In vivo analysis of cell recognition molecules involved in axonal pathfinding of motor neurons in the trunk of embryonic zebrafish *Danio rerio* (HAMILTON, 1822)

Dissertation

zur Erlangung des
Doktorgrades der Naturwissenschaften
des Fachbereichs Biologie der Universität Hamburg

vorgelegt von

Julia Feldner

aus Lübbecke

Hamburg
August 2005

Genehmigt vom
Fachbereich Biologie der
Universität Hamburg
auf Antrag von Frau Professor Dr. M. SCHACHNER
Weitere Gutachter der Dissertation:
Herr Professor Dr. L. RENWRANTZ
Tag der Disputation: 14. Oktober 2005

Hamburg, den 30. September 2005

Professor Dr. Arno Frühwald
Dekan

Gutachter

Herr Prof. Dr. L. Renwrantz

Frau Prof. Dr. M. Schachner

1 INTRODUCTION

1.1 Aims of the study

The aim of this study was to identify and characterize cell recognition molecules and their binding partners involved in the guidance of primary motor axons in the trunk of embryonic zebrafish. The outgrowth of primary motor axon in zebrafish was utilized as a model system to gain insight into the complex molecular interactions that govern axon guidance in vivo. The pathfinding of trunk motor axons in embryonic zebrafish is thought to be triggered by the interaction of class 3 semaphorins in the trunk environment with a receptor complex composed of neuropilins, plexins and the cell adhesion molecule L1 on motor axons. The expression patterns of the two zebrafish orthologs of semaphorin3A (semaphorin3A1 and semaphorin3A2) suggest that they are involved in the guidance of ventral trunk motor axons (Roos et al., 1999; Yee et al., 1999). Furthermore, homologs of the semaphorin3A receptor components neuropilin-1 and L1 are expressed in primary motor neuron somata (Tongiorgi et al., 1995; Lee et al., 2002; Yu et al., 2004; Bovenkamp et al., 2004; Martyn and Schulte-Merker, 2004).

To analyze the function of zebrafish neuropilin-1a and its ligands in motor axon outgrowth, specific morpholinos (anti-sense oligonucleotides with a stabilizing sugar backbone) and synthetic mRNAs were injected into zebrafish eggs to inhibit mRNA translation or to over-express proteins during motor axon development. Effects of perturbation agents were analyzed by labeling neurons and their axons at 24 hours post fertilization by immuno-histochemistry. To identify zebrafish homologs of the plexin family, which are potential co-receptors in the semaphorin3A signaling complex, the full-length plexinA3 gene was cloned, its expression patterns were described during development and the function of plexinA3 was analyzed by in vivo perturbation with morpholinos.

1.2 Zebrafish as a model system for axon guidance

The zebrafish (*Danio rerio*, formerly known as *Brachydanio rerio*) belongs to the family of cyprinids (*Cyprinidae*) in the class of ray-finned fishes (*Actinopterygii*) and within this class to the bony fishes (teleosts or *Teleostei*) to which most extant ray-finned fishes belong. Zebrafish are 2 to 4 cm long tropical freshwater fish and their natural habitats are rivers of South Asia, northern India, Bhutan, Pakistan and Nepal.

The zebrafish genome comprises approximately 1.5 x 10^9 bp on 25 chromosomes. It is assumed that large parts of the zebrafish genome were subject to an ancient genome duplication event during evolution of the ray-finned fishes (Taylor et al., 2001). This tetraploidization was followed by a functional specialization of some of the duplicated genes and the loss of other genes. Consequently an estimated 20% of mammalian genes have two zebrafish orthologs with distinct functions and expression domains (Van de Peer et al., 2002). In February 2001, the Sanger Institute started sequencing the genome of the zebrafish and sequences are currently being annotated by the Ensembl project of the Sanger Institute and the European Molecular Biology Laboratory. Preliminary genomic information is accessible through a genome browser on the Ensembl website.

The zebrafish is an ideal model system for studying developmental processes in vivo. Development of the nervous system takes place in a stereotyped pattern and is relatively simple. Patterning of the zebrafish nervous system and other fundamental organs occurs during the first 24 hours post fertilization (hpf) and juvenile fish hatch between two and three days post fertilization (dpf). On the fifth day of development the vast majority of cell types have differentiated and the organs have taken up their function. Zebrafish embryos are completely transparent during early development, which makes it possible to identify single neurons and their axons by immunohistochemistry, in situ hybridization or live imaging. Protein expression can easily be manipulated by injection of plasmid DNA, mRNA overexpression constructs or modified antisense oligonucleotides, so-called morpholinos, which inhibit mRNA translation. Such perturbation compounds can be injected directly into the yolk of fertilized eggs or into single cells at various developmental stages.

1.3 Motor axon outgrowth in the developing zebrafish

The outgrowth of primary motor axons in the trunk of embryonic zebrafish is a widely used model system to analyze the signals that pattern early motor axon growth (Beattie, 2000). This system is relatively simple, with three primary motor neurons per spinal hemisegment growing axons out of the spinal cord along a common pathway in the middle of each trunk segment up to the horizontal myoseptum. The axon of the caudal primary motor neuron (CaP) is the first to grow out of the spinal cord at 18 hpf (Fig. 1), followed by the axons of the middle (MiP) and rostral primary motor neurons (RoP). At the horizontal myoseptum axon paths diverge. The CaP axon continues its growth towards the ventral somite forming the ventral motor nerve, whereas the MiP axon retracts and grows towards the dorsal somite. The RoP axon takes a lateral path from the horizontal myoseptum. In half of the hemisegments a fourth primary motor neuron, called the variable primary motor neuron (VaP) is present. (Eisen et al., 1986; Myers et al., 1986; Westerfield et al., 1986; Eisen et al., 1990).

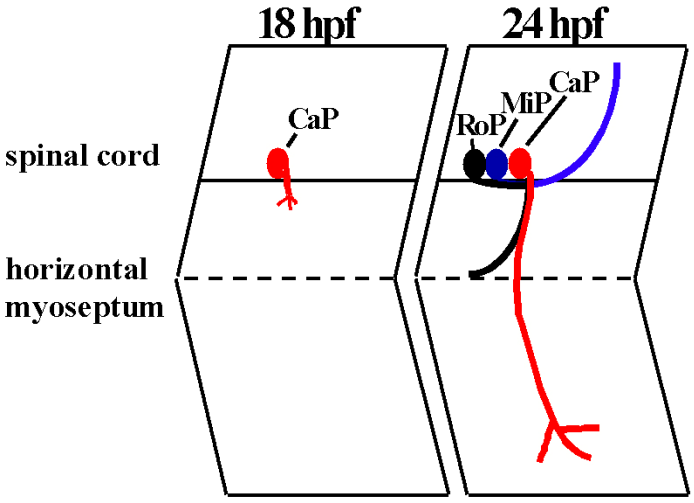

Fig. 1 Schematic illustration of primary motor axon outgrowth in embryonic zebrafish. A side view of zebrafish trunk segments at 18 and 24 hpf is given. At 18 hpf the caudal primary motor neuron (CaP) grows an axon out of the spinal cord. At 24 hpf, the axons of the middle (MiP) and rostral (RoP) primary motor neurons have followed on the common pathway to the horizontal myoseptum and the MiP has grown towards the dorsal somite. The CaP axon is the only one growing ventrally beyond the horizontal myoseptum.

By 24 hpf, when axon growth was analyzed by anti-tubulin immunohistochemistry, the CaP axon had reached the ventral myotome and the MiP axon had reached the dorsal myotome in

most trunk segments, with the exception of the youngest, most caudal segments, in which axon growth occurred later. The RoP axon has advanced as far as the horizontal myoseptum by 24 hpf (Eisen et al., 1986; Myers et al., 1986; Westerfield et al., 1986) (Fig. 1).

1.4 Cell recognition molecules in axon guidance

Throughout different stages of embryonic development, axons are directed by specific cell recognition molecules to follow specific pathways, to turn at particular guideposts and to identify their particular synaptic target cells. Guidance cues are present in the surrounding of a growing axon, either as diffusible secreted molecules (semaphorins, netrins, slits), which can act over long distances, or as molecules that act over short ranges that are either membrane-bound (ephrins, other semaphorins) or associated with the extracellular matrix (e.g. tenascins, proteoglycans). The presence of axon guidance cues is sensed by high-affinity cell surface receptors on growth cones (neuropilin, DCC, robo and ephrin receptors, integrins, Ig-CAMs, etc.). Receptor-ligand complexes initiate intracellular signaling cascades that result in the appropriate modulation of growth cone motility and define the eventual direction and extent of axon outgrowth. Guidance molecules can exhibit either attractive or repulsive effects and different axons can respond differently to the same cue (Tessier-Lavigne and Goodman, 1996; Nakamura et al., 2000; Yu and Bargmann, 2001; Dickson, 2002).

Several findings suggest that soluble semaphorin molecules play a major role as repulsive guidance cues by signaling through neuropilins and their receptor components during the development of primary motor axons in embryonic zebrafish:

1.4.1 Repulsive guidance cues of the semaphorin family

Semaphorins are a large family of transmembrane or secreted proteins (Fig. 2) known to mediate repulsive guidance events in neuronal development (Mark et al., 1997). The family is characterized by a conserved ~500 amino acid extracellular Sema domain and classification is based on domain organization within the primary structure and on species of origin (Kolodkin et al., 1993) (Fig. 2). Class 3 semaphorins are secreted molecules that contain an N-terminal Sema domain, one immunoglogbulin (Ig) domain and a basic amino rich C-terminal region, which might allow them to associate with the extracellular matrix (Nakamura et al., 2000).

Semaphorin 3A (sema3A, semaIII, semaD, collapsin-1) has been studied most extensively in the developing nervous system (Raper, 2000). Interactions of sema3A with axons expressing neuropilin-1 result in collapse of growth cones and repulsion of axons (Bagri and Tessier-Lavigne, 2002; He et al., 2002), but there is also evidence for attractive functions of sema3A (Bagnard et al., 1998; Castellani et al., 2000). Mice deficient for sema3A show defasciculation and target overshooting of cranial and spinal nerves (Taniguchi et al., 1997).

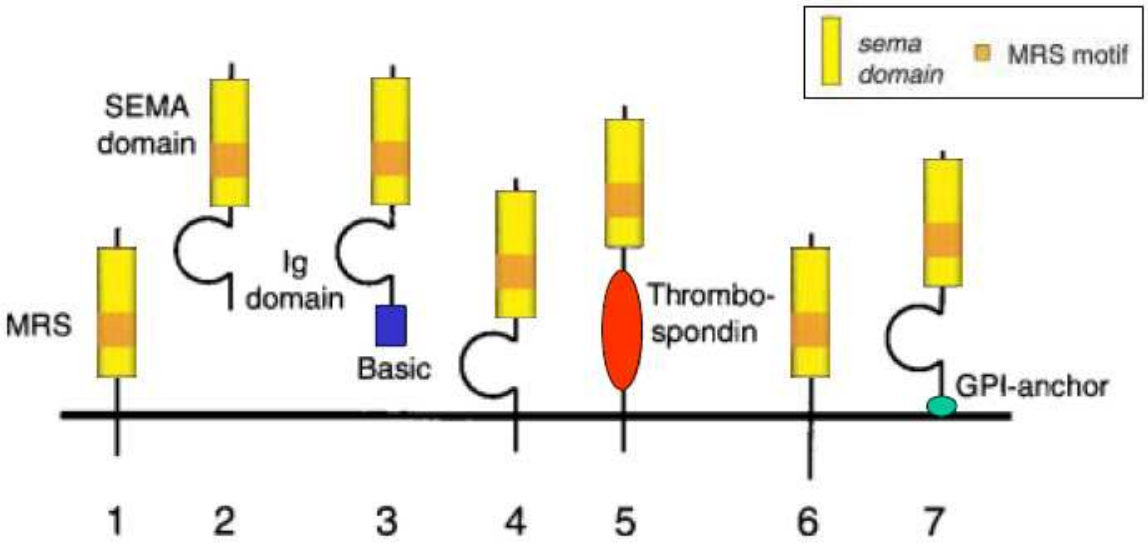

Fig. 2 Semaphorin subfamilies. Class 1 and 2 contain transmembrane and secreted semaphorins from invertebrates, respectively. Secreted semaphorins of vertebrates fall into class 3. The other vertebrate semaphorins are membrane-bound, either transmembrane (class 4, 5 and 6) or GPI-anchored (class 7, GPI-anchor in green). The Sema domain (yellow) is the hallmark of this protein family and it includes a Met-related sequence (MRS motif, orange). Other conserved domains are immunoglobulin domains (in classes 2, 3, 4 and 7), domains rich in basic amino acids (class 3, blue) and thrombospondin repeats (class 5, red). (source: http://www.ircc.it)

In zebrafish there are two homologs of Sema 3A designated Sema3A1 (semaZ1a) and Sema3A2 (semaZ1b). Sema3A1 mRNA is expressed at 15 hpf in the entire somite, but from 18–36 hpf its expression is restricted to the dorsal and ventral portions of the myotomes, leaving a corridor at the horizontal myoseptum negative of expression (Yee et al., 1999). Sema3A2 transcripts are found throughout the somite at 14 hpf, becoming progressively restricted to the posterior half of the somite and bordering the midsegmental pathway of the ventral motor nerve (Roos et al., 1999). Overexpression of the two sema3A homologs, sema3A1 (Halloran et al., 2000) and sema3A2 (Roos et al., 1999) in the trunk of embryonic

zebrafish induces truncations of primary motor nerves. This suggests axon-repellent functions of the molecules.

1.4.2 Neuropilins are receptors for class 3 semaphorins

Neuropilins are a small family of conserved proteins that function as cell surface receptors for soluble class 3 semaphorins. Two neuropilin molecules are known in mammals, designated neuropilin-1 (NRP1) and neuropilin-2 (NRP2), which share 44% amino acid identity (Kolodkin et al., 1997; Chen et al., 1997). Neuropilins are transmembrane glycoproteins containing two repeats of CUB (complement-binding) domains, two repeats of coagulation factor V/VIII homology domains, a MAM (meprin, A5 and receptor protein-tyrosine phosphatase µ) domain and a very short cytoplasmic domain (Fig. 3). Although the cytoplasmic domain contains a binding motif for neuropilin-1 interacting protein (NIP), which has been isolated in a yeast two hybrid screen as a potential binding partner for the C-terminus of neuropilin-1 (Cai and Reed, 1999), no evidence has been found that NIP contributes to transduction of the semaphorin signal (Nakamura et al., 1998). Thus, neuropilins rather contribute to specificity of ligand-binding and co-receptors are required for signal transduction.

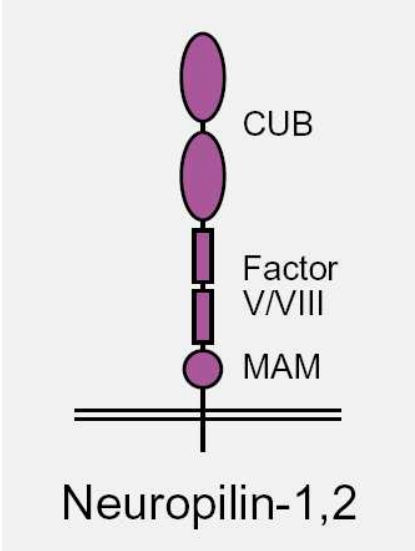

Fig. 3 Schematic representation of the neuropilin family members neuropilin-1 and neuropilin-2 (reproduced from Yu and Bargmann, 2001). The extracellular part of neuropilins is composed of two complement-binding domains (CUB), two coagulation factor V/VIII homology domains (Factor V/VIII), and a domain that has homology to domains found in meprin, A5 and receptor protein-tyrosine phosphatase µ (MAM).

Neuropilin-1 was first identified as an antigen expressed on retinal ganglion cell axons of developing *Xenopus* (Takagi et al., 1991). Using a COS cell expression cloning approach, two groups independently identified neuropilin-1 as a sema3A receptor (He and Tessier-Lavigne, 1997; Kolodkin et al., 1997). Mice deficient for neuropilin-1 show abnormalities in the peripheral projections of sensory neurons and some cranial motor neurons (Kitsukawa et al., 1997) similar to but more severe than those displayed in sema3A knockout mice (Taniguchi et al., 1997). Neuropilin-1 and neuropilin-2 exhibit different binding specificities for class 3 semaphorins. In vivo, neuropilin-1 binds sema3A preferentially, whereas neuropilin-2 preferentially binds sema3F (Nakamura et al., 2000). Explant and growth cone collapse assays suggest that sema3C signals through neuropilin-1/neuropilin-2 heterodimers (Chen et al., 1998; Takahashi et al., 1998). This binding specificity, together with restricted distribution of the molecules, explains the specificity of responses of different neurons to class 3 semaphorins.

For each mammalian neuropilin, two zebrafish orthologs have been identified, designated NRP1a and NRP1b and NRP2a and NRP2b, respectively (Lee et al., 2002; Yu et al., 2004; Bovenkamp et al., 2004; Martyn and Schulte-Merker, 2004). Of the four molecules, only NRP1a is expressed in the ventral spinal cord and thus, may be a receptor on motor neurons for the zebrafish sema3A orthologs sema3A1 and sema3A2, which are expressed in the zebrafish trunk.

1.4.3 Plexins are co-receptors for neuropilins

Neuropilins bind the secreted class 3 semaphorins with high affinity but require a member of the plexin family to form receptors that are able to activate down stream signal transducing cascades. In vertebrates, the plexin protein family was first identified as molecules predominantly expressed in the developing nervous system (Kameyama et al., 1996; Maestrini et al., 1996). Plexins comprise a large family of transmembrane molecules, divided into four subfamilies, (plexinA, plexinB, plexinC and plexinD) on the basis of sequence similarity (Tamagnone et al., 1999) (Fig. 4). They are characterized by a highly conserved cytoplasmic SP (Sex-Plexin) domain, which is required for signal transduction. The extracellular part of plexins contains a Sema domain, which shows a moderate degree of sequence identity to the corresponding domain in semaphorins (Winberg et al., 1998), two or three MRS repeats

(receptor protein tyrosine kinase Met-Related Sequence) and several IPT (Immunoglobulin-like fold shared by Plexins and Transcription factors) motifs (Fig. 4).

Several neurons in the developing central and peripheral nervous system express various plexins including hippocampal, cortical, sensory and sympathetic neurons (Cheng et al., 2001; Murakami et al., 2001). In addition to a role in signal transduction, complex formation of neuropilins with plexins changes their ligand-binding properties and increases specificity for particular secreted semaphorins. For example, neuropilin-1 and plexinA1 form a complex with an enhanced binding affinity for sema3A while a neuropilin-2/plexinA2 complex preferentially binds sema3F (Takahashi et al., 1999; Rohm et al., 2000). PlexinA3 regulates the development of hippocampal axonal projections, transduces repulsive signals in growth cones and contributes to sema3A and sema3F signaling in vivo (Cheng et al., 2001). The cytoplasmic SP domain is unique to plexins but has sequence similarities with GTPase activating proteins (GAPs) suggesting that plexins might regulate the activities of or interact with Ras-like GTPases (Rohm et al., 2000).

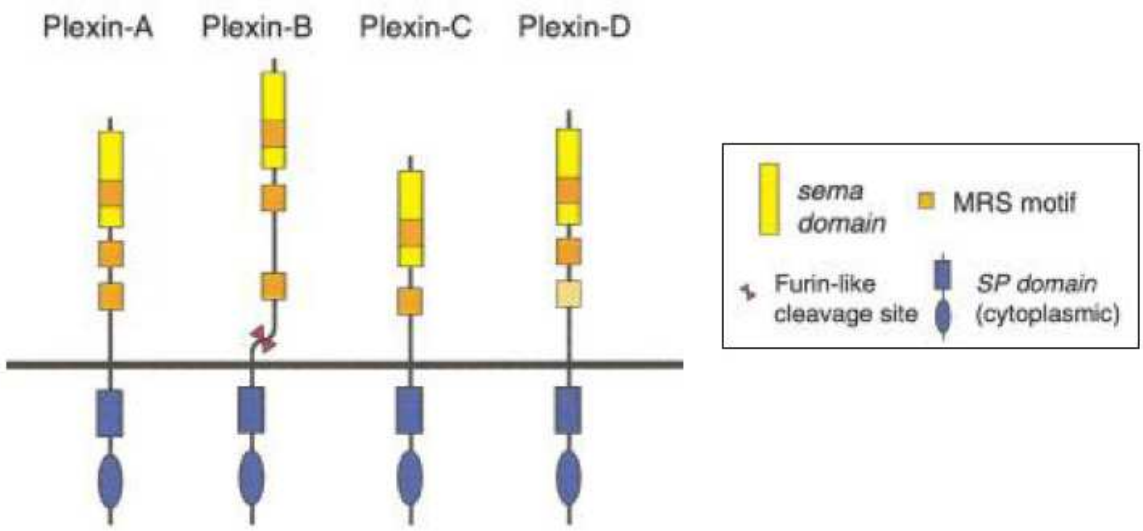

Fig. 4 Members of the plexin family. Nine human plexins are currently known, which fall into four homology groups (A, B, C and D subfamilies), based on sequence similarity, structural features, and tissue distribution. All plexins include a conserved cytoplasmic domain (Sex-Plexin domain, SP, blue) and a Sema domain (yellow). Repeated MRS motifs (orange) are found in the extracellular domain. Plexin-B subfamily members include potential cleavage sites for furin-like convertases (also found in plexin-B of *Drosophila*, here marked in red). The prototype member of the plexin-C subfamily (Vespr) is shorter, including only two MRS motifs. Plexin-D1 includes an atypical sequence in its third MRS (light orange). IPT (Immunoglobulin-like fold shared by plexins and transcription factors) motifs are not shown in this overview. (source: http://www.ircc.it)

In zebrafish to date two members of the plexin family have been cloned. PlexinD1 is expressed by epithelial cells of the embryonic vasculature and loss of plexinD1 function causes mispatterning of angiogenic intersegmental vessels in the trunk (Torres-Vazquez et al., 2004). PlexinA4, which is expressed by a number of neurons in the brain and spinal cord, promotes branching of the peripheral axons of primary sensory neurons (Yeo et al., 2004).

1.4.4 The neural cell adhesion molecule L1 modulates Sema3A signaling

In addition to the core complex that contains neuropilin and plexin, studies of mice lacking L1 activity suggest that a third molecule, the neural cell adhesion molecule L1 has a modulatory effect on sema3A signaling (Castellani et al., 2000).

L1 is a cell adhesion molecule (CAM) of a neural subfamily of the immunoglobulin (Ig) superfamily (Rathjen and Schachner, 1984) and has been implicated in a variety of morphogenetic processes, including axon growth, axon fasciculation, axon guidance, cell migration, myelination and synaptic plasticity (Walsh and Doherty, 1997; Haspel and Grumet, 2003). The L1 subfamily includes L1, a close homologue of L1 (CHL1), neurofascin, NrCAM, neuroglian, and tractin, and its members are found predominantly, but not exclusively, on axon tracts. L1 is a transmembrane glycoprotein similar in domain structure to members of the robo family (slit-receptors), and its extracellular domains consist of six immunoglobulin-like and five fibronectin type III domains (Fig. 5). A highly conserved intracellular region follows the transmembrane domain and contains a binding site for ankyrin, a protein connecting L1 to the spectrin cytoskeleton (Brümmendorf et al., 1998). Targeted disruption of the L1 gene in mice results in defects of the corticospinal tract (Dahme et al., 1997; Cohen et al., 1998). L1 can be co-immunoprecipitated with neuropilin-1 and dorsal root ganglion (DRG) neurons from L1 knockout mice do not respond to sema3A. In culture, addition of L1-Fc fusion proteins can turn the repulsive response of dorsal root ganglion neurons to sema3A into an attractive one, suggesting a modulatory function of L1 for semaphorin signaling (Castellani et al., 2000).

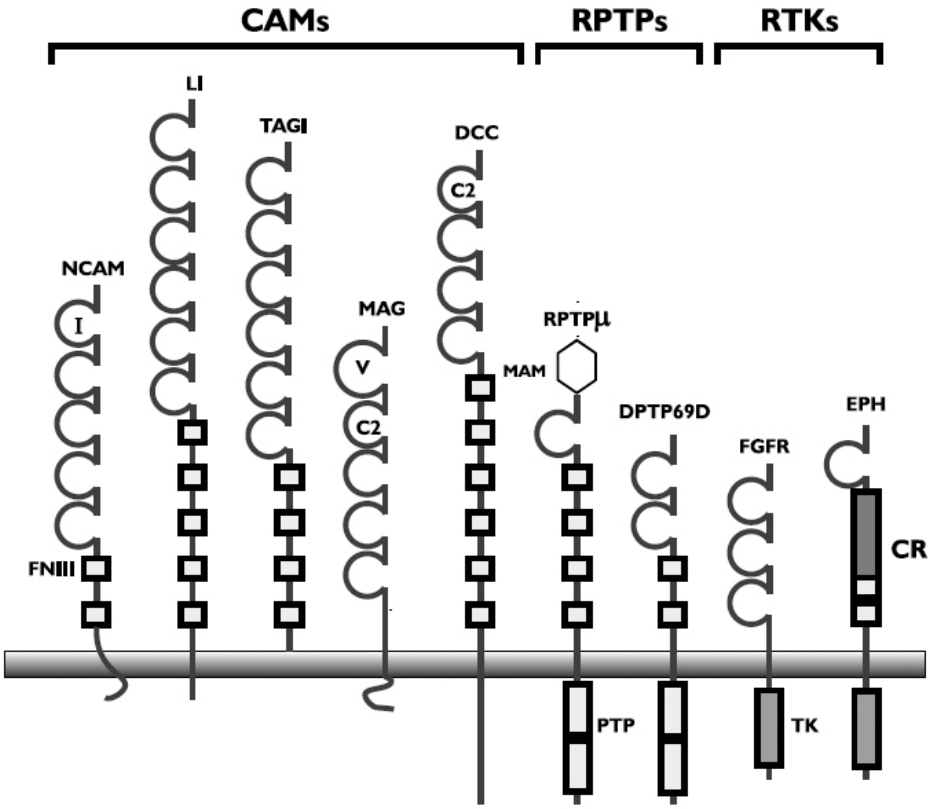

Fig. 5 Representatives of selected subfamilies of the immunoglobulin (Ig) superfamily implicated in growth and guidance in the nervous system (modified after Walsh and Doherty, 1997). Shown are examples of three main subgroups, namely cell adhesion molecules (CAMs), receptor protein tyrosine phosphatases (RPTPs), and receptor tyrosine kinases (RTKs). All molecules are typified by having Ig domains of various types; in the brain they are of C2, V, or I types. Members of the CAM subgroup all contain Ig domains, and with the exception of MAG, contain fibronectin type III (FNIII) repeats. NCAM, L1, and DCC are transmembrane proteins, whereas TAG 1 is GPI anchored. Two representatives of the RPTP family are shown: RPTPμ, which in addition to having an Ig domain and FNIII repeats, contains a MAM domain. DPTP69D contains Ig and FNIII repeats. Both RPTPs contain intracellular catalytic domains (PTP). Two representative RTKs are shown: FGFR and EPH. FGFR contains Ig domains. EPH contains an Ig domain, a cysteine-rich domain (CR), and FNIII repeats. Both contain intracellular catalytic domains (TK). EPH (ephrin), FGFR (fibroblast growth factor receptor), MAG (myelin-associated glycoprotein), NCAM (neural cell adhesion molecule), DCC (deleted in colonrectal carcinoma).

In zebrafish L1.1 and L1.2 have been identified as the two orthologs of mouse L1 (Tongiorgi et al., 1995). During embryonic development of the nervous system the onset of L1.1 and L1.2 expression correlates with the initiation of axonogenesis. L1.1 is expressed by all known classes of neurons, consistent with an important general function during axon outgrowth. Most of the neurons in the developing zebrafish also express L1.2, but L1.2 expression is lower or not detectable in subsets of neurons. The fact that primary motor neurons express L1.1 and L1.2 supports the idea that both L1 homologs could be part of the sema3A receptor complex and play a role in the guidance of primary motor axons in zebrafish. In adult

zebrafish, upregulation of L1.1 is an important part of the regenerative response of axotomized brainstem neurons after spinal cord transaction (Becker et al., 2004).

1.5 Neuropilins are receptors for in angiogenic signals

In addition to the nervous system, neuropilins are known to function in angiogenesis. Neuropilin-1 is expressed in endothelial cells and enhances vascular endothelial growth factor (VEGF) binding to VEGF receptor 2 (VEGFR2/Flk-1/KDR) (Soker et al., 1998) Similarly, neuropilin-2 forms complexes with VEGF receptor 1 (VEGFR1/Flt-1) in vitro (Gluzman-Poltorak et al., 2001). Thus, neuropilins are not only co-receptors for plexins in axonogenesis, but also act as co-receptors for VEGF receptors in the formation of blood vessels (Klagsbrun et al., 2002; Neufeld et al., 2002). Transgenic mice expressing high levels of neuropilin-1 exhibit major anomalies in the nervous and cardiovascular system, including excess capillary formation (Kitsukawa et al., 1995). In addition to severe abnormalities in the nervous system (Kitsukawa et al., 1997), neuropilin-1 knockout mouse embryos have defects in yolk sac, embryo and neuronal vascularization and in development of large vessels in the heart (Kawasaki et al., 1999).

During motor axon development, zebrafish VEGF is expressed in mesoderm giving rise to blood vessels, in the ventromedial somite of the trunk as well as in the anterior central nervous system (Liang et al., 1998).One of the zebrafish homologs of neuropilin-1, NRP1a, is expressed in the endothelium of major blood vessels in the trunk during angiogenesis and mediates VEGF-dependent development of intersegmental vessels in the trunk (Lee et al., 2002). Other zebrafish neuropilins are expressed in the dorsal aorta (NRP1b) and in the region of the posterior cardinal vein (NRP2a and NRP2b) and are involved in VEGF-mediated vessel development (Martyn and Schulte-Merker, 2004).

Recent observations suggest that semaphorin and VEGF signaling are probably not restricted to the nervous and vascular system, respectively. For example, sema3A acts as a repellent molecule for blood vessels in the quail forelimb (Bates et al., 2003). Both, sema3A/ neuropilin-1 and VEGF/neuropilin-1 signaling is needed for heart morphogenesis in mice (Gu et al., 2003). In vitro, VEGF promotes neurite outgrowth and neuronal survival (Sondell et al., 2000; Bocker-Meffert et al., 2002; Rosenstein et al., 2003). Thus, several signaling molecules may converge on one receptor, neuropilin-1, in the vascular and nervous system. In fact, there

is evidence for functional competition of VEGF and sema3A for overlapping binding sites on neuropilin-1 (Miao et al., 1999). In zebrafish, sema3A1 is involved in the development of the dorsal aorta in the trunk (Shoji et al., 2003).

2 MATERIAL AND METHODS

2.1 Material

2.1.1 Enzymes

Restriction endonucleases

various (5-20 U/µl)	New England Biolabs (Frankfurt, D) Roche (Mannheim, D)

DNA polymerases

Advantage™-2	BD Biosciences/Clontech (Heidelberg, D)
HotStarTaq®	Qiagen (Hilden, D)
Klenow Enzyme	Roche (Mannheim, D)
PfuUltra™ HF DNA Polymerase	Stratagene (Amsterdam, NL)
Taq DNA Polymerase	Invitrogen (Karlsruhe, D)

Reverse transcriptases (RT)

Omniscript™ RT	Qiagen (Hilden, D)
SuperScript II™ RT	Invitrogen (Karlsruhe, D)
RNasin® Plus RNase Inhibitor	Promega (Mannheim, D)

Miscellaneous

DNAse I	Roche (Mannheim, D)
RNAseH	Roche (Mannheim, D)
Shrimp Alkaline Phosphatase (SAP)	Roche (Mannheim, D)
T4 DNA Ligase	Roche (Mannheim, D)

2.1.2 Bacterial strains

E. Coli DH5α	Invitrogen (Karlsruhe, D)
E. Coli One Shot® TOP10 (Chemically Competent)	Invitrogen (Karlsruhe, D)
E. Coli NR 3704 (dam^-)	Institut Prof. Schachner, ZMNH (Hamburg, D)

2.1.3 Bacterial media

All media were autoclaved prior to use. Antibiotics were added if appropriate.

LB broth (1 l)	10 g NaCl
	10 g tryptone or peptone
	5 g yeast extract
	pH 7.0 with 5 M NaOH (optional)
LB agar (1 l)	10 g NaCl
	10 g tryptone or peptone
	5 g yeast extract
	20 g agar
	pH 7.0 with 5 M NaOH (optional)
Antibiotics (1000x)	100 mg/ml ampicillin (amp)
	25 mg/ml kanamycin (kan)

2.1.4 Vectors

pGEM®-T Easy	Promega (Mannheim, D)	TA cloning vector
pCR®-Blunt II TOPO®	Invitrogen (Karlsruhe, D)	TOPO cloning vector
pCS2+MT	Rupp et al., 1994	mRNA overexpression vector
zNRP1/pCR4	Lee et al., 2002	Cloning vector containing zf NRP1a cDNA

2.1.5 Kits

BCA Protein Assay Reagent Kit	Pierce (Rockford, USA)
ECL Western Blotting Detection Reagents	Amersham Pharmacia (Freiburg, D)
MEGAscript™ (T3/T7/SP6)	Ambion (Cambridge, UK)
mMESSAGE mMACHINE™ SP6	Ambion (Cambridge, UK)
Poly (A) Tailing Kit	Ambion (Cambridge, UK)
Rapid DNA Ligation Kit	Roche (Mannheim, D)
pGEM®-T Easy Vector System I	Promega (Mannheim, D)
Zero Blunt® TOPO® PCR Cloning Kit	Invitrogen (Karlsruhe, D)
JETstar Plasmid Purification MAXI Kit	Genomed (Bad Oeynhausen, D)

HiSpeed® Plasmid Midi Kit	Qiagen (Hilden, D)
GFX™ Micro Plasmid Prep Kit	Amersham Pharmacia (Freiburg, D)
QIAquick™ Gel Extraction Kit	Qiagen (Hilden, D)
QIAquick™ PCR Purification Kit	Qiagen (Hilden, D)
MiniElute™ Gel Extraction Kit	Qiagen (Hilden, D)
MiniElute™ PCR Purification Kit	Qiagen (Hilden, D)
High Pure PCR Product Purification Kit	Roche (Mannheim, D)
RNeasy® Midi Kit	Qiagen (Hilden, D)

2.1.6 DNA and protein standards

Ready-Load™ 1 kb Plus DNA Ladder	Invitrogen (Karlsruhe, D)
100 bp DNA Ladder	New England Biolabs (Frankfurt, D)
SmartLadder	Eurogentec (Heidelberg, D)
BenchMark™ Pre-Stained Protein Ladder	Invitrogen (Karlsruhe, D)

2.1.7 Oligonucleotides

Oligonucleotides/primers were synthesized and HPSF®-purified by MWG biotech AG (Ebersberg, D) or synthesized and salt-purified by Metabion (Planegg, Martinsried, D). Primer sequences are listed in the appendix.

2.1.8 Morpholinos

Morpholinos are synthetic antisense oligonucleotides containing a stabilizing sugar backbone with a morpholine ring instead of the standard ribose sugar found in DNA or RNA making them more resistant to a number of nucleases. Another advantage is, that morpholinos show a low toxicity and have a high affinity to RNA (Summerton et al., 1997). Ideally, morpholinos are selected against a sequence near the start codon of the mRNA of interest. By binding to the mRNA, the morpholino interferes with the 40S ribosomal subunit scanning the mRNA and blocks the initiation of translation (Ekker and Larson, 2001). The efficiency of morpholinos is restricted to target sites within the leader sequence and sequences surrounding the start codon (Summerton, 1999). Since protein synthesis of specific genes is not completely blocked by morpholino application, the effect is referred to as a “knockdown”.

Morpholinos were synthesized by Gene Tools LLC (Philomath, OR, USA) and 300 nmol lyophilized morpholinos were resuspended in 37.5 µl Danieau solution to obtain a stock solution of 8 mM (65 ng/nl). The stock solutions were split in 3 µl aliquots and stored at -20°C. Morpholinos were adjusted with Danieau solution to obtain concentrations between 0.1 and 2 mM. Sequences of morpholinos used in this study are listed in the appendix.

2.1.9 Antibodies

tubulin monoclonal antibody (mAb) against acetylated α-tubulin (6-11B-1; Sigma-Aldrich, Deisenhofen, D), used 1:1000 (immunohistochemistry) or 1:25000 (Western blot)

412 mAb to the HNK-1 epitope (Becker et al., 2001), used 1:50

CS-56 mAb to chondroitin sulfates (Sigma-Aldrich, Deisenhofen, D), used 1:200

Sus-ten polyclonal antibody (pAb) against tenascin-C of zebrafish (Bartsch, 1996), used 1:2000

9E10 mAb recognizing the myc-epitope (Santa Cruz Biotechnology, Santa Cruz, USA), used 1:600

40.2D6 antibody to islet-1/-2 (Dr. T.M. Jessell Columbia University, New York, USA), used 1:50

3A10 antibody to a neurofilament-associated antigen (Dr. T.M. Jessell Columbia University, New York, USA), used 1:50

4D9 antibody to engrailed (Patel et al., 1989), used 1:10

L1.1 polyclonal antiserum against bacterially expressed zebrafish L1.1 (Becker et al., 2004), used 1:25000

Antibodies 40.2D6, 3A10 and 4D9 were obtained as cell culture supernatants from the Developmental Studies Hybridoma Bank maintained by The University of Iowa, Department of Biological Sciences (Iowa City, IA, USA).

Secondary antibodies were Cy2-, Cy5- and horseradish peroxidase (HRP)-conjugated to rabbit and mouse (Dianova, Hamburg, Germany), used 1:200 for immunohistochemistry and 1:4000 for Western blot.

2.1.10 Buffers and stock solutions

General buffers and stock solutions are listed below. Method-specific solutions are specified in the corresponding sections.

Blocking buffer (Western blot)	0.05% Tween 20 in 1x PBS 3% skimmed milk powder
Blocking buffer (WMIHC)	1x PBS 1% (v/v) DMSO 1% (v/v) normal goat serum 1% (w/v) BSA 0.7% (v/v) Triton-X 100
Blotting buffer (1x)	25 mM Tris-HCl (pH 8.3) 192 mM glycine 20% methanol
DAB stock solution	6% (w/v) diaminobenzidine
Danieau solution	58 mM NaCl 0.7 mM KCl 0.4 mM $MgSO_4$ 0.6 mM $Ca(NO_3)_2$ 5 mM HEPES pH 7.6
DEPC-H_2O	0.1% (w/v) diethylpyrocarbonate autoclaved after stirring overnight
DNA sample buffer (5x) (DNA gel)	20% (w/v) glycerol in TAE buffer 0.025% (w/v) orange G

dNTP stock solutions (PCR)	dATP, dCTP, dGTP, dTTP, 25 mM each
EB buffer	10 mM Tris-HCl, pH 8.0
EDTA stock solution	0.5 M EDTA pH 8.0
Ethidiumbromide staining solution (DNA-gel)	10 µg/ml ethidiumbromide in 1x TAE
Loading buffer (5x) (RNA gel)	50% (v/v) glycerol 1 mM EDTA 0.25% (w/v) bromphenol blue 0.25% (w/v) cylene cyanol
PBST (Biochemistry)	0.05% (v/v) Tween 20 in 1x PBS
PBST (Morphology)	0.1% (v/v) Tween 20 in 1x PBS
PFA (4%)	4% (w/v) paraformaldehyde dissolved at 60°C under stirring in 1x PBS
Phosphate buffered saline (PBS) (10x)	1.36 M NaCl 0.1 M Na_2HPO_4 27 mM KCl 18 mM KH_2PO_4 pH 7.4
Running buffer (5x) (RNA gel)	0.1 M MOPS pH 7.0 40 mM sodium acetate 5 mM EDTA
Running buffer (10x) (SDS-Page)	250 mM Tris-HCl, pH 8.3 1.92 mM glycine 1% (w/v) SDS

Running gel (8.0%) (SDS-PAGE)	4.28 ml deionized water 4.65 ml 1 M Tris-HCl, pH 8.8 124 µl 10% SDS 3.34 ml 30% Acrylamide – Bis (37:5:1) 70 µl 10% APS 7 µl TEMED
Saline sodium citrate buffer (SSC) (20x)	3 M NaCl 0.3 M tri-sodium citrate pH 7.4
Sample buffer (5x) (SDS-Page)	62.5 mM Tris-HCl, pH 6.8 2% (w/v) SDS 5% (w/v) β-mercaptoethanol 20% (v/v) glycerol 0.04% (w/v) bromphenol blue
Stacking Gel (5%) (SDS-Page)	2.89 ml deionized water 1.25 ml 1 M Tris-HCl, pH 6.8 50 µl 10% SDS 830 µl 30% Acrylamide – Bis (37:5:1) 25 µl 10% APS 5 µl TEMED
Stripping buffer (Western blot)	0.5 M NaCl 0.5 M acetic acid
TAE (50x) (DNA gel)	2 M Tris-acetate, pH 8.0 100 mM EDTA
TE (10x)	0.1 M Tris-HCl, pH 7.5 10 mM EDTA

2.1.11 Chemicals

All chemicals were obtained from the following companies in *pro analysis* quality: Amersham Pharmacia Biotech (Freiburg, D), BioRad (München, D), Invitrogen (Karlsruhe, D), Carl Roth (Karlsruhe, D), Merck (Darmstadt, D), Serva (Heidelberg, D) and Sigma-Aldrich (Deisenhofen, D).

2.1.12 Equipment

Equipment not listed in the table below was of common laboratory standard. Particular devices are referenced throughout the respective protocols.

Centrifuge RC 5C Plus	Sorvall (Kendro, Hanau, D)
Rotors SLA3000, SLA1500, SA600 and HB-6	Sorvall (Kendro, Hanau, D)
Microcentrifuge 5415 D	Eppendorf (Hamburg, D)
Bench-top centrifuges 5417 R and 5804 R	Eppendorf (Hamburg, D)
E.A.S.Y. UV-light documentation	Herolab (Wiesloh, D)
Spectrophotometer Ultrospec 3000/DPV-411 printer	APB (Freiburg, D)
MJ PTC-200 DNA ENGINE™ Peltier Thermal Cycler	Biozym (Hessisch Oldendorf, D)
Rotor-stator homogenizer	(Kinematica, Luzern, CH)
Power Pac 200	BioRad (München, D)
Cryostat CM3050	Leica (Bensheim, D)
Axiophot	Zeiss (Göttingen, D)
Laser scanning microscope LSM510	Zeiss (Göttingen, D)

2.1.13 Zebrafish

Adult (body length > 2 cm, age > 4 months) and developing zebrafish, *Danio rerio*, were kept at a 14 hours light and 10 hours dark cycle and fed dried fish food and live brine shrimp several times a day. Embryos were collected from the ZMNH breeding colony according to standard procedures and staged in hours post fertilization (hpf) at the standard temperature of 28.5°C (Kimmel et al., 1995).

2.2 Molecular biological methods

If not otherwise indicated, standard biological techniques were carried out according to standard protocols (Sambrook et al., 1989).

2.2.1 Maintenance of bacterial strains

Strains were stored as glycerol stocks (LB broth, 25% (v/v) glycerol at –80°C). To regrow particular strains, an aliquot of the stock was streaked on an LB agar plate containing the appropriate antibiotic and incubated overnight at 37°C. Plates were stored up to 6 weeks at 4°C.

2.2.2 Production of competent bacteria

DH5α bacteria were streaked on LB agar dishes and grown overnight at 37°C with constant shaking. 50 ml of LB broth were inoculated with 5 colonies and grown at 37°C under constant shaking (>200 rpm) until the culture had reached an optical density (OD_{600}) of 0.35-0.45. Growth of bacteria was stopped by a 5 min incubation step on ice. Cells were pelleted at 1000x g for 15 min (4°C) and, after removal of the supernatant, resuspended in 17 ml prechilled RF1 (4°C). Following a 15 min incubation step on ice, the centrifugation was repeated. The cell pellet was resuspended in 4 ml prechilled RF2 (4°C) and incubated again for 15 min on ice. Bacteria were frozen in liquid nitrogen in 50 – 100 µl aliquots and stored at –80°C. Transformation capacity/efficacy of cells was tested by a transformation with a distinct quantity (pg-ng) of purified supercoiled plasmid DNA.

RF1	RF2
100mM RbCl	10 mM MOPS (pH 6.8)
50 mM $MnCl_2$	10 mM RbCl
30 mM KOAc	75 mM $CaCl_2$

10 mM $CaCl_2$ 150 g/l glycerol
pH 5.8 (with 0.2 M acetic acid)

2.2.3 Polymerase chain reaction (PCR)

The *in vitro* amplification of DNA fragments using the polymerase chain reaction (PCR) was performed in a MJ PTC-200 DNA ENGINE™ Peltier Thermal Cycler. Standard PCR reactions contained the following ingredients: template DNA (typically plasmid or first strand cDNA), primers (flanking the region to be amplified), dNTPs (25 mM each), DNA polymerase buffer and DNA polymerase. Primer sequences were selected manually or electronically determined with the PrimerSelect software from the Lasergene software suite (DNASTAR inc. WI, USA).

Table 1 Standard PCR cycling parameters for selected DNA polymerases.

	Taq polymerase	Pfu polymerase	HotStarTaq	Advantage-2
1.	94°C-95°C for 1'-5'	94°C-98°C for 1'	95°C for 15'	95°C for 1'
2.	94°C-96°C for 30''-1'	94°C-98°C for 1'	94°C for 30''-1'	95°C for 30''
3.	T_A for 30''–1'	T_A for 30''–1'	T_A for 30''–1'	T_A for 30''–1'
4.	72°C, 1 min per kb	72°C, 2 min per kb	72°C, 1 min per kb	68°C, 2 min per kb
5.	Goto2, 25-40x	Goto2, 25-40x	Goto2, 25-40x	Goto2, 25-35x
6.	72°C for 10'	72°C for 10'	72°C for 10'	72°C for 10'
7.	4°C for ever	4°C for ever	4°C for ever	4°C for ever
8.	End	End	End	End

PCR programs shown were general starting points, when using the above mentioned DNA polymerases. T_A = primer annealing temperature, ' = min, '' = s.

Routinely, 50 µl reactions were performed in 0.2 ml thin-walled tubes (Biozym, Hessisch Oldendorf, D). Taq and HotStarTaq® DNA polymerases were used for general PCR reactions, whereas the proof-reading DNA polymerase PfuUltra™ HF and the polymerase mix Advantage™-2, containing minor amounts of a proof-reading polymerase, were employed to amplify DNA for overexpression constructs or full-length genes. In Table 1 cycling parameters for these DNA polymerases are listed.

Number of cycles (25 - 40) required for optimum amplification varied depending on the amount of starting material and the efficiency of each amplification step. A final incubation step at the extension temperature ensured fully double stranded molecules from all nascent products. Following cycling, typically 5-10 µl aliquots up to complete reactions were analyzed by agarose gel electrophoresis to detect amplified products.

2.2.4 Nested PCR

Nested PCR is applied to prevent amplification of unspecific sequences of DNA from a pool of very similar sequences. Two pairs of PCR primers are used for a single locus. The first pair amplifies the locus as seen in any PCR experiment. The second pair of primers (nested primers) binds within the first PCR product and produces a second PCR product that will be shorter than the first one. Thus, if the wrong locus was amplified by mistake, the probability is very low that it would also be amplified a second time by a second pair of primers. Nested PCR reactions were set up using Taq and HotStarTaq® DNA polymerases as described above.

2.2.5 TA cloning

PCR products amplified with Taq, HotStarTaq® or Advantage™-2 DNA polymerases, were directly subjected to TA cloning. The latter two products are actually mixtures that contain minor amounts of a proof-reading polymerase, but TA cloning was still possible. PCR products derived from these enzymes contained an additional adenosine at their 3’ end, and were subjected to TA cloning using the pGEM®-T Easy Vector System I following the manufacturer’s instructions.

2.2.6 TOPO cloning

Due to the 3’→ 5’ exonuclease activity, a major fraction of DNA species amplified with Pfu DNA polymerases does not contain an additional adenosine at the 3’ end. Such blunt-end PCR fragments were cloned using the highly efficient vaccinia topoisomerase-I based TOPO® cloning system. PCR fragments were inserted into the pCR®-Blunt II TOPO® vector according to the manufactures instructions.

2.2.7 PCR/DNA fragment purification

For purification of DNA fragments, the silica matrix-based High Pure PCR Purification Kit or MiniElute™ PCR Purification Kit was used according to the manufacturer's protocol. The DNA was eluted from the column by addition of 50 µl EB buffer. The DNA concentration was determined using the 1:10 – 1:100 dilutions of the eluate.

2.2.8 Restriction enzyme digest of DNA

Restriction enzyme digests were performed by incubating double-stranded DNA with an appropriate amount of restriction enzyme(s), the respective buffer as recommended by the supplier, and at the optimal temperature for the specific enzyme(s), usually at 37°C. General digests were set up as 20 µl total volume reactions. For preparative restriction digests, the reaction volume was scaled up to 100 µl. Digest reactions contained DNA, 1x restriction buffer, the appropriate number of units of the respective enzyme(s) and the sufficient volume of nuclease-free H_2O to bring the mix to the calculated volume. Due to glycerol content the volume of the enzyme(s) added should not exceed 1/10 of the total volume. After incubation at the optimal temperature for a 1-3 hrs or overnight, enzymes were inactivated by incubation for 20 min at 65°C. If reaction conditions of enzymes were incompatible to each other, DNA was digested successively with the individual enzymes. Between individual reactions, the DNA was purified.

2.2.9 DNA agarose gel electrophoresis

To analyze restriction digests, quality of nucleic acid preparations, etc. horizontal agarose gel electrophoresesis was performed. Gels were prepared by heating 0.8-2.5% (w/v) agarose (electrophoresis grade) in 1x Tris-acetate buffer (TAE), the agarose concentration depending on the size of fragments to be separated. DNA samples were adjusted to 1x DNA sample buffer and were subjected to electrophoresis at 10 V/cm in BIO-Rad gel chambers in 1x TAE running buffer. Afterwards, gels were stained in a staining bath containing 0.5 µg/ml ethidiumbromide in 1x TAE for approximately 20 min. Thermo-photographs of trans-illuminated gels were taken, or bands were made visible on an UV screen (λ = 360 nm). If desired, fragments were cut out with a scalpel.

2.2.10 DNA fragment extraction from agarose gels

For isolation and purification of DNA fragments from agarose gels, ethidiumbromide-stained gels were illuminated with UV light and the appropriate DNA band was excised from the gel with a clean scalpel and transferred into an Eppendorf tube. The fragment was isolated utilizing Qiagen's silica matrix-based QIAquick™ or MiniElute™ Gel Extraction Kits following the manufacturer's protocol. The fragment was eluted from the column by addition of 50 µl EB buffer.

2.2.11 Dephosphorylation of linerarised DNA

To prevent self-circularization of fragments by DNA ligase, 5'-phosphates were removed using 1 U SAP (Shrimp Alkaline Phosphatase) per 50-80 ng of linarized plasmid DNA in 1x SAP buffer. The reaction was incubated at 37°C for 20 min and terminated by incubation at 65°C for 15 min. The plasmid DNA was used for ligation without further purification.

2.2.12 Ligation of DNA fragments

Ligation of DNA fragments was performed by mixing 50 ng vector DNA with the five-fold molar excess of insert DNA. 1 µl of T4 DNA Ligase and 2 µl of 10x ligation buffer were added and the reaction mix was brought to a final volume of 20 µl. The reaction was incubated either for 2 h at room temperature (sticky ends) or overnight at 16°C (blunt ends). The reaction mixture was used directly for transformation without any further purification.

2.2.13 Transformation of DNA into bacteria

2-10 µl of a ligation mixture were added to 100 µl of competent DH5α and incubated for 45 min on ice. After a heat shock (90 s, 42°C) and successive incubation on ice (3 min), 800 µl of LB broth were added to the bacteria suspension and incubated at 37°C for 60 min. Cells were then centrifuged (8000x g, 1 min, RT) and the supernatant was removed. Cells were resuspended 100 µl LB broth and plated on LB plates containing the appropriate antibiotic. Colonies formed after incubation at 37°C for 12-16 h.

2.2.14 Small scale plasmid isolation (Miniprep)

4 ml LB broth (containing 100 µg/ml ampicillin or 25 µg/ml kanamycin) were inoculated with a single colony and incubated over night at 37°C with constant agitation. 2 ml of the culture were transferred into a 2 ml Eppendorf tube and cells were pelleted by centrifugation (12000 rpm, 1min, RT). Plasmids were isolated from the bacteria using the GFX^{TM} Micro Plasmid Prep Kit, according to the manufacturer's protocol. The DNA was eluted from the columns by addition of 50 µl EB buffer with subsequent centrifugation (12000 rpm, 2 min, RT). Plasmid DNA was stored at -20°C.

2.2.15 Large scale plasmid isolation (Maxiprep)

For preparation of large quantities of DNA, the JETstar Plasmid Purification MAXI Kit was utilized. A single colony was inoculated in 2 ml LB broth (containing 100 µg/ml ampicillin or 25 µg/ml kanamycin) and grown at 37°C for 8 h with constant agitation. Afterwards, this culture was added to 300ml LB broth (containing 100 µg/ml ampicillin or 25 µg/ml kanamycin) and the culture was incubated at 37°C with constant agitation overnight. Cells were pelleted in a Beckmann centrifuge (6000x g, 15 min, 4°C) and the DNA was isolated as described in the manufacture's protocol. Finally, the DNA pellet was resuspended in 500 µl of 1x TE buffer and the DNA concentration was determined.

2.2.16 Photometric quantification of nucleic acids

DNA, RNA and oligonucleotides were measured directly in aqueous solutions. The concentration was determined by measuring absorption at λ = 260 nm against blank and then evaluated via factor. The linear range for measurements was between 0.1 and 1.0 OD (optical density). The absorption of 1 OD is equivalent to approximately 50 g/ml double-stranded DNA, 40 g/ml RNA and 30 g/ml for oligonucleotides. Interference by contaminants was recognized by the calculation of ratio. The ratio $OD_{260/280}$ was used to estimate the purity of nucleic acid, since proteins absorb at 280 nm. Pure DNA should have a ratio of 1.8, whereas pure RNA should give a value of approximately 2.0. Absorption at λ = 230 nm reflects contamination of the sample by substances such as carbohydrates, peptides, phenols or aromatic compounds. In the case of pure samples, the ratio $OD_{260/230}$ should be approximately 2.2.

2.2.17 Sequencing of DNA

Sequence determination of double-stranded DNA was performed by the sequencing facility of the ZMNH (Dr. W. Kullmann, M. Daeumigen). Fluorescent dye-labeled chain termination products (ABI Prism Dye Terminator Cycle Sequencing Ready Reaction Kit, Perkin Elmer, Wellesly, MA, USA) were analyzed with an ABI Prism 377 DNA Sequencer (Perkin Elmer). For preparation, 0.8-1 µg of DNA was diluted in 7 µl ddH_2O and 1 µl of the appropriate sequencing primer (10 pM) was added.

2.2.18 Precipitation of DNA

The salt concentration of an aqueous DNA solution was adjusted by adding 1/10 volume of sodium acetate (3 M, pH 4.9) and 2.5 volumes of cold ethanol, -20°C were added. Samples were mixed well, incubated on ice for 30 min and centrifuged for 15 min (16000x g, RT). The supernatant was removed and 800 µl of 70% ethanol were added for washing. For optimal purity, the pellet was loosened from the tube during this step. After centrifugation and removal of the supernatant, additional wash steps with 400 and 200 µl of 70% ethanol were performed, followed by a quick 1-2 s centrifugation step to collect residual ethanol. This was removed and the DNA pellet was air dried (approximately 15 min at RT) and resuspended in an appropriate volume of ddH_2O or EB buffer.

2.2.19 Total RNA isolation from zebrafish brain tissue

Total RNA was purified using the silica-gel-membrane technology adopted in Qiagen's RNeasy® Midi Kit system. All buffers used were provided by the manufacturer. Adult zebrafish brains were quickly isolated and frozen in liquid nitrogen. 250 mg brain tissue was homogenized in 4 ml buffer RLT with a rotor-stator homogenizer (Kinematica, Luzern, CH) for 60 s at maximum speed. The total RNA was isolated following the manufacturer's protocol. Finally, the total RNA was eluted in 200 µl DEPC-treated water. Integrity of the purified total RNA was assessed by spectrophotometry (scan from λ = 200-350 nm) and agarose electrophoresis under denaturing conditions. RNA samples were stored at -80°C.

2.2.20 Denaturing RNA gel electrophoresis

Denaturating gel electrophoresis of total RNA samples was performed according to standard procedures (Sambrook et al., 1989). Briefly, total RNA (30 µg in a volume of 7 µl) was complemented with 3 µl 10x MOPS and 20 µl F/FA mix. RNA was denaturated by incubating samples for 10 min at 65°C. 3 µl 10x RNA loading buffer were added. A thin, low percentage agarose gel (0.7 % agarose, length 15 cm) containing 0.7 M formaldehyde in 1x MOPS buffer was cast and pre-run for 30 min at 100 mV. Samples were loaded and the gel was run until bromphenol blue had moved 3-4 cm into the gel. The buffer was circulated from anode to cathode every 30min.

MOPS (10x)	RNA loading buffer (10x)
500 mM MOPS	400 g/l sucrose
10 mM EDTA	2 g/l bromophenol blue
pH to 7.5 (with 5 N NaOH)	2 g/l xylene cyanol

F/FA mix
75 % formamide, deionized
25 % formaldehyde (37 % solution)

2.2.21 First strand cDNA synthesis, RT-PCR

For reverse transcription *in vitro*, the RNA-dependent DNA polymerase activity and hybrid-dependent exoribonuclease (RNase H) activity of reverse transcriptase (RT) enzymes were employed to produce single-stranded cDNA from RNA. Routinely, Omniscript™ or SuperScript II™ reverse transcriptases were used to produce first strand cDNA from 50 – 500 ng of total RNA as starting material. After denaturating total RNA samples for 5 min at 65°C, the following reaction was set up by adding the components listed below in a master mix to the RNA solution. The first strand synthesis reaction was incubated for 60 min at 42°C. First strand cDNA was stored at –20°C or directly subjected to PCR.

1x Omniscript™ RT buffer
0.5 mM each dNTP (5mM dNTPs supplied)

0.5 µM oligo dT primer (mostly RoRi dT_{17})
0.2 U/µl Omniscript™ RT (40 U/µl)
0.5 U/µl RNasin® (40 U/µl)
DEPC-treated H_2O to a total volume of 20 µl

2.2.22 *In vitro* transcription

To generate *in vitro* transcribed RNAs, 5-10 µg of plasmid DNA containing the desired insert flanked by a T3, T7 or SP6 polymerase promotor were digested with restriction endonucleases overnight, at positions that were located 3' of the designated RNA polymerase promoter and 3'of the DNA strand to be transcribed. This way, the DNA polymerase transcribed only the strand of interest and no vector-specific sequences. Linearized DNA was purified using the MiniElute™ PCR Purification Kit according to manufacturer's instructions. In order to obtain digoxigenin (DIG)-labeled RNA probes for *in situ* hybridization, transcription of the desired template was performed with Ambion's MEGAscript™ system. For the generation of DIG-labeled RNAs, the DIG-UTP mix shown below was used instead of the NTPs provided by the manufacturer. For double-labeling experiments fluorescein-labeled RNA probes were used to differentiate different mRNAs. In this case reactions were carried out using Fluorescein-12-UTP (Roche, Mannheim, D) instead of DIG-11-UTP.

DIG-UTP mix (10x)
10 mM ATP
10 mM CTP
10 mM GTP
6.5 mM UTP
3.5 mM DIG-11-dUTP (Roche, Mannheim, D)

To generate mRNA for overexpression studies, Ambion's mMESSAGE mMACHINE™ kit was employed. In both cases, 20 µl *in vitro* transcriptions were performed as recommended by the manufacturer. After the incubation time, the template DNA was removed by adding 1 µl DNase, supplied by the manufacturer, to the reaction mix and incubating it for 15 min at 37°C. Generated RNAs were purified by lithium chloride precipitation, analyzed on a denaturating agarose gel and stored at –80°C.

2.2.23 Lithium chloride precipitation

To remove unincorporated proteins and most proteins, MEGAscript™ and mMESSAGE mMACHINE™ reactions were subjected to lithium chloride (LiCl) precipitation. The RNA was precipitated by adding 30 µl nuclease-free water and 30 µl LiCl precipitation solution (each supplied by the manufacturer). The mixture was chilled at -20°C for at least 30 min and centrifuged (15 min, 16000x g, 4°C). The supernatant was removed and the pellet was washed with 1 ml nuclease-free 70% ethanol, re-centrifuged, air dried and resuspended in 20 µl nuclease-free water.

2.3 Biochemical methods

2.3.1 Protein isolation from adult zebrafish brains

The brains of 10 adult zebrafish were homogenized in 1 ml lysis buffer C I with a rotor-stator homogenizer (Kinematica, Luzern, CH) and were subjected to constant rotary motion for 4 h at 4°C. The homogenates were cleared by centrifugating them three times at 12000x g for 30 min at 4°C. Aliquots were stored at -20°C.

Lysis buffer C I
25 mM Tris pH 7.5
1 mM EDTA
1% NP-40
1 Complete™ Protease protease inhibitor cocktail tablet (Roche, Mannheim, D)
total volume: 50 ml

2.3.2 Determination of protein concentration

The protein concentration of cell lysates was determined using the BCA Protein Assay Reagent Kit. Solution A and B were mixed in a ratio of 1:50 and 200 µl of the resulting solution were applied to 10 µl of the cell lysate in microtiter plates and incubated for 30 min at 37°C. BSA standards ranging from 100 µg/ml to 2 mg/ml were co-incubated. The

extinction of the samples was determined in a microtiter plate at 562 nm using an ELISA reader and protein concentrations were determined from their relative extinction compared to BSA standards.

2.3.3 Protein isolation from three day old zebrafish larvae

1 - 2 three day old zebrafish larvae were transfered to 1.5 ml Eppendorf tubes, shock frozen in liquid nitrogen and stored at -80°C until use. Samples were thawed on ice and 1 µl buffer C II was added. The tissue was homogenized in the Eppendorf tube using the glass pestle of a 0.1 ml Micro-Homogenisator (Wheaton, Millville, NJ, USA). The pestle was rinsed in 19 µl 1x SDS sample buffer, which were then added to the homogenate. The samples were mixed, and boiled at 98°C for 5 minutes. Prior to loading on SDS polyacrylamide gels samples were centrifuged for 2 min at 13000 rpm.

Lysis buffer C II
20 mM Tris pH 7.4
0.15 M NaCl
0.5 % NP-40
1 Complete™ Protease protease inhibitor cocktail tablet (Roche, Mannheim, D)
total volume: 50 ml

2.3.4 SDS-polyacrylamide gel electrophoresis (SDS-PAGE)

Separation of proteins was performed by means of the discontinuous SDS polyacrylamide gel electrophoresis (SDS-PAGE) using the Mini-Protean II system (BioRad, München, D). Gel concentrations were 8% for the running gel and 5% for the stacking gel. The heights of running and stacking gel were 4.5 cm and 0.8 cm, respectively. Combs were either for 10 or 15-wells with a thickness of 0.75 mm. After complete polymerization of the gel, the chamber was assembled as described in the manufacturer's protocol. The entire homogenate from one three day old zebrafish was used to load one gel pocket and the gel was run in 1x running buffer at constant voltage of 140 V until the probes had entered the running gel and then at 160 V until the bromphenol blue line had reached the end of the gel. Gels were then subjected to Western blotting.

2.3.5 Western blotting

Proteins were transferred from a SDS gel onto a PROTEAN® Nitrocellulose Transfer Membrane (Schleicher & Schüll, Dassel, D) using the Mini-Protean II system. The blotting sandwich was assembled as described in the manufacturer's protocol. Proteins were transferred electrophoretically in 1x blotting buffer at constant voltage (80 V for 90 min at 4°C). The BenchMark™ Pre-Stained Protein Ladder was used as a molecular weight marker and to control the efficiency of the electrophoretic transfer.

2.3.6 Immunological detection of proteins on nitrocellulose membranes

After electrophoretic transfer, the membrane was removed from the sandwich, placed with the protein-binding site upwards into a glass vessel, washed once in PBST and incubated in blocking buffer for 1 h at room temperature. Afterwards, the primary antibody was added in the appropriate dilution overnight at 4°C. The primary antibody was removed and membranes were washed three times for 10 min with PBST. The appropriate secondary antibody was applied for 1 h at RT. The membrane was washed again three times for 10 min with PBST and immunoreactive bands were visualized using the enhanced chemiluminescence (ECL) detection system.

2.3.7 Immunological detection using enhanced chemiluminescence (ECL)

The immunocomplex composed of nitrocellulose membrane bound protein, primary antibody and secondary antibody coupled with horse-reddish peroxidase (HRP) was detected using the ECL Western Blotting Detection Reagents. The membrane was soaked for 1 min in detection solution (1:1 mixture of solutions I and II). The solution was removed and the blot was placed between two foils. The membrane was exposed to Biomax-MR X-ray film (Kodak, Stuttgart, D) for varying time periods.

2.4 Morphological methods

2.4.1 Microinjection into freshly fertilized zebrafish eggs

Freshly fertilized eggs were harvested and disinfected with 1x HBSS (Invitrogen, Karlsruhe,D) containing 0.5% PFA. Eggs were washed three times with 1x HBSS and arranged in a line in a petri dish containing 2% agarose in 1x PBS. To visualize the amount of injected liquid, 0.5 µl of 5% rhodamine dextran (M_W = 10000) were added to a 3 µl aliquot of morpholino, mRNA, or Danieau solution. A glass micropipette (3 µm, GB 150F-8P, Science Products GmbH, Hofheim, D) was filled with the required solution by capillary force and attached to a micromanipulator. RNA was injected with a Picospritzer (PLI-100, Medical systems Corp., Greenvale, USA) at 6 psi and 90 ms directly into the yolk of 1 - 4 cell staged eggs. Injected eggs were incubated in 1x HBSS at 28.5°C until the desired developmental stage was reached and embryos were subjected to phenotypic analysis.

2.4.2 Whole mount mRNA in situ hybridization (WMISH)

To detect the expression patterns of mRNAs in 16-24 hpf zebrafish embryos, non-radioactive whole mount in situ hybridization was performed. Embryos at the desired developmental stages were deeply anesthetized in 0.1% aninobenzoic acid ethyl methyl ester (MS222, Sigma-Aldrich, Deisenhofen, D), dechorionated and fixed overnight in 4% PFA at 4°C. The following day, the embryos were washed 4 times with PBST and incubated in 100% methanol for 30 min at –20°C. Methanol was removed by subjecting the embryos to a descending methanol series (75, 50 and 25% methanol in PBST). Afterwards embryos were washed twice in PBST. To achieve sufficient penetration of mRNA probes, embryos were digested with 1.4 µg/ml recombinant Proteinase K (Roche, Mannheim, D) in PBST for 10 min at RT, followed by two wash steps in 2 mg/ml glycine in PBST. Embryos were post-fixed in 4% PFA for 20 min at RT and subsequently washed 4 times with PBST to remove residual PFA. Embryos were prehybridized in hybridization buffer at 55°C for at least 3 hours. Hybridization with the DIG-labeled probes occurred at 55°C overnight. DIG-labeled probes were diluted 1:250-1:4000 in hybridization buffer. After hybridization, embryos were washed twice in with 2x SSCT containing 50% formamide for 30 min, followed by a washing step in 2x SSCT for 15 min and two washing steps with 0.2x SSCT for 30 min. All washing steps were executed at 55°C. To prevent unspecific binding of the anti-DIG AP-conjugated antibodies, embryos were

incubated for 30 min in 1% w/v Blocking Reagent (Roche, Mannheim, D) in PBST. Anti-Digoxigenin-AP antibodies (Roche, Mannheim, D) were diluted 1:2000 in Blocking Reagent and applied overnight at 4°C. To remove unbound antibody, embryos were washed 6 times in 1x PBST for 20 min. The washing solution was removed and the signal was developed in the dark with SIGMA FAST™ BCIP/NBT tablets (Sigma-Aldrich, Deisenhofen, D) until the reaction product became visible under a stereomicroscope. Sense probes were developed in parallel under the same conditions as the antisense probes and did not show any labeling. Finally, embryos were washed 3 times in 1x PBS and cleared in an ascending glycerol series (30, 50 and 70% glycerol in 1x PBS). The yolk sack was removed and embryos were mounted in 70% glycerol.

Whole mount hybridisation buffer

5 ml deionized formamide
2.5 ml 20x SSC
10 µl Tween 20
100 µl 100 mg/ml yeast RNA (Sigma Aldrich, Deisenhofen, D)
2.38 ml DEPC-H_2O
10 µl 50 mg/ml heparin

For double labeling with immunohistochemistry SIGMA FAST™ Fast Red TR/Naphthol AS-MX tablets (Sigma-Aldrich, Deisenhofen, D) were used to yield a red precipitate. The sense probes served as negative controls and did not show a signal.

Double in situ hybridization was performed with the NRP1a probe labeled with fluorescein and the islet-1/-2 probes labeled with digoxygenin according to previously published protocols (Jowett, 2001). Embryos were simultaneously incubated with the probes and sequentially detected with Anti-Fluorescein-AP (Roche, Mannheim, D) and Anti-Digoxygenin-AP antibodies. NRP1a probes were developed with SIGMA FAST™ Fast Red TR/Naphthol AS-MX tablets and, after inactivation of the alkaline phosphatase with 0.1 M glycine-HCl, 0.1% Tween 20, pH 2.2, islet-1/-2 probes were developed with SIGMA FAST™ BCIP/NBT tablets. Specificity of the labeling was tested by omitting the islet probes, which did not yield a brown precipitate.

2.4.3 mRNA in situ hybridization (ISH) on cryosections

To perform non-radioactive detection of mRNAs, 14 µm sections were cut from fresh-frozen tissue on a cryostat and mounted on glas slides. The sections were fixed in 4% PFA overnight. The next day, sections were washed 3 times in 1x PBS, treated with 0.1 M HCl for 20 min, acetylated in 0.1 M triethanolamine containing 0.25% acetic anhydride and dehydrated in an ascending ethanol series. Finally, sections were air dried and prehybridized for 3 hours at 37°C with hybridization mix. Hybridization with the DIG-labeled probes occurred at 55°C overnight in humid chambers. DIG-labeled probes were diluted 1:250 - 1:4000 in hybridization buffer. After hybridization, sections were washed twice in 0.2x SSC at 55°C, followed by three washing steps in 0.2x SSC containing 50% formamide (each 90 minutes at 55°C). To prevent unspecific binding, sections were incubated in blocking buffer for 30 min before Anti-Digoxigenin-AP antibodies (Roche, Mannheim, D), diluted 1:2000 in blocking buffer, were applied overnight at 4°C. To remove unbound antibody, sections were washed twice in DIG-buffer 1 for 15 min. The washing solution was removed and the sections were equilibrated for 5 min with DIG-buffer 3. The signal was developed in the dark with DIG-buffer 3 containing 0.35 g/l 4-nitroblue tetrazolium chloride (NBT, Roche, Mannheim, D), 0.175 g/l 5-bromo-4-chloro-3-indolyl phosphate (BCIP, Roche, Mannheim, D) and 0.25 g/l levamisole (Sigma-Aldrich, Deisenhofen, D) until signals became visible under a stereomicroscope. Sense probes, developed in parallel under the same conditions as the antisense probes, did not show any labeling. Finally, sections were washed in 1x PBS and coverslipped.

Hybridisation buffer	10x “Grundmix”
25 ml deionized formamide	2 ml 1 M Tris pH 7.5
5 ml 10x “Grundmix”	200 µl 0.5 M EDTA
3.3 ml 5M NaCl	2 ml 50x Denhardt’s solution
2.5 ml 2M DTT	2 ml tRNA (25 mg/ml)
4.7 ml DEPC-H_2O	1 ml poly A^+-RNA (10 mg/ml)
10 ml dextransulfate	2.8 ml DEPC-H_2O
DIG-buffer 1	Blocking buffer
100 mM Tris	1% (w/v) Blocking Reagent
150 mM NaCl	0.5% (w/v) BSA
pH 7.5	in DIG-buffer 1

DIG-buffer 3

10 mM $MgCl_2$

100 mM Tris

100 mM NaCl

pH 9.5

2.4.4 Whole mount immunohistochemistry (WMIHC)

To detect the expression patterns of proteins in 16-24 hpf zebrafish embryos, whole mount immunohistochemistry was performed. The chorions of animals at the desired developmental stages were removed and yolks were opened using two fine forceps. Afterwards, embryos were fixed in 4% PFA containing 1% (v/v) DMSO for 45 min at RT. Embryos were washed in 1x PBS and incubated with blocking buffer to prevent unspecific binding of the primary antibody for 30 min at RT. Primary antibodies were diluted in blocking buffer and applied to the embryos overnight at 4°C. Unbound primary antibody was removed by three washing steps with 1x PBS for 15 min each. To visualize primary antibodies, fluorescence- or HRP-labeled secondary antibodies were diluted 1:200 in blocking buffer and applied to the embryos overnight at 4°C. Unbound secondary antibody was removed by three washing steps with 1x PBS for 15 min each. To visualize the HRP signals, embryos were incubated in 0.5 mg/ml diaminobenzidine in 1x PBS for 20 min at 4°C. The brownish precipitate was developed by adding 1/10 volume of a 0.035% H_2O_2 solution in 1x PBS. After 5 - 10 min, the staining solution was removed, embryos were washed 3 times in 1x PBS and cleared in an ascending glycerol series (30, 50 and 70% glycerol in 1x PBS). Embryos were mounted in 70% glycerol.

2.4.5 Microangiography

Microangiography was performed as previously described (Lee et al., 2002; Goishi et al., 2003). Briefly, FITC-dextran (Sigma-Aldrich, Deisenhofen, D) in 75 mM NaCl solution was injected into the sinus venosa, which results in labeling of the entire vascular system. For fluorescent microscopy, a FITC filter was used. Zebrafish embryos were visualized with an Olympus SZX12 stereomicroscope and photographed using an Olympus DP11 digital camera. These experiments were carried out by Michael Klagsbrun’s group at the Children's Hospital and Harvard Medical School, Boston, USA.

2.4.6 Quantitative analysis of trunk ventral motor growth

Anti-tubulin labeled peripheral nerves were analyzed in whole-mounted 24 hpf embryos. Only the ventral motor nerve was clearly visible at this stage, because the dorsal motor nerve was obscured by the underlying spinal cord and no axons had grown into the specific pathway of the medial motor nerve at that stage. Only the rostral 12 pairs of motor nerves were scored, because all of these had grown beyond the ventral edge of the notochord into the ventral somite in uninjected embryos at 24 hpf. Trunk hemisegments were scored as abnormal when nerves were branched at or above the ventral edge of the notochord. This is to exclude naturally occurring branching that is sometimes observed ventral to the notochord. We also scored trunk hemisegments as abnormal when nerves were truncated (i.e. did not grow beyond the horizontal myoseptum), more than one anti-tubulin immunolabeled axon fascicle exited the spinal cord (multiple exits) and when tubulin immunopositive cells were present in the ventral motor pathway. Embryos were scored as affected by the respective phenotypes when more than one of 24 nerves were aberrantly branched or truncated, and at least one of 24 hemisegments showed multiple exits of nerves or anti-tubulin positive cells in the ventral somite. Embryos were scored as severely affected by branching when more than two of the motor nerves were aberrant. For each treatment at least two and for most treatments three or more experiments were performed. Values for affected embryos are given as mean ± standard error of the mean (SEM). Statistical analyses were done using Fisher's exact test.

2.5 Cloning and analysis of plexinA3

To identify predicted genes, partially cloned sequences were subjected to a BLAST/SSAHA search of the zebrafish genome using the Ensembl Zebrafish Genome Browser (http://www.ensembl.org/Danio_rerio/). Homology searches were performed using BLAST (Altschul et al., 1990) located at http://www.ncbi.nlm.nih.gov/BLAST/. Alignments of the deduced amino acid sequences of the novel plexinA3 gene were done using the ClustalW method implemented in the BioEdit suite available through http://www.mbio.ncsu.edu/BioEdit/bioedit.html. The modular architecture of the protein was predicted by searching the Protein Families Database of Alignments and Hidden Markov Models (Bateman et al., 2000)

and the transmembrane domain was predicted using the TransMembrane Hidden Markov Model (TMHMM) algorithm (Sonnhammer et al., 1998).

3 RESULTS

3.1 NRP1a is expressed in trunk motor neurons

Zebrafish NRP1a was first described as a molecule involved in angiogenesis (Lee et al., 2002). Expression was found in cell clusters in the ventral spinal cord which appeared to be motor neurons (Lee et al., 2002; Yu et al., 2004; Bovenkamp et al., 2004; Martyn and Schulte-Merker, 2004). To confirm these findings, expression of NRP1a mRNA was analysed in the trunk during the outgrowth of motor axons by in situ hybridization. Digoxigenin (DIG)-labeled sense and antisense probes for NRP1a mRNA were generated from a plasmid containing the full length gene (Lee et al., 2002; gift from Michael Klagsbrun) using the MEGAscript™ system according to the manufacturer's instructions and in situ hybridization was performed in 16 hpf and 24 hpf embryos.

At 16 hpf, embryos show conspicuous expression of NRP1a mRNA in small clusters of cells at the ventral edge of the spinal cord consistent with the position of primary motor neurons in the trunk. There was also expression in the dorsal aspect of the spinal cord, in the hypochord and in putative angioblasts in the ventral somite (Shoji et al., 2003) (Fig. 6).

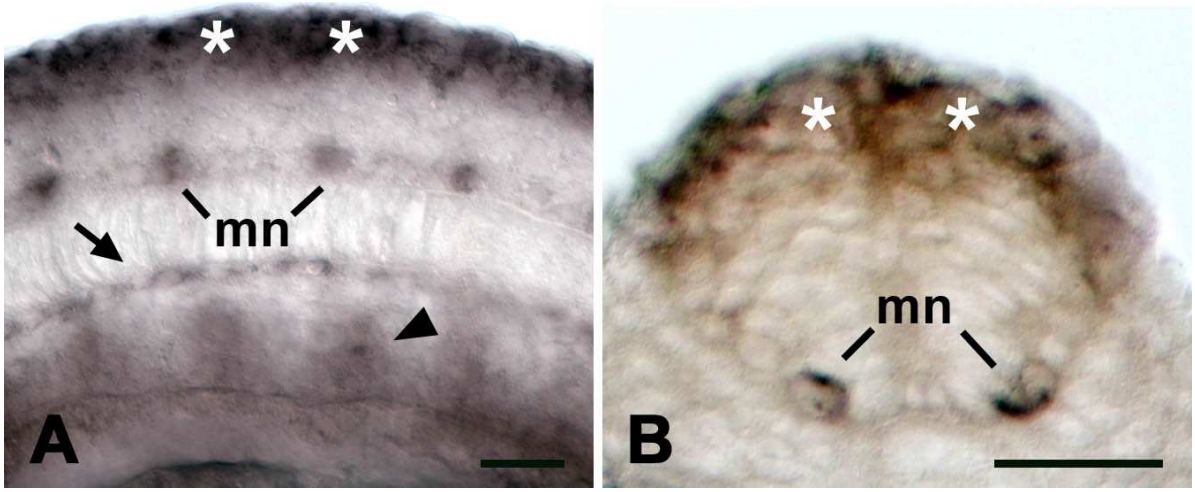

Fig. 6 Expression of NRP1a in the trunk of embryonic zebrafish at 16 hpf. A: In a lateral view of a whole-mounted 16 hpf embryo at mid-trunk level (rostral is left) NRP1a mRNA is expressed in the dorsal spinal cord (asterisks), in motor neurons (mn) and in the hypochord (arrow). Arrowhead indicates expression in putative angioblasts. B: In a cross section through the trunk at 16 hpf, expression is obvious in the dorsal spinal cord (asterisks) and the motor neurons (mn). Bar in A = 25 µm; bar in B = 25 µm.

At 24 hpf, expression of NRP1a mRNA in the position of motor neurons was strongest in the youngest, most caudal trunk segments. This indicates a developmental down-regulation of NRP1a mRNA in more mature rostral trunk segments. Expression in the dorsal spinal cord and in the ventral somite was strongly reduced at 24 hpf (Fig. 7A). Hybridization with sense probes did not yield any signal (Fig. 7B).

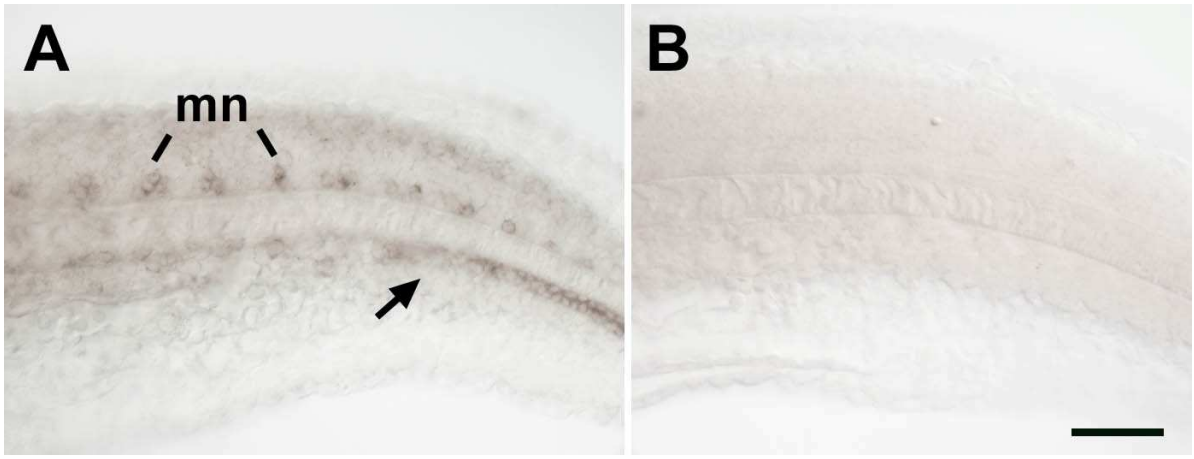

Fig. 7 Expression of NRP1a in the trunk of embryonic zebrafish at 24 hpf. A: In a lateral view of the caudal trunk of a 24 hpf embryo, expression of NRP1a is reduced in the dorsal spinal cord, but is still strong in motor neurons (mn) and in a forming blood vessel (arrow). B: In situ hybridization with an NRP1a sense mRNA probe did not yield a signal (age and orientation as in A). Bar in B = 50 µm for A and B.

To directly demonstrate that expression of NRP1a mRNA in the ventral spinal cord occurred in primary motor neurons, NRP1a mRNA was double labeled together with probes for islet-1, a marker for RoP and MiP (Inoue et al., 1994), and islet-2, a marker for CaP and VaP (Appel et al., 1995; Tokumoto et al., 1995) by in situ hybridization. This goes beyond previous studies in which motor neurons were identified only by position (Lee et al., 2002; Yu et al., 2004; Bovenkamp et al., 2004; Martyn and Schulte-Merker, 2004). Islet-1 and islet-2 probes have been described (Tokumoto et al., 1995). Both probes were applied simultaneously and developed in brown to label all primary motor neurons. Developing the NRP1a signal in the same embryos (n = 19) in red yielded double labeled cells, with no cells detectable that were only labeled in red (Fig. 8D). Omitting the islet probes as a negative control yielded only cells labeled in red (Fig. 8A, n = 17 embryos). Thus NRP1a is expressed only in primary motor neurons in the ventral spinal cord. The NRP1a signal (red) appeared to be weaker in the most rostral islet-1/-2 labeled cell, suggesting lower expression of NRP1a in RoP. This was also

found when NRP1a was labeled together with islet-1 alone (n = 15). As expected, there were cells caudal to the double labeled cells that were only labeled for NRP1a (Fig. 8B). These were probably CaP and VaP, the most caudal primary motor neurons, which are not labeled by the islet-1 probe. Conversely, double labeling of NRP1a with islet-2 alone (n = 17) yielded double labeled cells and cells that were only labeled for NRP1a rostral to the double labeled cells (Fig. 8C). This is because islet-2 only labels CaP and VaP, but not the two most rostral primary motor neurons RoP and MiP.

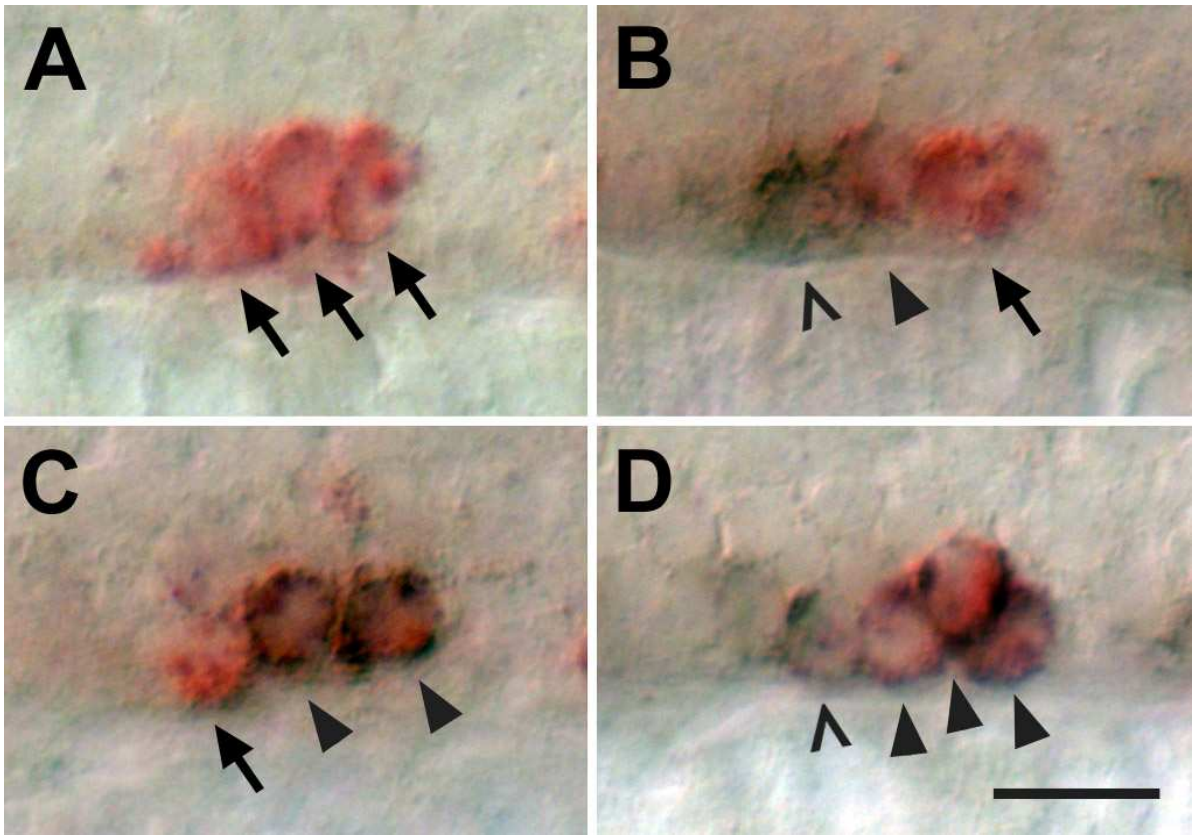

Fig. 8 Double labeling of NRP1a (red) and islet-1/-2 (brown) mRNAs at 24 hpf. Lateral trunk views are shown, rostral is left. In A, the islet probes were omitted. In B, the NRP1a probe was combined with the islet-1 probe and in C with the islet-2 probe. In D, the NRP1a probe was combined with both probes. Arrows indicate cells labeled in red only (NRP1a). Arrowheads indicate double labeled cells and open arrowheads cells labeled only in brown (islets). Bar in D = 12.5 µm for A-D.

Double labeling of NRP1a mRNA and tubulin protein showed a close apposition of ventral motor nerves to the NRP1a positive somata, further demonstrating that NRP1a positive cells are motor neurons (Fig. 9). Taken together, these results suggest expression of NRP1a in VaP, CaP, MiP and to lower levels in RoP.

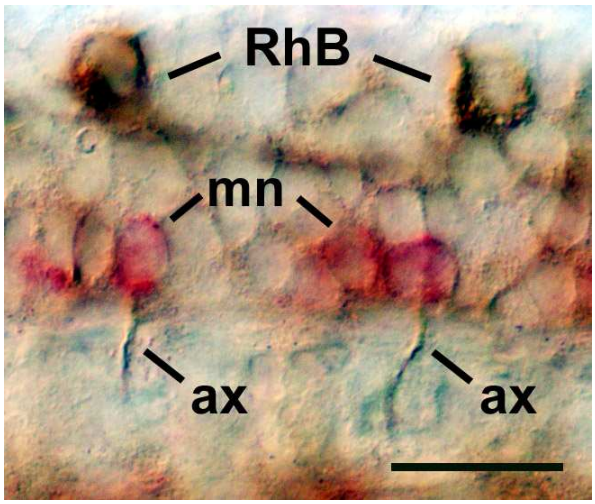

Fig. 9 Double-labeling of motor neuron somata and axons in zebrafish embryos at 24 hpf. A lateral view of a whole-mounted 24 hpf embryo is shown at caudal trunk level. NRP1a mRNA is labeled in red and tubulin protein in brown. Anti-tubulin immunopositive motor axons (ax) can be seen to emerge from NRP1a mRNA labeled motor neurons (mn). Rohon-Beard neurons (RhB) are labeled by the anti-tubulin antibody, but not by the NRP1a in situ hybridization probe. Bar = 25 µm.

3.2 Expression of putative NRP1a ligands and other co-receptors

Sema3A2, one of the two Sema3A homologs in zebrafish, is a putative ligand for NRP1a and/or plexinA3. The probe for detecting Sema3A2 has been described (Roos et al., 1999). Similar to NRP1a, sema3A2 was also most strongly expressed in caudal trunk segments, where it was found in the posterior half of each somite (Roos et al., 1999) (Fig. 1F).

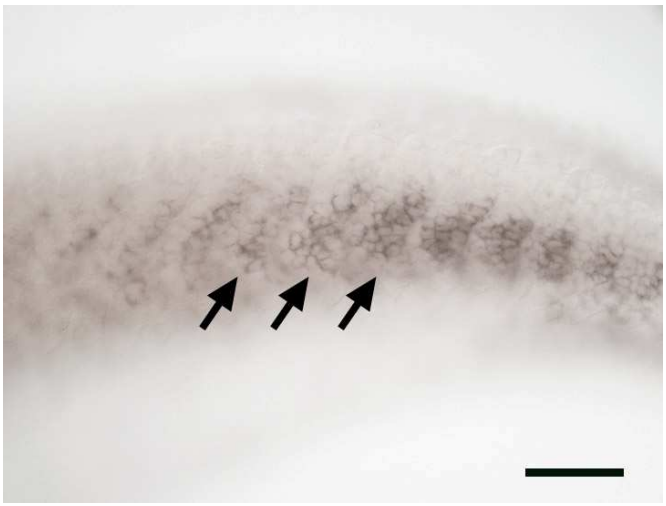

Fig. 10 Expression of sema3A2 in the trunk of embryonic zebrafish at 24 hpf. A: In a lateral view of the caudal trunk of a 24 hpf embryo (rostral is left), Sema3A2 is expressed in the caudal half of trunk myotomes (arrows). Bar = 50 µm.

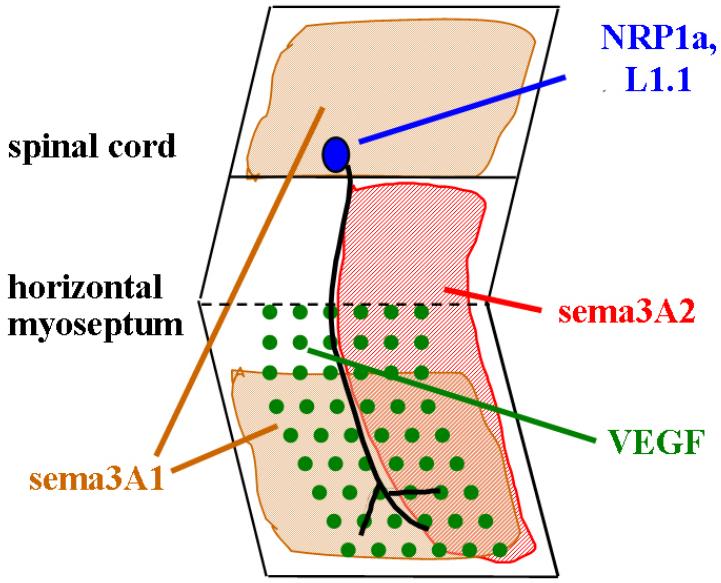

Fig. 11 Expression patterns of the receptor components NRP1a and L1.1 (blue) and their potential ligands sema3A1 (orange), sema3A2 (red) and VEGF (green) are summarized for CaP in one trunk hemisegment.

Other putative NRP1a ligands, such as sema3A1 and VEGF are also expressed during the outgrowth of primary motor axons (Fig. 11). Sema3A1 mRNA is located in the dorsal and ventral somite, with a gap of expression at the horizontal myoseptum (Shoji et al., 1998) and VEGF mRNA is found in the ventromedial somite (Liang et al., 1998). L1.1, one of the two L1 homologs in zebrafish and a putative co-receptor for NRP1a, is expressed in primary motor neurons (Tongiorgi et al., 1995) (Fig. 11).

3.3 Morpholinos to NRP1a induce errors in the growth of primary motor axons

To analyze the function of NRP1a in motor axon outgrowth, the expression of NRP1a was reduced by specific morpholinos. The efficiency of NRP1a morpholino1 (Lee et al., 2002), has previously been demonstrated. Labeling of ventral motor nerves with an antibody to tubulin at 24 hpf revealed three major types of aberrations in the growth of these nerves after application of 1mM NRP1a morpholino1 (Fig. 12).

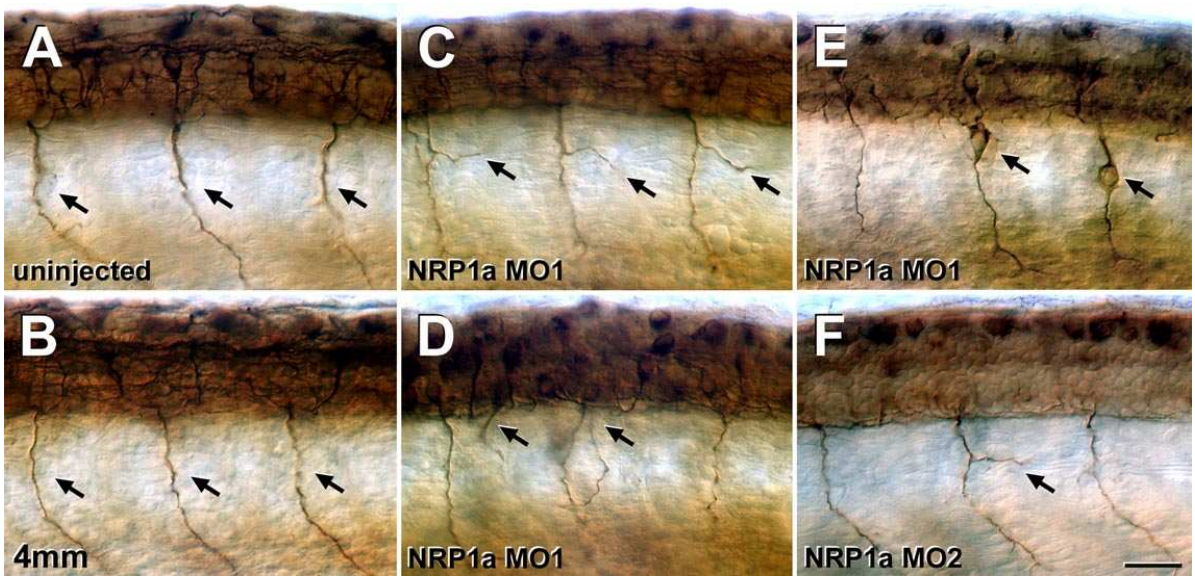

Fig. 12 NRP1a morpholinos induce aberrations of primary motor nerves. A-F: Lateral views of anti-tubulin labeled whole-mounted 24 hpf embryos at mid-trunk levels are shown (rostral is left). In uninjected embryos (A) or those injected with 1 mM NRP1a 4mm morpholino (4mm, B), single unbranched motor nerves (arrows in A,B) grow ventrally out of the spinal cord. Injection of 1 mM NRP1a morpholino1 induced branching (arrows in C), a second exit point for motor axons per hemisegment (arrows in D) or anti-tubulin labeled cells that appear to have migrated out of the spinal cord along the pathway of the ventral motor nerve (arrows in E). Injection of 1 mM NRP1a morpholino2 also induced aberrant branching (arrow in F) of the ventral motor nerve. Bar in F = 25 µm for A-F.

Embryos (n = 53) were affected by aberrant branching of ventral motor nerves (79.4% affected embryos, $P < 0.0001$ against all controls), multiple exits points of ventral motor nerves (77.6% affected embryos, $P < 0.0001$ against all controls), or ventrally displaced neuronal somata (63.4% affected embryos, $P < 0.0001$ against all controls), compared to 7.9%, 7.9% and 13.9% for the respective phenotypes in controls injected with a morpholino in which 4 bases were mismatched (1 mM NRP1a 4mm morpholino, n = 64, Table 2). Percentages of embryos with aberrations differed also significantly from those in uninjected embryos, in embryos injected with a standard control morpholino at 2 mM and in embryos injected with buffer for all phenotypes (Table 2). Taking all three phenotypes together, 35.1% (438 of 1247) analyzed hemisegments in 53 embryos were abnormal.

3.4 Phenotypes after injection of 1mM NRP1a morpholino1

3.4.1 Aberrant branching

Instead of growing ventrally from the spinal cord as a single nerve towards the ventral myotome in an unbranched way (Fig. 12A,B), 40.7% of the nerves in affected hemisegments were aberrantly branched (Fig. 12C). Most of these branches (69.6%) were directed caudally. This nerve branching could be due to axonal branching with one axonal branch remaining on the midsegmental pathway, or due to one of the primary motor axons taking an aberrant course. Rostrally (20.2%) and bilaterally (10.2%) branched nerves were observed less frequently. On average, 4.2 ± 0.4 (SEM) hemisegments/embryo had aberrant branches in affected embryos.

3.4.2 Mutiple exit points of ventral motor nerves

Instead of exiting the spinal cord only in one position in the middle of each hemisegment, nerves in 35.6% of the affected hemisegments showed mostly one additional exit point, with a nerve of variable length growing ventrally (Fig. 12D). This second nerve either ran parallel to the main nerve or joined it at variable positions on the somite. In those segments in which the segment borders could be visualized in differential interference contrast, it was possible to determine where additional nerve exit points were located. Most of the additional exit points were found in the posterior half of the somites (74.7%), 22.4% were located in the anterior half of the somite and 2.9% of the hemisegments had additional exit points rostral and caudal to the midsegmental pathway. On average, 3.7 ± 0.4 hemisegments/embryo showed multiple exits in affected embryos.

3.4.3 Ventrally displaced neurons

In several of the affected hemisegments (18.7%), anti-tubulin positive neuronal somata were found in the midsegmental pathway outside the spinal cord in contact with the nerve (Fig. 12E). This was almost never observed in controls (1 displaced cell in 84 uninjected embryos). Most of these cells were dorso-ventrally elongated along the nerve, giving the impression of

having migrated out of the spinal cord along the nerve. On average, 2.5 ± 0.3 hemisegments/embryo showed ventrally displaced neurons in affected embryos.

Truncations were rare, amounting to 5.0% of all aberrations. This corresponds to 6.3% ± 3.0% affected embryos, which was not significantly different from uninjected controls (1.8% ± 1.2%; $P > 0.05$).

3.5 The effect of NRP1a morpholino1 was dose-dependent

Injecting increasing concentrations of NRP1a morpholino1 revealed a dose-dependent effect of the morpholino on aberrant motor axon growth. Results are summarized in Table 2.

Table 2 Morpholinos to NRP1a induce aberrant ventral motor nerve growth.

Injection type	n	Embryos with aberrant ventral motor nerve branching (%)	Embryos with multiple exits of ventral motor nerves (%)	Embryos with displaced neurons (%)
Uninjected	96	6.5 ± 3.4	2.3 ± 1.1	1.4 ± 1.4
Vehicle	41	4.8 ± 4.8	2.4 ± 2.4	0.0 ± 0.0
Standard control MO (2 mM)	54	4.8 ± 4.8	1.6 ± 1.6	3.2 ± 1.6
NRP1a 4mm MO (1 mM)	65	7.9 ± 3.2	7.9 ± 3.2	13.9 ± 6.2
NRP1a MO1 (0.1 mM)	70	18.0 ± 3.7	11.0 ± 4.7	9.8 ± 7.6
NRP1a MO1 (0.25 mM)	34	17.9 ± 2.1	27.0 ± 20.4 **	17.9 ± 2.1
NRP1a MO1 (0.5 mM)	178	50.5 ± 7.2 ***	60.5 ± 6.4 ***	56.8 ± 5.5 ***
NRP1a MO1 (1 mM)	53	79.4 ± 6.2 ***	77.6 ± 3.9 ***	63.4 ± 8.9 ***
NRP1a MO2 (0.25 mM)	38	12.8 ± 7.2	13.1 ± 1.9	5.0 ± 5.0
NRP1a MO2 (1 mM)	53	50.6 ± 4.9 ***	12.6 ± 4.0	5.6 ± 5.6
NRP1a MO2 (2 mM)	69	35.6 ± 14.4 ***	21.7 ± 0.5*	2.9 ± 0.1

Morpholino doses are indicated in brackets. n = numbers of embryos analyzed. MO = morpholino, NRP1a MO1/MO2: morpholino1/2 against NRP1a, NRP1a 4mm MO: morpholino with 4 mismatched bases based on NRP1a morpholino1, * = $P < 0.05$, ** = $P < 0.01$, *** = $P < 0.001$ (Fisher's Exact Test) tested against all controls.

NRP1a morpholino1 had no significant effect on ventral motor nerve branching at 0.1 mM and 0.25 mM (18.0% and 17.9% affected embryos, n = 70 and n = 34, respectively), but significantly increased the number of embryos with aberrant ventral motor nerve branching at

0.5 mM (50.5%, n = 178, P < 0.0001 against all controls) and 1 mM (see above), compared to uninjected controls (6.5% affected embryos, n = 96), buffer injected embryos (4.8% affected embryos, n = 41), embryos injected with standard control morpholino at 2 mM (4.8% affected embryos, n = 54) and embryos injected with NRP1a 4mm morpholino at 1 mM (7.9% affected embryos, n = 65). Multiple exits of ventral motor nerves were significantly increased at 0.25 mM (27.0% affected embryos, P < 0.01 against all controls), at 0.5 mM (60.5% affected embryos, P < 0.0001 against all controls) and 1 mM (see above), but not at 0.1 mM (11.0% affected embryos) compared to all controls (2.3% of uninjected embryos, 2.4% of embryos injected with vehicle, 1.6% of embryos injected with 2 mM standard control morpholino and 7.9% of embryos injected with 1 mM NRP1a 4mm morpholino). At 0.1 mM and 0.25 mM, displaced neurons were found in 9.8 % and 17.9% of the embryos respectively, which was not significantly more than in all controls (uninjected: 1.4%, vehicle injected: 0%, standard control morpholino injected: 3.2% and NRP1a 4mm morpholino injected: 13.9%), whereas at concentrations of 0.5 mM and 1 mM, the frequency of this phenotype was significantly increased to 56.8% (P < 0.0001 against all controls) and 63.4% of the embryos, respectively.

3.6 A second morpholino to NRP1a induces similar phenotypes in a dose-dependent manner

A second morpholino to NRP1a (NRP1a morpholino2) of non-overlapping sequence with morpholino1 also induced aberrant ventral motor nerve branching (Fig. 12) and additional exits of ventral motor nerves, but not displaced neurons (Table 2). At 0.25 mM, NRP1a morpholino2 was ineffective with 12.8% of embryos (n = 38) showing aberrant ventral motor nerve branching and 13.1% of embryos showing multiple exits of ventral motor nerves. At 1 mM, 50.6% of the embryos were affected by aberrant ventral motor nerve branching (n = 53), which was significantly more than in all controls (P < 0.0001 against all controls). This percentage was not increased by a higher concentration of 2 mM (35.6%, n = 69, P < 0.001 against all controls). The frequency of multiple exits of ventral motor nerves was not significantly different from all controls at 1 mM (12.6%), but at 2 mM (21.7%, P < 0.05

against all controls). Thus, NRP1a morpholino2 confirmed most of the effects of NRP1a morpholino1 on motor axon growth, but was less effective than NRP1a morpholino1.

3.7 Overexpression of NRP1a mRNA

3.7.1 Generation of a NRP1a mRNA overexpression construct

RNA overexpression leads to an ectopic expression of the desired protein in almost every cell of the developing embryo. Cells, which normally do not express the gene of interest e.g. a receptor for repulsive guidance cues are forced to express this gene and their axons may respond to their environment in a way that differs from wildtype embryos thereby giving insights into the protein's function, for example see (Shoji et al., 1998). Furthermore, cells which normally express the designated gene are forced to synthesize higher amounts of the protein which also can give information about the protein's function. Last but not least the presence of an exogeneous mRNA can compensate the knockdown effects of a morpholino and thus rescue the phenotypes cause by the morpholino.

An overexpression vector containing the full length sequence of NRP1a was generated in the following manner. Total brain polyA mRNA was isolated and reverse transcribed with an oligodT primer. Proofreading PCR was performed using the polymerase Advantage^{TM}-2 and primers NRP1ClaI low and NRP1ClaI up. The obtained product was inserted into the ClaI site of the overexpression vector pCS2+MT (Rupp et al., 1994), in frame with a C-terminal myc-tag. In vitro synthesis of capped mRNA from the linearized pCS2+MT-NRP1a construct was carried out using Ambion's mMessage mMachine^{TM} and polyA tailing kits. The mRNA was precipitated with $LiCl_2$ and the RNA concentration was determined spectrophotometrically. Concentrations between 1 and 2 µg/µl were used for injections.

3.7.2 Overexpression of NRP1a mRNA has no effect on motor axon outgrowth

Expression of myc-tagged NRP1a protein translated from the injected mRNA was demonstrated by immunohistochemistry (Fig. 13A,B). The outlines of individual cells were most strongly labeled, suggesting that the exogenous protein was associated with the plasma membrane. With progressing development, less protein was detectable. The protein was

detected at 5 hpf in 16 of 17 embryos, at 16 hpf in 7 of 10 embryos, at 18 hpf in 3 of 10 embryos and at 24 hpf in 1 of 19 embryos. The mRNA was expressed throughout the embryos in a mosaic pattern i.e. the mRNA was not expressed in all cells (Fig. 13A). This is commonly observed with this type of mRNA overexpression study (McWhorter et al., 2003).

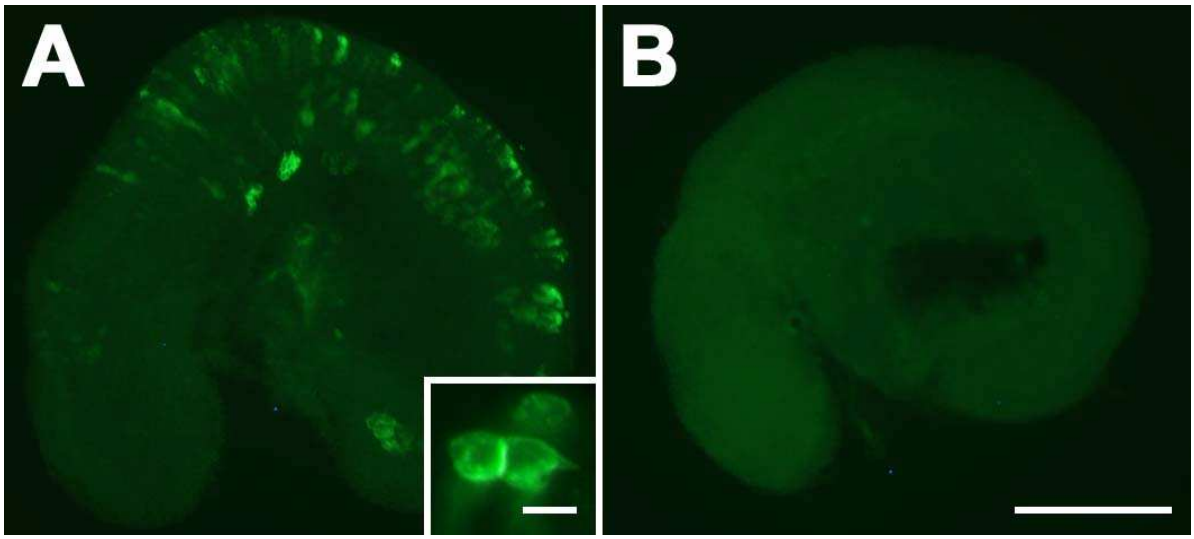

Fig. 13 Overexpression of NRP1a mRNA. A,B: In lateral views of 16 hpf whole-mount embryos (rostral is left, dorsal is up; yolk sac has been removed) myc-tagged NRP1a mRNA is expressed in a mosaic pattern (A). No signal is observed in uninjected animals (B). The insert in A shows that outlines of cells are most prominently labeled, suggesting membrane-associated expression of the exogenous protein. Bar in B = 250 µm for A,B; bar in inset = 10 µm.

Analyzing motor axon outgrowth with anti-tubulin immunolabeling in 24 hpf embryos indicated that injection of the NRP1a mRNA alone had no significant effect on the growth of ventral motor nerves in the trunk (10.4% of NRP1a mRNA injected embryos displayed branched nerves vs. 6.5% in uninjected controls; 7.7% NRP1a mRNA injected embryos had multiple exits of motor nerves vs. 2.3% in uninjected controls; 0% of NRP1a mRNA injected embryos had displaced neurons vs. 1.4% in uninjected controls; n = 36 NRP1a mRNA injected embryos).

3.7.3 The effect of NRP1a morpholinos can be partially rescued by NRP1a mRNA overexpression

To show the specificity of the observed effects of morpholinos to NRP1a, NRP1a mRNA and NRP1a morpholino1 were co-injected to rescue the morpholino induced phenotype. Paired experiments, in which 0.5 mM NRP1a morpholino1 was injected either alone or in combination with the NRP1a mRNA, were performed. NRP1a morpholino1 is not complementary to the sequence of the overexpression construct and can, thus, only bind to endogenous NRP1a mRNA.

Table 3 Overexpression of NRP1a mRNA partially rescues the motor axon phenotype.

Injection type	n	Embryos with severe aberrant ventral motor nerve branching (%)	Embryos with multiple exits of ventral motor nerves (%)	Embryos with displaced neurons (%)
NRP1a MO1 (0.5 mM)	133	42.3 ± 6.8	65.9 ± 6.0	62.9 ± 5.1
NRP1a MO1 (0.5 mM) + NRP1a mRNA	140	34.1 ± 6.2 *	46.5 ± 4.0 ***	40.3 ± 5.1 ***

Morpholino doses are indicated in brackets. n = number of embryos analyzed, NRP1a MO1: morpholino1 against NRP1a, * = $P < 0.05$, *** = $P < 0.001$ (Fisher's Exact Test).

In these experiments, the proportion of affected animals was significantly reduced for severe aberrant branching (> 2 branched nerves per animal: 42.3% affected animals with NRP1a morpholino1 vs. 34.1% in co-injected animals, $P = 0.023$), for multiple exits (65.9% in NRP1a morpholino1 injected vs. 46.5% in co-injected animals, $P < 0.0001$) and for displaced neurons (62.9% in NRP1a morpholino1 injected vs. 40.3% in co-injected animals, $P = 0.0002$) (Table 3). Thus, all three observed motor axon phenotypes in NRP1a morpholino1 injected animals could be partially rescued by overexpression of NRP1a mRNA.

3.7.4 NRP1a morpholino2 efficiently suppresses detectability of the myc-tagged NRP1a mRNA

The sequence of NRP1a morpholino2 overlaps with the NRP1a overexpression construct. Therefore the activity of the morpholino could be tested by co-injecting NRP1a mRNA and

morpholino2 followed by immunohistochemistry using an anti-myc antibody. Co-injection of NRP1a mRNA with 0.5 mM NRP1a morpholino2 suppressed detectability of the myc epitope in 23 out of 25 embryos (Fig. 14C), whereas injection of the overexpression construct alone led to detectability of the myc epitope in 20 out of 20 embryos at 5 hpf (Fig. 14B). Uninjected embryos did not show any myc-labeling (n = 16, Fig. 14A). Thus, NRP1a morpholino2 binds to the injected NRP1a mRNA and suppresses its translation.

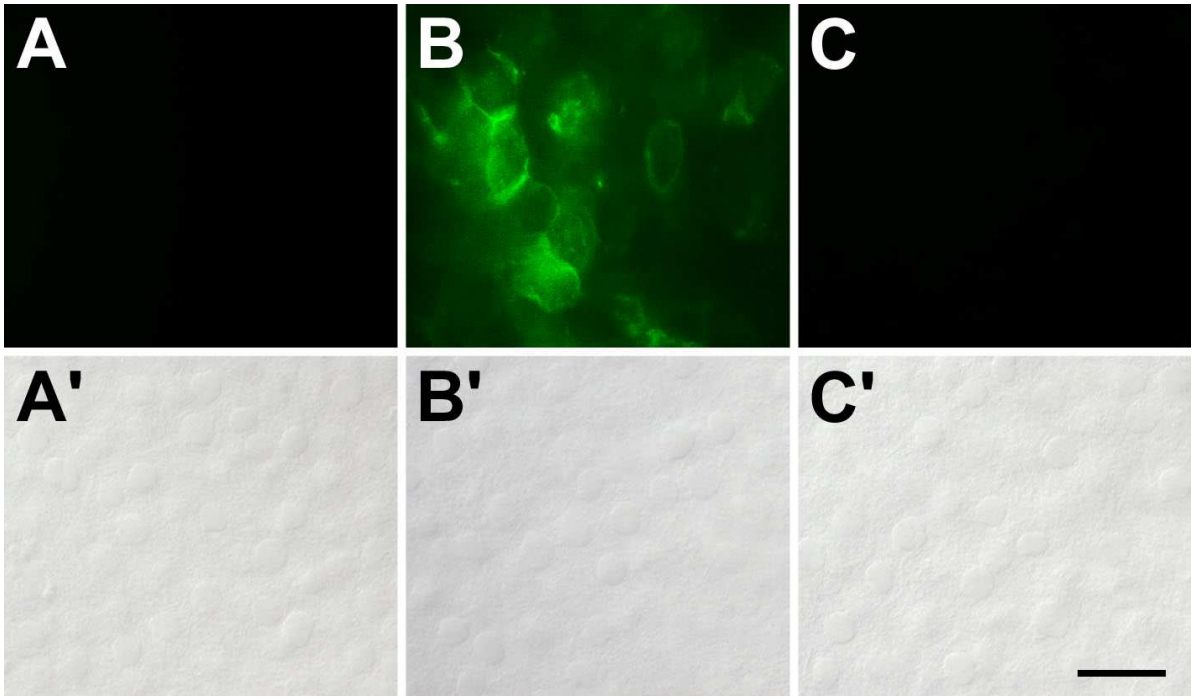

Fig. 14 Expression of myc-tagged NRP1a mRNA is blocked by NRP1a morpholino2. A,B,C: Myc-labeling of cells in zebrafish at 5 hpf. A',B',C': Phase contrast of the corresponding section. No signal is observed in uninjected animals (A,A'). Myc-tagged NRP1a mRNA is detectable after injection of NRP1a mRNA (B,B'), but not after co-injection of NRP1a mRNA and NRP1a morpholino2 (C,C'). Bar in C' = 25 µm for A-C'.

3.8 Trunk structures and other axon trajectories appeared unaffected in NRP1a morpholino treated embryos

To exclude that the effect of the morpholino treatment was secondary to possible alterations of trunk morphogenesis, several structures were labeled after application of 1 mM NRP1a morpholino1, which had the strongest effect on ventral motor nerves, and patterns were compared with those in uninjected embryos.

The notochord, which underlies the pathway of ventral motor axons, and the spinal floor plate were labeled with antibodies to chondroitin sulfates (Bernhardt and Schachner, 2000) and appeared normal (Fig. 15A,B; n = 22 NRP1a morpholino1 injected embryos).

In double labeling experiments, vertical myosepta, labeled with antibodies to tenascin-C (Bernhardt et al., 1998; Schweitzer et al., 2005), appeared normal in segments in which motor axons, labeled with anti-HNK-1 antibodies, grew aberrantly (Fig. 15C,D; n = 6 NRP1a morpholino1 injected embryos).

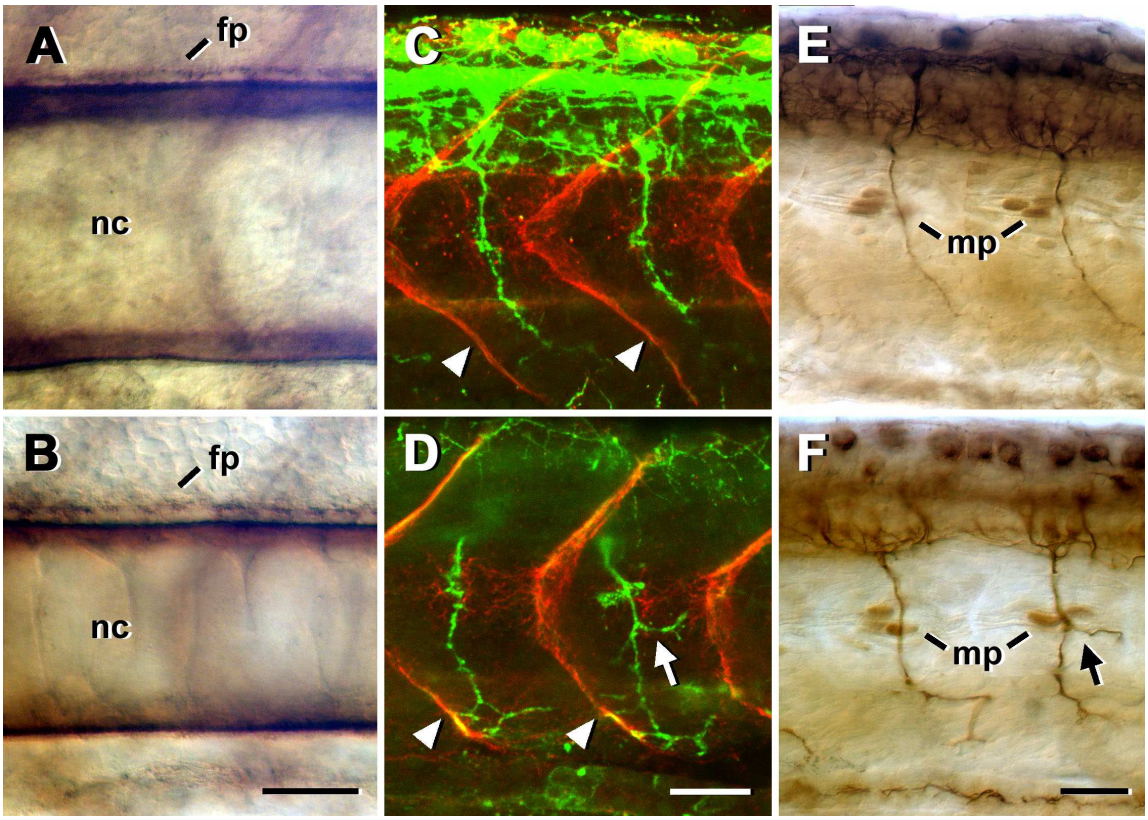

Fig. 15 Trunk structures appear normal after injection of 1 mM NRP1a morpholino1. Lateral views of whole-mounted 24 hpf embryos at mid-trunk levels are shown (rostral is left). Notochord (nc) and spinal floor plate (fp), labeled with an anti-chondroitin sulfate antibody (A,B), vertical myosepta (arrowheads), labeled with an anti-tenascin-C antibody (red) and ventral motor axons labeled with an anti-HNK-1 antibody (green) (C,D), as well as muscle pioneer cells (mp) at the horizontal myoseptum, labeled with an antibody to engrailed and ventral motor axons labeled with an anti-tubulin antibody (E,F), did not show systematic differences between uninjected embryos (A,C,E) and those injected with 1 mM NRP1a morpholino1 (B,D,F). Arrows in D and F indicate aberrant branches of ventral motor nerves. Bar in B = 25 µm for A,B; bar in D = 25 µm for C,D; bar in F = 25 µm for E,F.

At the horizontal myoseptum, an important choice point for growing motor axons in the trunk, double labeling of muscle pioneer cells (Melancon et al., 1997) with antibodies to the

engrailed protein and motor axons with anti-tubulin antibodies (Fig. 15E,F; n = 16 NRP1a morpholino1 injected embryos) indicated normal differentiation of muscle pioneer cells in segments with aberrant motor axons. For each labeling pattern analyzed, 10 to 24 uninjected control embryos were used as a reference. Thus, aberrations in motor axons were probably not caused by aberrations in trunk structures, such as vertical myosepta, notochord and muscle pioneer cells at the horizontal myoseptum.

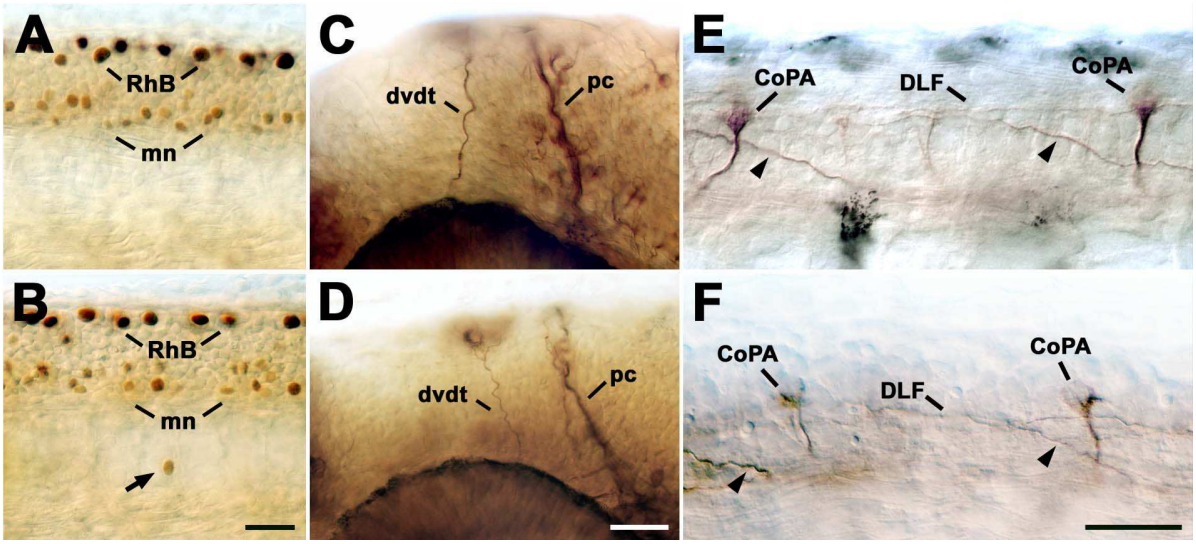

Fig. 16 Other neurons and axons in the head and spinal cord are not affected by NRP1a morpholino1. Lateral views of 24 hpf whole-mounted embryos at mid-trunk (A,B,E,F) or head (C,D) levels are shown (rostral is left). A,B: Labeling Rohon-Beard (RhB) and motor neurons (mn) with an antibody to islet-1 indicates comparable numbers of these cell types in uninjected embryos (A) and those injected with 1mM NRP1a morpholino1 (B). Whereas Rohon-Beard neurons and most motor neurons are found in their correct locations, one immunopositive cell (arrow) is displaced ventral to the spinal cord in B. C,D: Anti-tubulin labeling of the dorsoventral diencephalic tract (dvdt) and the posterior commissure (pc) reveals no significant differences between uninjected embryos (C) and those injected with 1 mM NRP1a morpholino1 (D). E,F: Labeling of commissural primary ascending interneurons in the spinal cord with the 3A10 antibody indicated normal positioning of somata (CoPA) and contralateral axons (arrowheads), which eventually join the dorsal longitudinal fascicle (DLF) in uninjected embryos (E) and those injected with 1mM NRP1a morpholino1 (F). Bar in B = 25 µm for A,B; bar in D = 25 µm for C,D; bar in F = 25 µm for E,F.

The presence and normal positioning of motor neurons was controlled with an antibody to islet-1/-2 proteins (Becker et al., 2002). In embryos injected with 1 mM NRP1a morpholino1, immunopositve cells in the ventral spinal cord were labeled at a density that was not significantly different from that in uninjected control embryos (60.3 ± 3.4 cells in segments 5-7 of 6 NRP1a morpholino1 injected embryos vs. 58.7 ± 2.1 cells in segments 5-7 of 6 uninjected embryos, Fig. 16A,B). The only exception was occasional labeling of single cell

nuclei ventral to the spinal cord in some hemisegments (Fig. 16B). These ectopic cells reflect the presence of the anti-tubulin antibody labeled cells in the somitic pathway of motor nerves. Therefore, these cells may be motor neurons that had migrated out of the spinal cord. Intensely labeled large nuclei of putative Rohon-Beard cells in the dorsal spinal cord were located in their normal position and density (26.8 ± 2.0 Rohon-Beard cells in segments 5-7 of 6 NRP1a morpholino1 injected embryos vs. 25.7 ± 1.6 Rohon-Beard cells in segments 5-7 of 6 uninjected embryos).

Trajectories of other axons were also analyzed in anti-tubulin labeled embryos. In the head of embryos injected with 1 mM NRP1a morpholino1, the prominently visible dorso-ventral diencephalic tract and the posterior commissure appeared normal (n = 12; Fig. 16C,D). In the spinal cord, Rohon-Beard cells, the dorsal longitudinal fascicle and the medial longitudinal fascicle, peripheral processes of Rohon-Beard neurons, as well as trigeminal neurons and axons appeared normal as compared to uninjected embryos (n = 21; not shown). MiP and RoP primary motor axons could not be evaluated, because their trajectories are not discernable in anti-tubulin immunohistochemistry.

The 3A10 antibody to a neurofilament-associated protein specifically labels somata and axons of the Mauthner neurons in the brainstem and the commissural primary ascending interneurons in the spinal cord at 24 hpf, similar to the CON1 antibody (Bernhardt et al., 1990). In embryos injected with 1 mM NRP1a morpholino1 (n = 11), the Mauthner neurons were normally positioned and sent their crossed axons into the spinal cord in a manner that was indistinguishable from uninjected controls (n = 10; not shown). Large commissural primary ascending interneurons were also normally located in the dorsal spinal cord, projected ventrally, crossed the midline and projected in the contralateral dorsal longitudinal fascicle, as in uninjected controls (Fig. 16E,F). Thus, several other axon trajectories were not affected by the injection of NRP1a morpholino1.

3.9 Formation of primary motor nerves does not depend on the presence of blood vessels

Injection of NRP1a morpholino1 also disturbs the formation of blood vessels in the trunk so that aberrations in motor axon growth could be secondary to the loss of blood vessels (Lee et

al., 2002). To analyze if motor axons would grow in their normal pathway in the absence of blood vessels in the trunk, morpholinos to VEGF, which is known to inhibit blood vessel development (Nasevicius et al., 2000; Lee et al., 2002), were injected. Injection of 1 mM VEGF morpholino did not induce ventral motor axon aberrations (2.5% embryos with ventral motor nerve branching, 1.7% embryos with multiple exits of ventral motor nerves or displaced neurons, n = 49) (Fig. 17B,D) (Table 4).

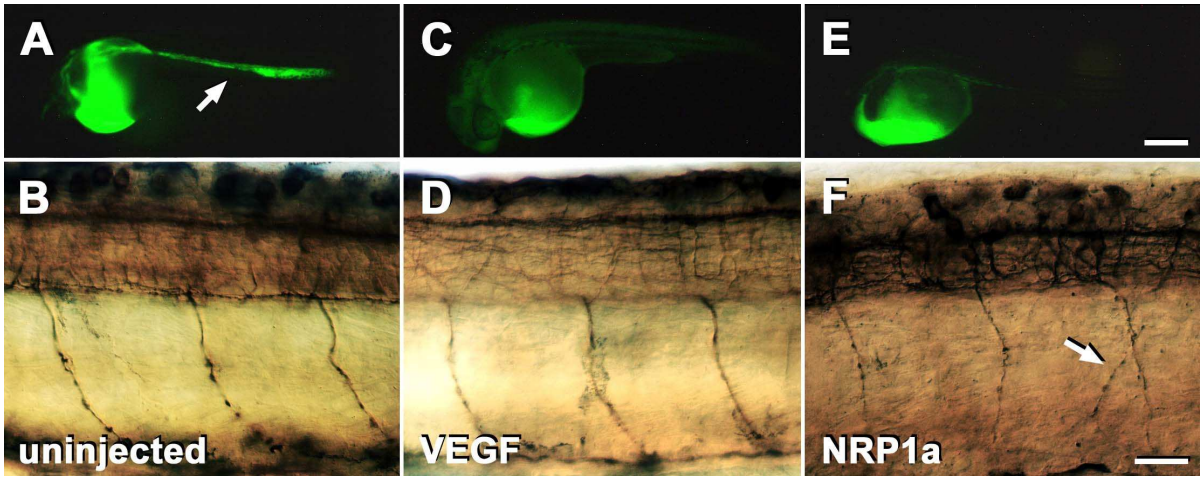

Fig. 17 Differential effects of different morpholinos on blood vessel and on motor axon development in the trunk of 24 hpf embryos. Lateral views of whole embryos subjected to microangiography are shown in A,C,E. Fluorescence of yolk sacs is near the injection site and does not indicate the presence of blood vessels. Mid-trunk levels of embryos labeled with anti-tubulin antibodies subsequent to microangiography are shown in B,D,F (rostral is left). In uninjected embryos, the trunk vasculature (A, arrow) and ventral motor nerves (B) develop normally. In embryos injected with 1 mM VEGF morpholino trunk vessels fail to develop (C), but motor nerves grow normally (D). In embryos injected with 1 mM NRP1a morpholino1, no trunk vessels are labeled (E) and ventral motor nerves grow abnormally (F). Arrow in F indicates a branched ventral motor nerve. Bar in E = 250 µm for A,C,E; bar in F = 25 µm for B,D,F.

To analyze the effect on blood vessels and motor axons in the same set of embryos, microangiography was performed on uninjected embryos (n = 7), on embryos injected with 1mM NRP1a morpholino1 (n = 8), and on embryos injected with 1 mM VEGF morpholino (n = 11) before labeling of motor axons with an anti-tubulin antibody. In all uninjected embryos, blood flow through axial trunk blood vessels at 24 h could be detected by microangiography (Fig. 17A). At this developmental stage, intersegmental vessels are just beginning to form (Childs et al., 2002) and are not filled by microangiography. However, there was no blood flow through axial vessels in VEGF morpholino and NRP1a morpholino1 injected embryos (Fig. 17C,E). Subsequent analysis of ventral motor axon growth revealed that aberrations of

ventral motor nerves were only present in those embryos injected with NRP1a morpholino1 (Fig. 17B,D,F). Thus, primary motor axons can grow correctly in the absence of normal blood vessel differentiation in the trunk, as shown in VEGF morpholino injected embryos.

3.10 Morpholinos to potential NRP1a ligands had no effect on motor axon growth when injected alone

To determine the contribution of potential NRP1a ligands to the motor axon phenotype observed after NRP1a morpholino treatment, morpholinos to potential ligands of NRP1a were injected (Table 4).

Table 4 Morpholinos to potential NRP1a ligands and co-receptors are non-effective.

Injection type	n	Embryos with aberrant ventral motor nerve branching (%)	Embryos with multiple exits of ventral motor nerves (%)	Embryos with displaced neurons (%)
Uninjected	96	6.5 ± 3.4	2.3 ± 1.1	1.4 ± 1.4
Vehicle	41	4.8 ± 4.8	2.4 ± 2.4	0.0 ± 0.0
Standard control MO (2 mM)	54	4.8 ± 4.8	1.6 ± 1.6	3.2 ± 1.6
Sema3A1 MO (2 mM)	47	14.0 ± 14.0	10.0 ± 5.0	1.8 ± 1.8
Sema3A2 MO (2 mM)	43	14.9 ± 3.7	3.3 ± 3.3	6.7 ± 6.7
VEGF MO (1 mM)	49	2.5 ± 2.5	1.7 ± 1.7	1.7 ± 1.7
L1.1 MO (2 mM)	51	4.9 ± 3.4	9.8 ± 6.7	0.0 ± 0.0

Morpholino doses are indicated in brackets. n = numbers of embryos analyzed. MO = morpholino, tested against all controls (Fisher's Exact Test).

Similar to injecting VEGF morpholinos, injection of morpholinos to the sema3A homologs sema3A1 and sema3A2 had no significant effects on the growth of ventral motor axons when injected at a concentration of 2 mM (sema3A1 morpholino: 14.0% embryos with aberrantly branched ventral motor nerves, 10.0% embryos with multiple exits of ventral motor nerves, and 1.8% embryos with displaced neurons, n = 47, sema3A2 morpholino: 14.9% embryos with aberrantly branched ventral motor nerves, 3.3% embryos with multiple exits of ventral motor nerves, and 6.7% embryos with displaced neurons, n = 43). There are several potential

NRP1a ligands expressed in the trunk, which may act redundantly and could compensate for the reduction in the expression of single ligands, such as VEGF, sema3A1 and sema3A2.

3.11 VEGF, sema3A1 and sema3A2 morpholinos act synergistically with NRP1a morpholino

Compensation might not be possible if the availability of NRP1a was reduced in experimental embryos and thus, experiments were performed where NRP1a expression was slightly reduced by injecting 0.1 mM NRP1a morpholino1, a concentration that is ineffective on its own to elicit a motor axon phenotype, in combination with 1 mM VEGF, 2 mM sema3A1 or 2 mM sema3A2 morpholinos, which also did not affect motor axon outgrowth when injected alone. Results are summarized in Table 5.

Table 5 Synergistic effects of NRP1a morpholino1 with potential ligands and co-receptors.

Injection type	n	Embryos with aberrant ventral motor nerve branching (%)	Embryos with multiple exits of ventral motor nerves (%)	Embryos with displaced neurons (%)
NRP1a MO1 + VEGF 4mm MO	81	0.0 ± 0.0	7.2 ± 0.8	5.2 ± 3.7
NRP1a 4mm MO + VEGF MO	71	23.0 ± 7.2	12.8 ± 4.8	0.0 ± 0.0
NRP1a MO1 + VEGF MO	61	44.2 ± 15.1 **	15.1 ± 3.1	31.8 ± 3.1 ***
NRP1a 4mm MO + Sema3A1 MO	76	19.7 ± 5.1	9.8 ± 4.6	2.8 ± 1.7
NRP1a MO1 + Sema3A1 MO	62	34.3 ± 8.2	17.5 ± 3.5	30.4 ± 18.2 ***
NRP1a 4mm MO + Sema3A2 MO	66	10.8 ± 5.8	13.0 ± 4.6	0.0 ± 0.0
NRP1a MO1 + Sema3A2 MO	80	32.2 ± 8.9 ***	18.4 ± 7.1	9.7 ± 3.7 ***
NRP1a 4mm MO + L1.1 MO	49	4.2 ± 2.4	0.0 ± 0.0	2.3 ± 2.3
NRP1a MO1 + L1.1 MO	47	11.5 ± 7.8	8.7 ± 2.1	7.0 ± 7.0

Morpholino doses are indicated in the text. n = numbers of embryos analyzed. MO = morpholino, NRP1a MO1: morpholino1 against NRP1a, NRP1a 4mm MO: morpholino with 4 mismatched bases based on NRP1a morpholino1, VEGF 4mm MO: morpholino with 4 mismatched bases derived from the VEGF morpholino, ** = $P < 0.01$, *** = $P < 0.001$ (Fisher's Exact Test).

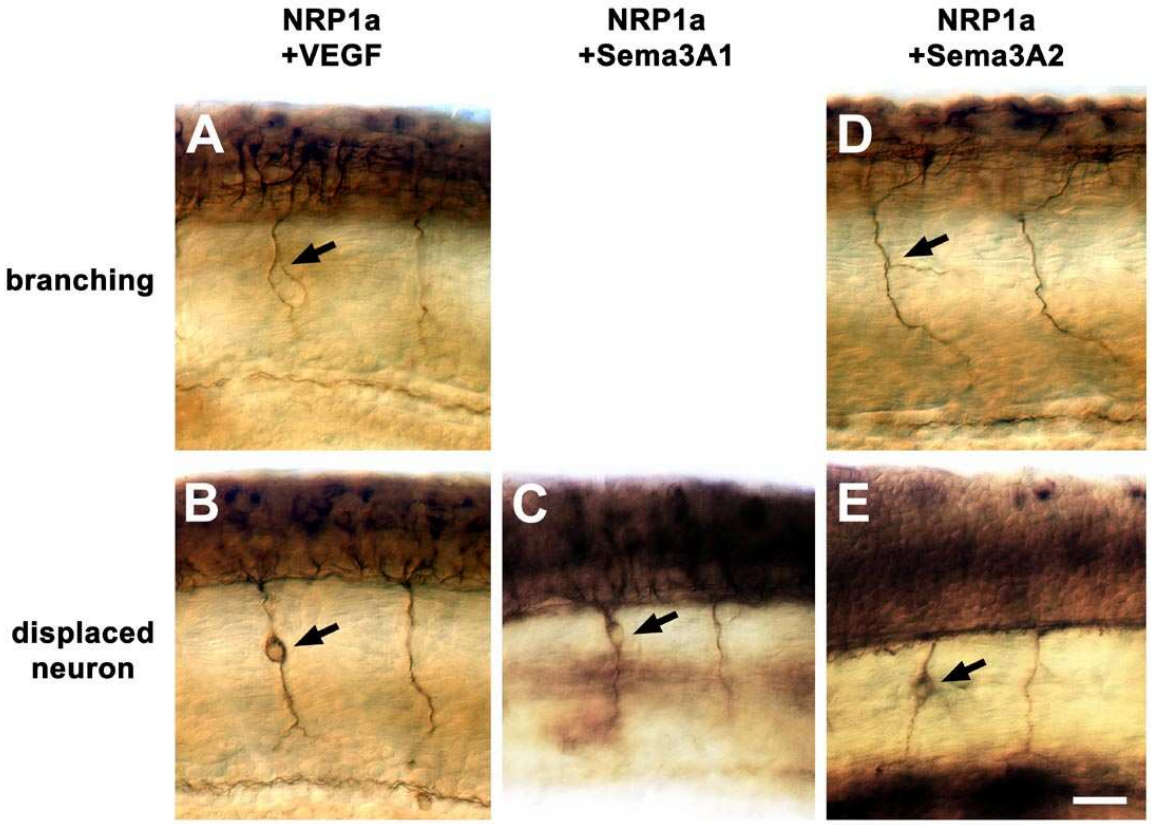

Fig. 18 Sub-threshold concentrations of NRP1a morpholino1 in combination with VEGF, sema3A1 or sema3A2 morpholinos induce aberrant growth of motor nerves. Lateral views of anti-tubulin labeled whole-mounted 24 hpf embryos at mid-trunk levels are shown (rostral is left). Combinations of NRP1a morpholino1 with VEGF (A) or sema3A2 (D) morpholinos induce aberrant motor nerve branching (arrows in A,D), whereas displaced neurons in the path of the ventral motor nerve (arrows in B,C,E) occur after combination of NRP1a morpholino1 with VEGF (B), sema3A1 (C) or sema3A2 (E) morpholinos. Bar in E = 25 µm for A-E.

Co-injections of NRP1a morpholino1 with either VEGF or sema3A2 morpholinos significantly induced motor axon branching (+ VEGF morpholino: 44.2%, n = 61, P = 0.0032; + sema3A2 morpholino: 32.2% affected embryos, n = 80, P = 0.0008) (Fig. 18A,D) and displaced neurons (+ VEGF morpholino: 31.8%, P < 0.0001; + sema3A2 morpholino: 9.7%, P = 0.0082) (Fig. 18B,E) compared to combinations with 0.1 mM NRP1a 4 mismatch morpholino (+ VEGF morpholino: 23.0% embryos with aberrant branching and 0% embryos with displaced neurons, n = 71; + sema3A2 morpholino: 10.8% embryos with aberrant branching and 0% embryos with displaced neurons, n = 66), but not multiple exits of motor nerves (+ VEGF morpholino: 15.1% vs. 12.8% control embryos; + sema3A2 morpholino: 18.4% vs. 13.0% control embryos). The combination with Sema3A1 morpholino showed only a significant increase of the percentage of embryos with displaced neurons (30.4%, n = 62,

$P < 0.0001$) (Fig. 18C) compared to the control combination (2.8%, n = 76) whereas no significant differences were found regarding motor nerve branching (34.3% vs. 19.7%) and multiple exits (17.5% vs. 9.8%).

As an additional control, sub-threshold concentrations of NRP1a morpholino1 (0.1 mM) were injected in combination with a 4 base mismatch control morpholino for VEGF (1 mM), which did not elicit aberrant growth of motor axons (0% embryos with aberrant ventral motor nerve branching, 7.2% embryos with multiple exits of ventral motor nerves, and 5.2% embryos with displaced neurons, n = 81). The synergistic effects observed in the experiments with sub threshold amounts of morpholinos indicate a contribution of VEGF as well as of sema3A1 and sema3A2 signaling to the correct outgrowth of the ventral motor nerve in the trunk.

3.12 Efficiency of morpholinos against putative NRP1a ligands

The activitities of the sema3A1 and sema3A2 morpholinos were tested using myc-tagged reporter constructs co-injected with the morpholino of overlapping sequence. Sema3A1 and sema3A2 overexpression constructs, were generated from PCR products, containing only the first ~300bp of the coding sequence including the morpholino binding site using primers sema3Ab/Bam-5' and sema3Ab/Cla-3' for sema3A1 and primers sema3Aa/Bam-5' and sema3Aa/Cla-NEW-3'for sema3A2. Each PCR product was cloned into the overexpression vector pCS2+MT (Rupp et al., 1994), in frame with a C-terminal myc-tag using the ClaI and BamHI restriction sites of the vector. Capped mRNA was synthesized from these constructs with the mMESSAGE mMACHINE^{TM} kit according to the manufacturer's instructions. For the sema3A2 construct polyA tailing was required, whereas the myc-tagged protein of the sema3A1 construct was sufficiently detectable in 16 hpf embryos without polyA tailing. Concentrations of mRNA between 1 and 2 µg/µl were used for injections.

Injecting the sema3A1 construct alone induced protein expression in 19 of 21 embryos. Protein expression was not detectable in any of the 16 embryos co-injected with the mRNA and the sema3A1 morpholino. After injection of the sema3A2 construct, 9 of 10 embryos expressed the protein compared to 0 of 7 embryos co-injected with the mRNA and the sema3A2 morpholino. This indicates specific binding of morpholinos to sema3A1 and sema3A2.

The efficiency of the VEGF morpholino has previously been demonstrated (Nasevicius et al., 2000).

3.13 L1.1 morpholino does not co-act with NRP1a morpholino

The cell recognition molecule L1.1 (Castellani et al., 2000), which is expressed in primary motor neurons (Tongiorgi et al., 1995) (Fig. 11), is a potential co-receptor for NRP1a and was tested for interaction with NRP1a. Injection of L1.1 morpholino alone had no significant effect on the growth of ventral motor axons when injected at a concentration of 2 mM (4.9% embryos with aberrant ventral motor nerve branching, 9.8% embryos with multiple exits of ventral motor nerves, and 0% embryos with displaced neurons, n =51) (Table 4). Injecting a concentration of 2 mM L1.1 morpholino in combination with the sub-threshold concentration of NRP1a morpholino1 (0.1 mM) did also not induce a significant increase of either aberrant branching of ventral motor nerves (11.5% vs. 4.2% embryos co-injected with 0.1 mM NRP1a 4mm morpholino, n = 49 and 47 respectively), of additional exits of ventral motor nerves (8.7% vs. 0% embryos co-injected with 0.1 mM NRP1a 4mm morpholino) or of displaced neurons (7.0% vs. 2.3% embryos co-injected with 0.1 mM NRP1a 4mm morpholino) (Table 5). This indicates that in the context of primary motor axon outgrowth, L1.1 may not play a major role.

3.14 Efficiency of the morpholino to L1.1

To demonstrate the efficiency of the morpholino to L1.1 3-day old uninjected and L1.1 morpholino-injected zebrafish were homogenized and L1.1 protein was analyzed by Western blot. The entire homogenates from single larvae were used to load one gel pocket of a SDS-polyacrylamide gel. Stripping the filters and reprobing them with an anti-tubulin antibody served as a loading control.

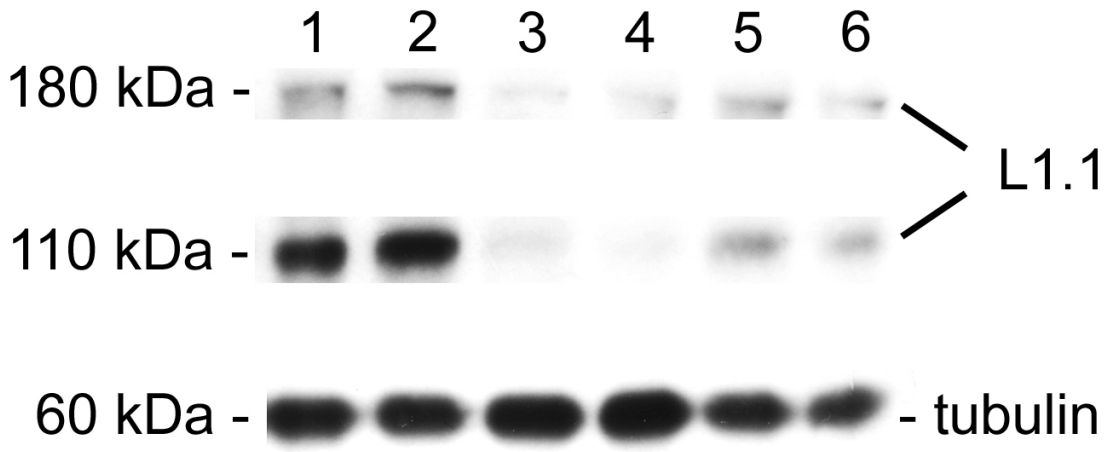

Fig. 19 Western blot analysis of single 3-day old zebrafish larvae indicates decreased L1.1 immunoreactivity in bands at 180 kD and 110 kD, in embryos injected with 2 mM L1.1 morpholino (lanes 3 and 4) and those that had received 0.5 mM L1.1 morpholino (lanes 5 and 6), compared to uninjected controls (lanes 1 and 2). Anti-tubulin labeling of a band at 60 kDa served as a loading control.

In uninjected zebrafish, L1.1 protein was represented by two bands, one thick band at 110 kDa and a thinner band at 180 kDa, which are also found in adult zebrafish brain homogenates. In animals injected with 2 mM of L1.1 morpholino, detectability of L1.1 protein was reduced compared to uninjected animals. Injection of 0.5 mM L1.1 morpholino also led to a reduction of L1.1 protein, but to a lower extent than injection of 2 mM L1.1 morpholino. Thus, L1.1 morpholino efficiently reduces L1.1 protein expression in a dose-dependent manner.

3.15 Cloning of PlexinA3 cDNA

Members of the plexinA family have been described as the signal-transducing components of semaphorin3A/neuropilin signaling complex (Rohm et al., 2000). To isolate the zebrafish plexinA1 cDNA, degenerate RT-PCR with oligonucleotide primer sequences based on the conserved sequences of human and mouse plexinA1 was performed using the Consensus-Degenerate Hybrid Oligonucleotide Primer (CODEHOP) program (Rose et al., 1998).

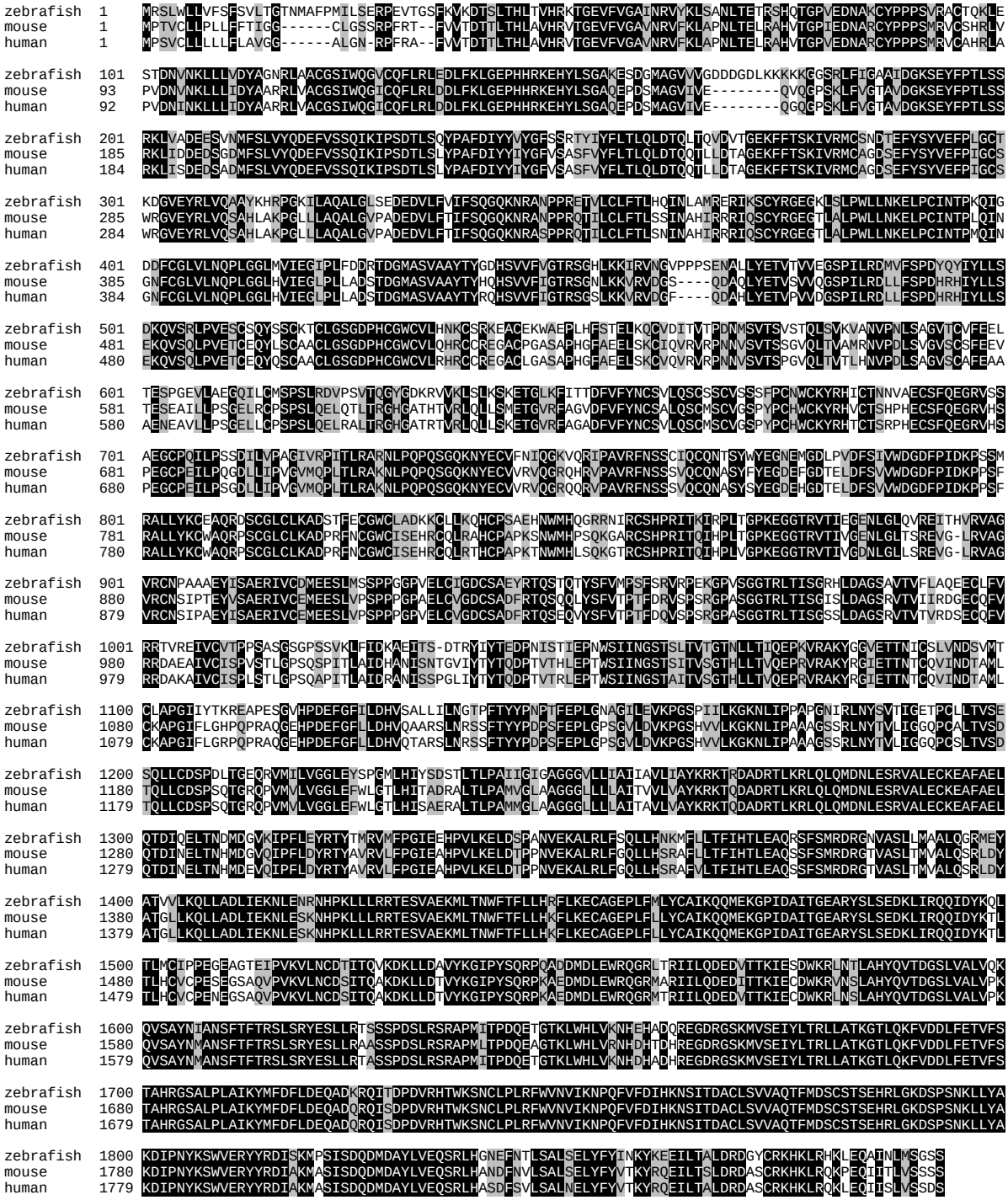

Fig. 20 Zebrafish plexinA3 shares structural homologies with plexinA3 proteins of other vertebrate species. The deduced amino acid sequence of zebrafish plexinA3 is aligned with mouse and human plexinA3. Black and gray shading represents identical and similar amino acids, respectively.

Total RNA from adult zebrafish brains was isolated and reversely transcribed using the nested oligo dT anchor primer RoRi dT_{17}, followed by PCR using primers plexinU2-5' and

plexinY1-3', yielding a 850 bp partial plexin fragment, which was cloned and sequenced. Based on this sequence, a 3' nested PCR was carried out with a combination of two nested 3' oligo dT coupled adapter primers Ro and Ri and two nested 5' gene-specific primers plexinN1a-5' and plexinN2a-5', located in the most 3' end of the newly cloned plexin fragment. The nested PCR product was cloned and sequencing revealed, that the 1020 bp plexin fragment contained 390 bp of 3' UTR and 630 bp of the 3' coding region of the plexin gene. To obtain the full-length plexin cDNA, the sequence of the nested PCR product was used to search the Ensembl Zebrafish Genome Browser. Subjecting the short plexin sequence to a BLAST/SSAHA search revealed that the coding region of the nested PCR fragment was highly homologous to the 3' region of a 5496 bp transcript (ENSDART00000020604) of the gene ENSDARG00000016216 located on chromosome 8 of the zebrafish genome. Homology searching of the database using BLAST (Altschul et al., 1990) revealed that the 5496 bp transcript was most closely related to human and mouse plexinA3 and that the 5' region, containing the start codon, was not included in the transcript.

To identify the 5' region of zebrafish plexinA3, the zebrafish EST database was screened using BLAST (Altschul et al., 1990) and the 520 bp EST clone 24185179 was obtained. This 520 bp EST clone contained 260 bp of plexinA3 5'UTR, the start codon followed by 100 bp of novel 5'coding region and 260 bp overlapping with the 5' region of the 5496 bp plexinA3 transcript. The full length plexinA3 gene was amplified using the proof-reading polymerase PfuUltra and primers Plexin5496Chr8-5'5 and Plexin5496Chr8-3', based on the 5'- and 3' UTR regions of the predicted sequence, yielding a 6420 bp PCR fragment, which was cloned and sequenced using sequencing primers based on the predicted sequence (see Appendix).

Full length plexinA3 encodes a deduced protein of 1892 amino acids. The start codon was predicted from the presence of stop codons preceding the N-terminal end of the deduced protein. The general domain structure of zebrafish plexinA3, comprising a Sema domain, followed by three MRS (Met Related Sequence) domains, four IPT (Immunoglobulin-like fold shared by Plexins and Transcription factors) motifs and the highly conserved intracellular SP (Sex Plexin) domain at the C-terminus, is identical to that of homologs in other vertebrate species. The transmembrane domain of zebrafish plexinA3 was located between the TPT motifs and the SP domain and comprised amino acids 1241-1263. Alignment of the zebrafish

molecule with those of human (Maestrini et al., 1996) and mouse (Kameyama et al., 1996) plexinA3 indicated significant structural homology among the three molecules (Fig. 20).

Table 6 Zebrafish plexinA3 is related to other members of the plexinA subfamily.

	zPlexA3	zPlexA4	mPlexA1	mPlexA2	mPlexA3	mPlexA4	hPlexA1	hPlexA2	hPlexA3	xPlexA	dPlexA
zPlexA3	100	60	67	61	73	61	67	61	73	68	39
zPlexA4		100	62	66	58	79	62	67	59	62	39
mPlexA1			100	62	65	63	95	63	66	84	39
mPlexA2				100	59	67	63	96	59	62	39
mPlexA3					100	59	66	59	94	64	37
mPlexA4						100	63	67	59	63	39
hPlexA1							100	63	66	83	39
hPlexA2								100	59	63	39
hPlexA3									100	64	38
xPlexA										100	39
dPlexA											100

Pair-wise comparisons show high percentage of amino acid identities of zebrafish plexinA3 and identified plexinAs of other species. Numbers indicate percentage of amino acid identity. *Drosophila* plexinA was added as an outgroup. Plex, Plexin; z, zebrafish; m, mouse; h, human; x, *Xenopus*; d, *Drosophila*.

The highest overall identity of amino acid sequences was found between the zebrafish gene and human as well as mouse plexinA3 (73%, Table 6). The degree of amino acid identity between the zebrafish protein and other plexinA proteins (except *Drosophila* plexinA, which served as an outgroup) was between 60% and 68% (Table 6). In *Xenopus* only one A-type plexin has been identified, which is most closely related to plexinA1 from other species (Ohta et al., 1995).

A phylogenetic tree using the Clustal method (Chenna et al., 2003) was constructed with known plexinAs from human, mouse, zebrafish and *Xenopus* species and *Drosophila* plexinA as an outgroup. The novel zebrafish plexinA3 segregated with its species homologs as expected from pair-wise comparisons (Fig. 21).

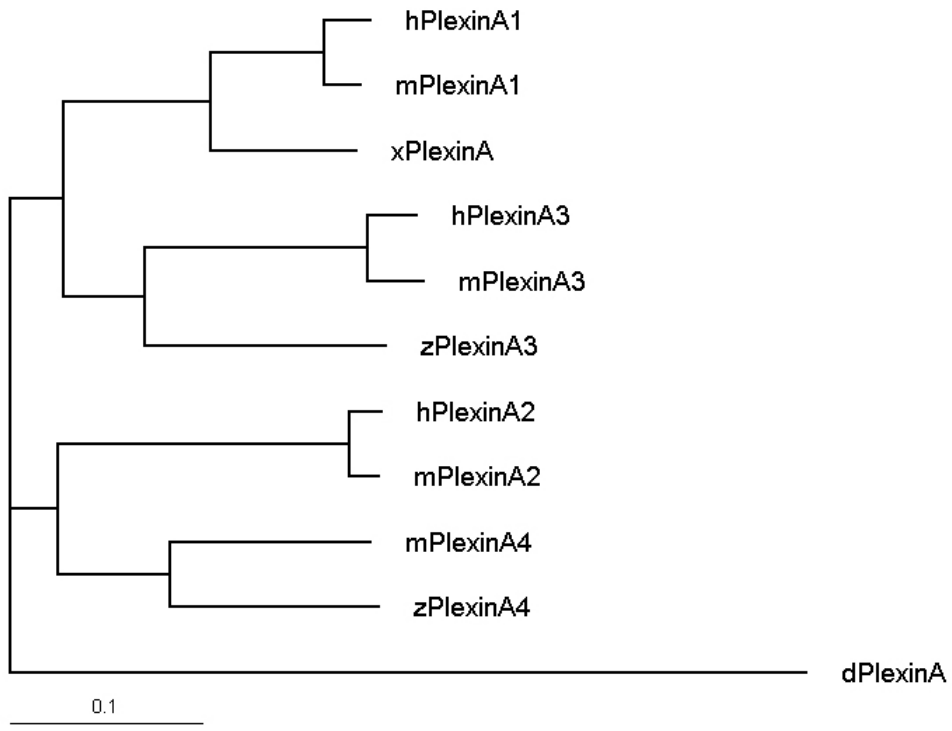

Fig. 21 Multiple comparisons in a phylogenetic tree group zebrafish plexinA3 with plexinA3 homologs in other vertebrates. Drosophila plexinA was added as an outgroup. The scale bar represents 10 substitutions per 100 amino acids. z, zebrafish; m, mouse; h, human; x, *Xenopus*; d, *Drosophila*.

3.16 PlexinA3 is expressed in primary motor neurons

To test whether the novel zebrafish plexinA3 could function as a co-receptor for semaphorin/neuropilin signaling in motor axon outgrowth, plexinA3 mRNA expression was analyzed by in situ hybridization. Digoxigenin (DIG)-labeled antisense and sense probes specific for plexinA3 mRNA, were obtained from the pCR®-Blunt II TOPO® vector containing the complete plexinA3 ORF plus additional 5' and 3' untranslated regions. In situ hybridization was performed in 16 and 24 hpf zebrafish embryos (Fig. 22).

In 16 hpf embryos, diffused reactivity of plexinA3 mRNA was found in the nervous system, including trigeminal sensory ganglion neurons, hindbrain and spinal cord. In a higher magnification, cell clusters at the ventral edge of the spinal cord, which seemed to be motor neurons, could be detected (Fig. 23A). Interestingly, plexinA3 was also expressed outside the nervous system in ventral regions of the tail.

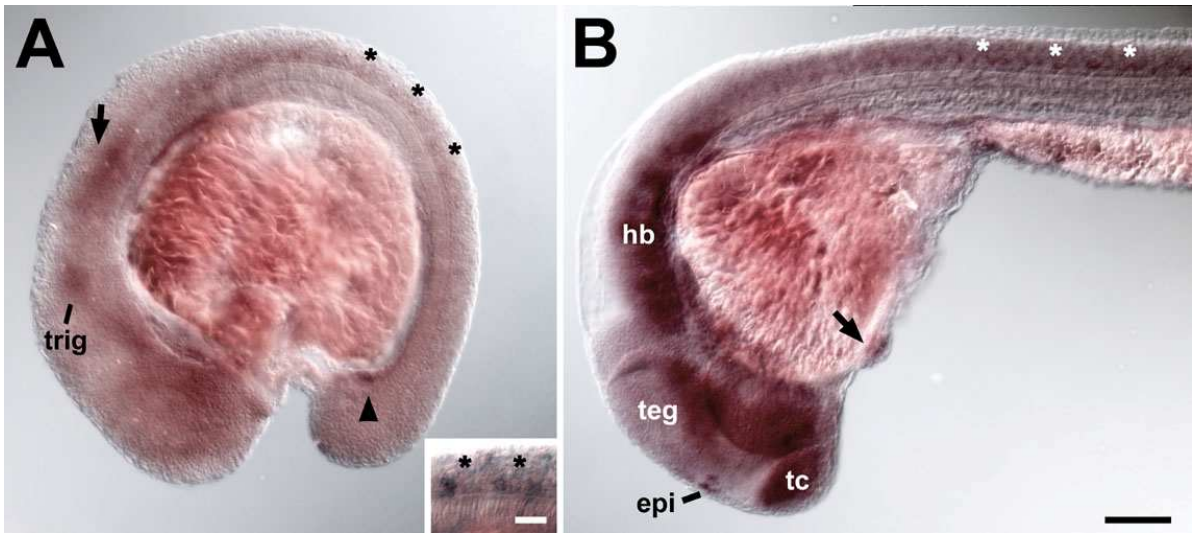

Fig. 22 Expression pattern of plexinA3 in embryonic zebrafish. Lateral views of whole-mounted 16 hpf (A) and 24 hpf (B) embryos are shown (rostral is left) A: At 16 hpf, plexinA3 mRNA is expressed in the nervous system within defined regions of the trigeminal ganglion (trig), the hindbrain (arrow in A) and in cell clusters in the ventral spinal cord (asterisks). The insert in A shows a magnified view of these cell clusters which appear to be motor neurons (asterisks). At 16 hpf plexinA3 is also expressed in tail regions outside the nervous system (arrowhead). B: At 24 hpf plexinA3 is expressed in the telencephalon (tc), the epiphysis (epi), the tegmentum (teg), the hindbrain (hb) and in the spinal cord (asterisks). Outside the nervous system, plexinA3 mRNA was found in the developing heart (arrow in B). Bar in B = 100 µm for A and B; bar in insert = 25 µm.

At 24 hpf, plexinA3 was expressed in various regions of the nervous system with structures of the telencephalon, epiphysis and tegmentum being most prominent (Fig. 22B). Strong expression was also found in the hindbrain and in the heart.

PlexinA3 was detectable in the spinal cord (Fig. 22B) and a higher magnification of a caudal trunk region revealed expression in cells clusters at the ventral edge of the spinal cord (Fig. 23A). These cells were similar in number and position to the cells expressing NRP1a suggesting that plexinA3, like NRP1a, is expressed in primary motor neurons. Also similar to NRP1a (Lee et al., 2002) (Fig. 7A), PlexinA3 mRNA was found in tail regions ventral of the notochord, outside the nervous system, identical with the position of tail angioblasts involved in blood vessel formation (Fig. 23A). Embryos treated with the sense probe did not show any labeling (Fig. 23B).

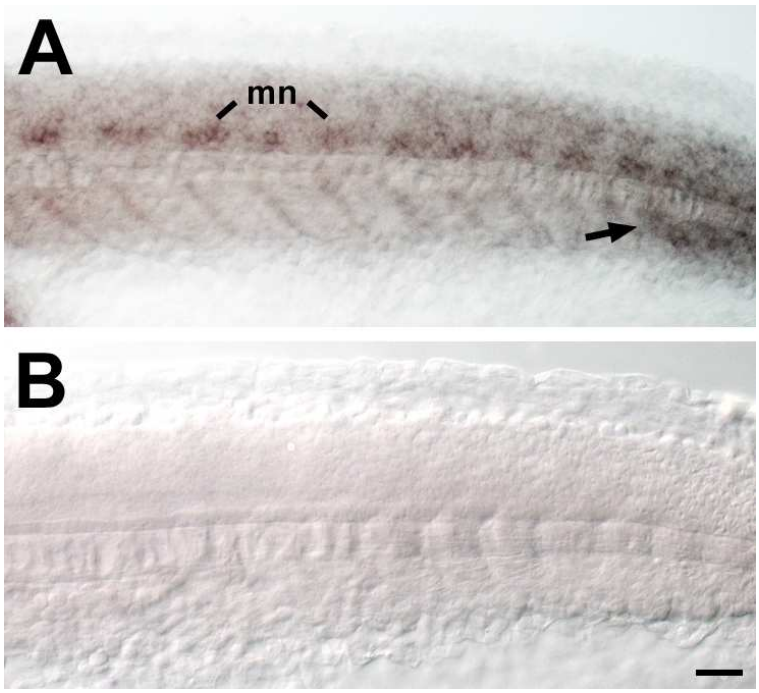

Fig. 23 Expression of plexinA3 in the trunk of embryonic zebrafish at 24 hpf. A: In a lateral view of the caudal trunk of a 24 hpf embryo plexinA3 mRNA is expressed in cells in the ventral spinal cord in the position of motor neurons (mn) and outside the nervous system in a ventral region of the tail (arrow). B: In situ hybridization with a plexinA3 sense mRNA probe did not yield a signal (age and orientation as in A). Bar in B = 25 µm for A and B.

3.17 Morpholinos against plexinA3 are active in vivo

To test whether a lack of plexinA3 would influence the growth of motor axons, fertilized eggs were injected with two anti-sense morpholinos of non-overlapping sequence, designated plexinA3 morpholino1 and plexinA3 morpholino2, to inhibit the translation of plexinA3. The efficiency of both PlexinA3 morpholinos was tested by co-injection of 1 mM plexinA3 morpholino1 or morpholino2 with a myc-tagged 420 bp plexinA3 mRNA contruct containing the first 330 bp of the coding region plus 5'untranslated regions including the binding sites for both morpholinos. The plexinA3 mRNA was translated in vitro and injected into zebrafish eggs. Expression was analyzed in 16 hpf embryos by immunohistochemistry using an anti-myc antibody.

In 38 of 43 embryos, injected with plexinA3 mRNA, myc expression could be detected (Fig. 24B), whereas none of 30 uninjected embryos showed myc expression (Fig. 24). PlexinA3 morpholino1 was co-injected with plexinA3 mRNA and suppressed protein expression of plexinA3 mRNA in 27 of 29 embryos (Fig. 24C), whereas co-injection of PlexinA3

morpholino2 with plexinA3 mRNA resulted in suppression of plexinA3 mRNA expression in 31 of 33 embryos (Fig. 24D). Thus, both plexinA3 morpholinos efficiently bind to their target sequence in vivo.

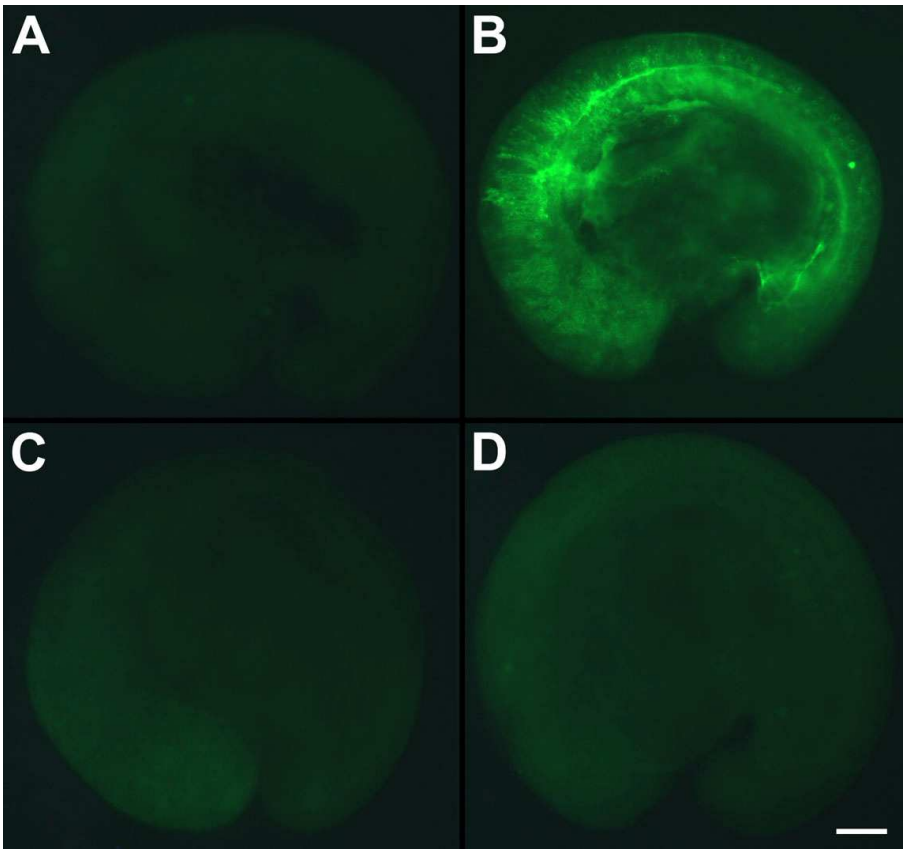

Fig. 24 Expression of a short myc-tagged plexinA3 mRNA fragment is inhibited by plexinA3 morpholino1/2. Embryos at 16 hpf were labeled with the anti-myc antibody. The myc-epitope is not detectable in uninjected animals (A). Embryos injected with the plexinA3 mRNA construct show diffuse expression of the mRNA, suggesting an intracellular localization of the protein (B). Co-injection of plexinA3 mRNA with plexinA3 morpholino1 (C) or plexinA3 morpholino2 (D) abolishes detectability of the myc-epitope. Bar in D = 100 µm for A-D.

3.18 Reduction of plexinA3 expression leads to aberrant branching and multiple exits of primary motor axons

Axon growth in plexinA3 morpholino injected embryos was analyzed at 24 hpf using the anti-tubulin antibody (Fig. 25). Injection of 1mM plexinA3 morpholino1 led to abnormal growth of primary motor axons in 28.9% (471 of 1611) analyzed hemisegments in 68 embryos. Aberrations of ventral motor nerves, which have normally grown one unbranched

nerve beyond the ventral edge of the notochord at 24 hpf (Fig. 25A,B), can be grouped into two categories. Nerves were either abnormally branched (Fig. 25C,D) or hemisegments showed an additional nerve exiting the spinal cord (Fig. 25E,F).

For embryos that had received 1 mM plexinA3 morpholino1, these phenotypes were analyzed in more detail: 34.8% of the nerves in affected hemisegments showed aberrant branching (Fig. 25C). The vast majority of these branches (81.9%) were directed caudally. Rostrally (5.0%) and bilaterally (3.3%) branched nerves were observed less frequently. On average, 3.4 ± 0.2 hemisegments/embryo showed aberrant branching in affected embryos.

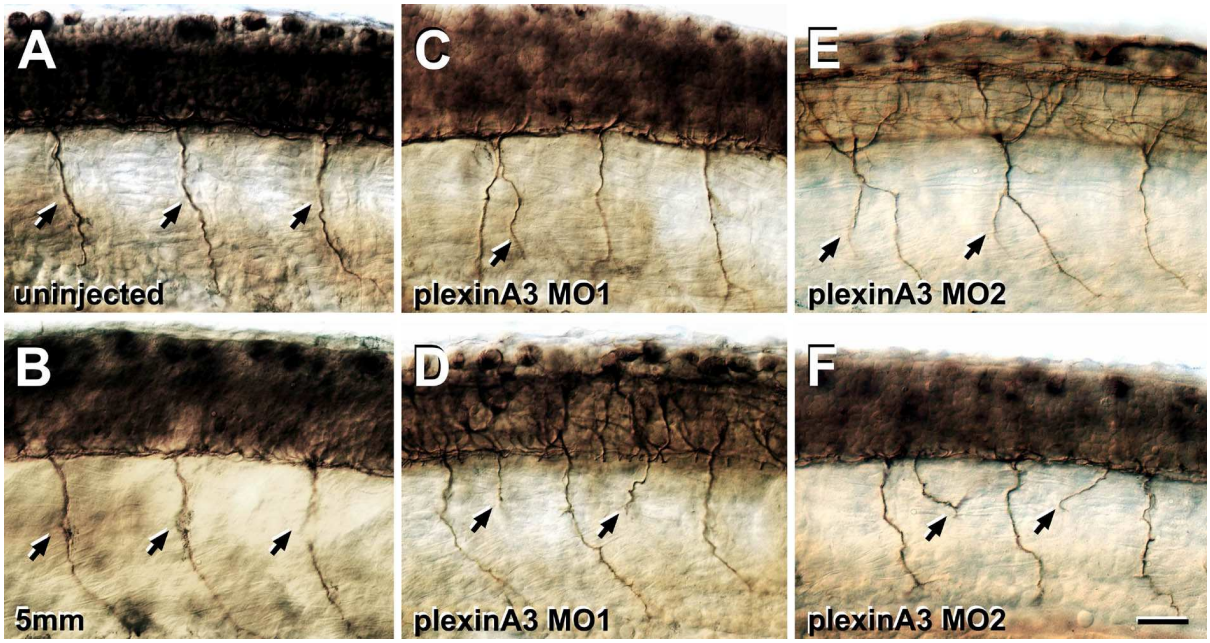

Fig. 25 PlexinA3 morpholinos induce aberrant branching and multiple exits of primary motor nerves. A-F: Lateral views of anti-tubulin labeled whole-mounted 24 hpf embryos at mid-trunk levels are shown (rostral is left). In uninjected embryos (A) or those injected with 1 mM plexinA3 5mm morpholino (5mm, B), single unbranched motor nerves (arrows in A,B) grow ventrally out of the spinal cord. Injection of 1 mM plexinA3 morpholino1 induced branching (arrow in C) or a second spinal exit point for motor axons per hemisegment (arrows indicated additional nerves in D). Injection of 1 mM plexinA3 morpholino2 also induced aberrant branching (arrows in E) of the ventral motor nerve and additional nerves exiting the spinal cord (arrows in F). Bar in F = 25 µm for A-F.

In 63.5% of the affected hemisegments mostly one additional nerve of variable length grew ventrally from an additional exit point in the ventral spinal cord (Fig. 25D). The additional nerve ran parallel to the main nerve or joined it at variable positions dorsal of the horizontal myoseptum. In 67.5% of the hemisegments showing additional exit points, it was not possible

to determine whether the additional nerve emanated from the spinal cord in the rostral or caudal half of a segment, because it grew close to the segment border, which could not be visualized. In the remaining 32.5% of hemisegments with multiple exits of motor nerves, the additional nerve could be localized in the anterior or posterior half of the somite and the frequency of rostral or caudal exits points could be calculated. Most of these additional exit points (72.8%) were located in the posterior half of the somites, whereas 25.1% were found in the anterior half of the somite and 2.1% of the hemisegments had additional exit points rostral and caudal to the main nerve. This indicates that additional nerves originate from the posterior half of the trunk segments, rather than from the anterior part. On average, 4.7 ± 0.4 hemisegments/embryo had multiple exits in affected embryos.

Ventrally displaced neurons and truncations were almost never found after injection of plexinA3 morpholino. Only 0.2% of all aberrations were displaced neurons and 1.5% of aberrations were truncations. This corresponds to 1.4% ± 1.4% embryos with displaced neurons and 1.7% ± 1.7% embryos with truncations, which was not different from uninjected controls (displaced neurons: 0% ± 0%; $P > 0.05$, truncations: 4.8% ± 3.0%; $P > 0.05$).

3.19 Aberrations induced by plexinA3 morpholino1 are dose-dependent

PlexinA3 morpholino1 was injected at concentrations ranging from 0.1 mM to 1 mM. Aberrant growth of motor nerves was observed in a dose-dependent manner (Table 7). Injecting 0.1 mM or 0.25 mM plexinA3 morpholino1 did not lead to significant differences in aberrant branching of ventral motor nerves (16.8% and 26.0% affected embryos, $n = 63$ and $n = 53$, respectively) compared to uninjected controls (1.7 % affected embryos, $n = 50$), buffer injected embryos (11.5% affected embryos, $n = 53$), embryos injected with standard control morpholino at 2 mM (4.8% affected embryos, $n = 54$) and embryos injected with plexinA3 5mm morpholino at 1 mM (13.8% affected embryos, $n = 51$). In contrast, injection of 0.5 mM and 1 mM plexinA3 morpholino1 significantly increased the proportion of embryos with branched nerves (43.2% and 63.8% affected embryos, $n = 65$ and $n = 68$, $P < 0.01$, $P < 0.001$, respectively) compared to all controls.

Table 7 Morpholinos to plexinA3 induce aberrant ventral motor nerve growth.

Injection type	n	Embryos with aberrant ventral motor nerve branching (%)	Embryos with multiple exits of ventral motor nerves (%)
Uninjected	50	1.7 ± 1.7	4.9 ± 3.0
Vehicle	53	11.5 ± 7.3	4.4 ± 2.4
Standard control MO (2 mM)	54	4.8 ± 4.8	1.6 ± 1.6
PlexinA3 5mm MO (1 mM)	51	13.8 ± 5.3	12.0 ± 0.3
PlexinA3 MO1 (0.1 mM)	63	16.8 ± 5.8	19.7 ± 4.8
PlexinA3 MO1 (0.25 mM)	53	26.0 ± 10.4	17.5 ± 5.2
PlexinA3 MO1 (0.5 mM)	65	43.2 ± 14.7 **	56.0 ± 11.7 ***
PlexinA3 MO1 (1 mM)	68	63.8 ± 7.3 ***	93.9 ± 2.7 ***
PlexinA3 MO2 (1 mM)	66	82.9 ± 6.5 ***	94.7 ± 2.5 ***

Morpholino doses are indicated in brackets. n = numbers of embryos analyzed. MO = morpholino, plexinA3 MO1/MO2: morpholino1/2 against plexinA3, plexinA3 5mm MO: morpholino with 5 mismatched bases based on plexinA3 morpholino1, ** = $P < 0.01$, *** = $P < 0.001$ (Fisher's Exact Test) tested against all controls.

At 0.1 mM and 0.25 mM, multiple exits were found in 19.7% and 17.5% of the embryos respectively, which was not significantly more than in all controls (uninjected: 4.9%, vehicle injected: 4.4%, standard control morpholino injected: 1.6% and plexinA3 5mm morpholino injected: 12.0%), whereas at concentrations of 0.5 mM and 1 mM, the percentage of embryos with multiple exits of motor nerves was significantly increased to 56.0% and 93.9% of the embryos, respectively ($P < 0.001$ against all controls for both concentrations).

3.20 A second morpholino to plexinA3 induces the same phenotypes as plexinA3 morpholino1

To exclude that aberrations caused by plexinA3 morpholino1 are non-specific, a second morpholino to plexinA3, called plexinA3 morpholino2, was used to knockdown the protein levels of plexinA3. PlexinA3 morpholino2 was non-overlapping with the sequence of morpholino1 and was designed against a region further upstream than plexinA3 morpholino1. Injection of 1 mM plexinA3 morpholino2 resulted in the same phenotypes observed after injection of plexinA3 morpholino1: branching of ventral motor nerves (Fig. 25E) and multiple exit points (Fig. 25F). Using 1 mM plexinA3 morpholino2 significantly increased

the frequencies of ventral motor nerve branching (82.9 % affected embryos, n = 66) and multiple exits (94.7 % affected embryos) compared to all controls (Table 7). Thus a second morpholino against plexinA3 recapitulates aberrations induced by plexinA3 morpholino1.

3.21 Cellular differentiation of trunk structures other axon tracts were not affected by plexinA3 morpholino injections

The effect of the plexinA3 morpholinos could be secondary to potential changes of important spinal cord or trunk structures, which was assessed by labeling relevant structures with specific antibodies.

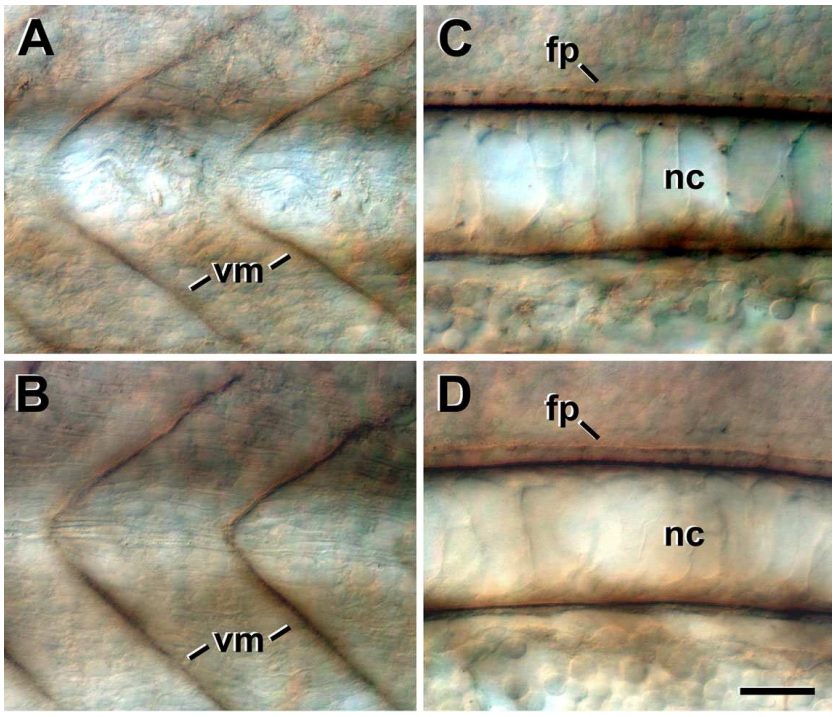

Fig. 26 Trunk structures appeared unaltered after injection of 1 mM plexinA3 morpholino1. Lateral views of whole-mounted 24 hpf embryos at mid-trunk levels are shown (rostral is left) labeled with an antibody to chondroitin sulfates. Vertical myosepta (vm) (A,B), the surface of the notochord (nc) and spinal floor plate (fp) (C,D) are indistinguishable in uninjected (A,B) and plexinA3 morpholino1 injected embryos (B, D). Bar in D = 25 µm (applies to A-D).

Trunk structures were visualized with antibodies to chondroitin sulfates labeling vertical myosepta, spinal floor plate and the notochord surface (Bernhardt and Schachner, 2000) at

24 hpf. Immunolabeling of chondroitin sulfates was unaltered in embryos injected with 1 mM plexinA3 morpholino1 (n = 11, Fig. 26B,D) compared to uninjected embryos (n = 13, Fig. 26A,C).

The presence of neurons and axon trajectories was analyzed in the spinal cord, where the somata of motor neurons are located (Fig. 27). The islet antibody (Becker et al., 2002), was used to reveal the location of primary motor neurons and Rohon-Beard neurons (Fig. 27A,B). After injection of 1 mM plexinA3 morpholino1 (n = 15, Fig. 27B) somata of motor and Rohon-Beard neurons were normally distributed in the spinal cord compared to uninjected control embryos (n = 14, Fig. 27A).

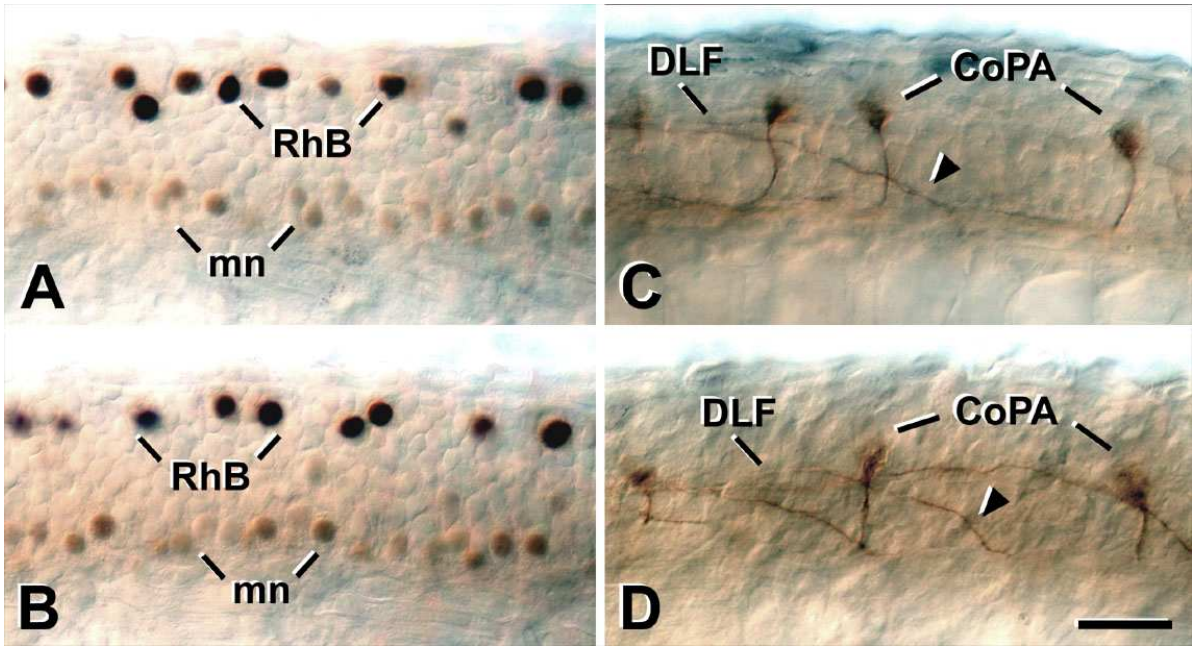

Fig. 27 Other neurons and axons in the spinal cord are unaffected by plexinA3 morpholino1. Lateral views of 24 hpf whole-mounted embryos at the level of the spinal cord are shown (rostral is left). A,B: Labeling Rohon-Beard (RhB) and motor neurons (mn) with an antibody to islet-1 indicates comparable numbers of these cell types in uninjected embryos (A) and those injected with 1mM plexinA3 morpholino1 (B). C,D: Labeling of commissural primary ascending interneurons (CoPA) in the spinal cord with the 3A10 antibody indicated normal positioning of somata (CoPA) and contralateral axons (arrowheads), which eventually join the dorsal longitudinal fascicle (DLF) in uninjected embryos (C) and in those embryos injected with 1mM plexinA3 morpholino1 (D). Bar in D = 25 µm for A-D.

The neurofilament antibody 3A10 was used to demonstrate that the somata of commissural primary ascending interneurons were located in their normal positions in the dorsal spinal cord. Their axons grew ventrally, crossed the midline and projected in the contralateral dorsal

longitudinal fascicle (Fig. 27C,D) in embryos injected with 1 mM plexinA3 morpholino1 (n = 14, Fig. 27D) indistinguishably from uninjected controls (n = 13, Fig. 27C). Additionally, the 3A10 antibody labels the somata of Mauthner neurons, positioned in the brainstem, and their axons crossing the midline and extending into the spinal cord, and no differences were observed comparing 1 mM plexinA3 morpholino1-injected embryos (n = 14) with uninjected embryos (n = 13; not shown).

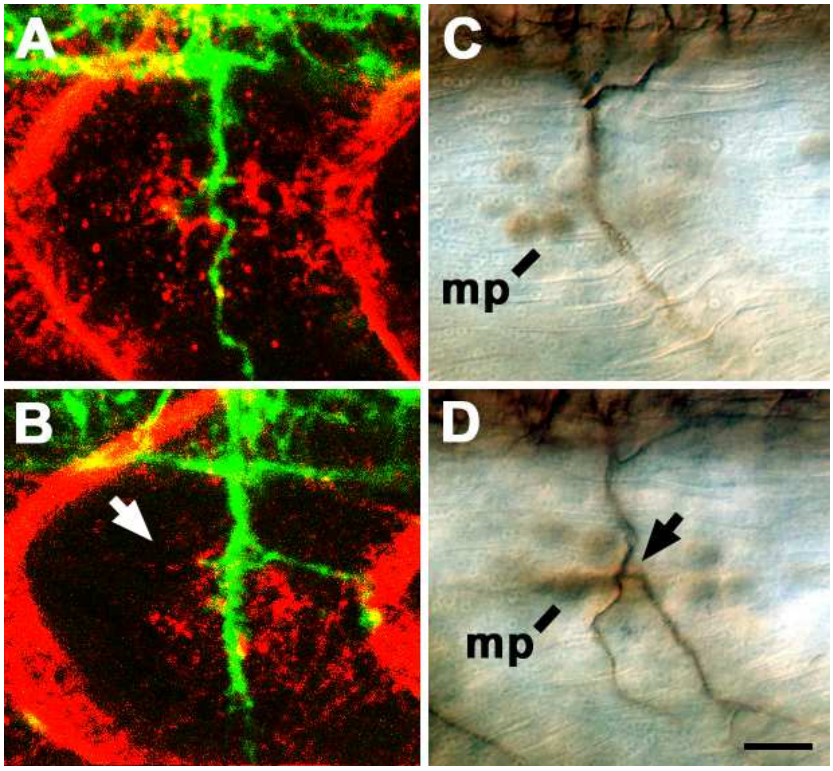

Fig. 28 The horizontal myoseptum appeared normal after injection of 1 mM plexinA3 morpholino1. Lateral views of whole-mounted 24 hpf embryos at the level of the horizontal myoseptum are shown (rostral is left). Tenascin-C expression (red) at the horizontal myoseptum and ventral motor axons (green) labeled with an anti-HNK-1 antibody (A,B) and muscle pioneer cells (mp) at the horizontal myoseptum, labeled with an antibody to engrailed and ventral motor axons labeled with an anti-tubulin antibody (C,D) did not show systematic differences between uninjected embryos (A,C) and those injected with 1 mM plexinA3 morpholino1 (B,D). Arrows in B and D indicate aberrant branches of ventral motor nerves. Bar in D = 12.5 µm for A-D.

The horizontal myoseptum is an important choice region where trajectories of primary motor axons diverge to grow into different regions of the somite (Eisen, 1994). Expression of tenascin-C at the horizontal myoseptum (Fig. 28A,B), indicated by immunolabeling with antibodies to tenascin-C (Bernhardt et al., 1998; Schweitzer et al., 2005), did not differ between segments in which axons, labeled with the anti-HNK-1 antibody in the same

embryos, were abnormally branched in 1 mM plexinA3 morpholino1-injected embryos (n = 15, Fig. 28B) and uninjected embryos (n = 14, Fig. 28A), where ventral motor axons grew unbranched.

Double immunohistochemisty of muscle pioneer cells, which are located at the level of the horizontal myoseptum in 24 hpf embryos and were labeled with an antibody to the engrailed protein (Melancon et al., 1997) and ventral motor axons visualized with anti-tubulin antibodies (Fig. 28C,D) revealed that muscle pioneer cells differentiated indistinguishably in embryos injected with 1 mM plexinA3 morpholino1 (Fig. 28D; n = 25) and uninjected embryos (Fig. 28C; n = 28), although abnormal branching occurred in plexinA3 morpholino1-injected embryos (Fig. 28D).

These observations suggest that plexinA3 morpholino1 injection did not affect differentiation of the trunk or growth of some axon fascicles and other neurons other than primary motor nerves.

3.22 Sema3A1 and sema3A2 morpholinos act synergistically with plexinA3 morpholino1

The two homologues of semaphorin3A, sema3A1 and sema3A2 are ligands that might signal through plexinA3. Morpholinos against sema3A1 and sema3A2, each at 2 mM, did not induce aberrant growth of ventral motor axons (sema3A1 morpholino: 14.0% embryos with aberrantly branched ventral motor nerves, 10.0% embryos with multiple exits of ventral motor nerves, n = 47, sema3A2 morpholino: 14.9% embryos with aberrantly branched ventral motor nerves, 3.3% embryos with multiple exits of ventral motor nerves, n = 43) (Table 4). However, co-injections of 2mM sema3A1 or sema3A2 morpholinos with 0.1 mM plexinA3 morpholino1 induced significant aberrations of motor axon growth such as branching (sema3A1: 60.2% affected embryos, n = 77, sema3A2: 33.9% affected embryos, n = 54) and multiple exits (sema3A1: 37.8% affected embryos, sema3A2: 52.3% affected embryos) compared to embryos co-injected with 0.1 mM plexinA3 5mm morpholino in combination with 2mM sema3A1 morpholino (20.2% with aberrantly branched ventral motor nerves and 19.0% embryos with multiple exits of ventral motor nerves, n = 58), which served as a control for both combinations (Table 8). These results show that both ligands, sema3A1 and

sema3A2, contribute to the correct outgrowth of the ventral motor nerves probably by signaling through plexinA3.

Table 8 Synergistic effects of plexinA3 morpholino1 with potential ligands and co-receptors.

Injection type	n	Embryos with aberrant ventral motor nerve branching (%)	Embryos with multiple exits of ventral motor nerves (%)
PlexinA3 5mm MO (0.1 mM) + Sema3A1 MO (2 mM)	58	20.2 ± 4.8	19.0 ± 0.2
PlexinA3 MO1 (0.1 mM) + Sema3A1 MO (2 mM)	77	60.2 ± 9.6 ***	37.8 ± 9.5 *
PlexinA3 MO1 (0.1 mM) + Sema3A2 MO (2 mM)	54	33.9 ± 7.9 *	52.3 ± 4.8 ***
PlexinA3 MO1 (0.1 mM) + VEGF MO (0.1 mM)	89	29.5 ± 7.8	34.0 ± 5.1 *
PlexinA3 MO1 (0.1 mM) + NRP1a MO1 (0.1 mM)	88	21.5 ± 10.6	27.9 ± 14.7
PlexinA3 MO1 (0.1 mM) + L1.1 MO (2 mM)	48	11.6 ± 4.7	13.3 ± 4.7

Morpholino doses are indicated in brackets. n = numbers of embryos analyzed. MO = morpholino, plexinA3 MO1: morpholino1 against plexinA3, plexinA3 5mm MO: morpholino with 5 mismatched bases based on plexinA3 morpholino1, NRP1a MO1: morpholino1 against NRP1a, * = $P < 0.05$, *** = $P < 0.001$ (Fisher's Exact Test) tested against PlexinA3 5mm MO (0.1 mM) + Sema3A1 MO (2 mM).

3.23 Co-injection of VEGF and plexinA3 morpholinos induces multiple exits of motor nerves

Since VEGF is a ligand for NRP1a present in the trunk environment, it might also function through plexinA3. Indeed, sub-threshold experiments with ineffective concentrations of VEGF and plexinA3 morpholinos revealed, that a combination of plexinA3 morpholino at 0.1 mM and VEGF morpholino at 1 mM induces multiple exits of motor nerves (34.0% affected embryos, n = 89) at a frequency significantly different from the control combination of 0.1 mM plexinA3 5mm morpholino and 2mM sema3A1 morpholino. However, branching of ventral motor nerves (29.5% affected embryos) was not significantly different from this control (Table 8). Thus, it seems that VEGF might, at least partially, participate in plexinA3 mediated signaling.

3.24 Sub-threshold experiments of plexinA3 and the potential co-receptors NRP1a or L1.1 fail to show synergistic effects

Morpholinos to both, plexinA3 and NRP1a induce aberrant branching and multiple exits of ventral motor nerves. Thus plexinA3 could be a co-receptor of NRP1a necessary for the signal transduction of sema3A in motor axon outgrowth. To test this hypothesis, NPR1a and plexinA3 morpholinos were co-injected at sub-threshold concentrations that did not elicit aberrant motor axon growth when injected alone (Table 2, Table 7). Co-injections of NRP1a morpholino1 with plexinA3 morpholino1, each at 0.1 mM, did not induce ventral motor axon branching (21.5% affected embryos, n = 88) or multiple exits (27.9% affected embryos) compared to embryos co-injected with 0.1 mM plexinA3 5mm morpholino and 2mM sema3A1 morpholino, which served as a control (Table 8).

Another potential co-receptor for NRP1a and plexinA3 is the cell recognition molecule L1.1, which is also expressed in primary motor neurons. However, co-injection of 2 mM L1.1 morpholino together with 0.1 mM plexinA3 morpholino1, both of which have no effect when injected alone at these concentrations, did not increase aberrant growth of motor nerves (branching: 11.6% affected embryos, multiple exits: 13.3% affected embryos, n = 48) at a significant frequency compared with embryos injected with 0.1 mM plexinA3 5mm morpholino and 2mM sema3A1 (Table 8). Thus, co-injections of sub-threshold concentrations of NRP1a and L1.1 morpholinos with 0.1 mM plexinA3 morpholino1 are not sufficient to induce aberrant growth of primary motor axons.

4 DISCUSSION

Expression of NRP1a and plexinA3 in motor neurons is necessary for the correct outgrowth of ventral motor nerves in embryonic zebrafish. Synergistic effects of injecting morpholinos to NRP1a or plexinA3 together with morpholinos to the potential ligands VEGF, sema3A1 and sema3A2 suggest a role of NRP1a and plexinA3 in integrating signals of several ligands in the trunk environment.

4.1 Identification of a plexinA3 homolog in zebrafish

The full length cDNA of plexinA3 was cloned using a combination of PCR-based techniques. The structure of plexinA3, comprising a Sema domain, three MRS (Met Related Sequence) domains, four IPT (Immunoglobulin-like fold shared by Plexins and Transcription factors) motifs and a highly conserved intracellular SP (Sex Plexin) domain, is identical to that of other A-type plexin molecules, indicating that the cloned molecule is a member of the plexinA subfamily. Other subgroups of the plexin family contain less than three or atypical MRS motifs or potential cleavage sites for furin-like convertases, which distinguishes them from A-type plexins.

PlexinA3 in zebrafish shares 73% amino acid identity with human and mouse plexinA3. The observed degrees of amino acid identities are above the expected range for related recognition molecules in phylogenetically distinct species. For example, the zebrafish L1-homologs L1.1 and L1.2 share only about 40% amino acid identity with human L1 (Tongiorgi et al., 1995). Zebrafish plexinA3 and plexinA4 share approximately 60% amino acid identity and compared to other members of the plexinA family, amino acid identity ranges between 60% and 68%. This indicates an overall high degree of homology within the plexinA subfamily. For identification of novel plexins in zebrafish, degenerate primers based on known plexinA1 sequences were used, but the obtained plexin turned out to be plexinA3. This may be explained by comparing the zebrafish plexinA3 amino acid sequence with sequences of human and mouse plexinA1, as well as *Xenopus* plexinA, which is the only identified plexinA in *Xenopus* to date and is the *Xenopus* homolog of plexinA1 (Ohta et al., 1995). The degree of amino acid identities between zebrafish plexinA3 and plexinA1 homologs is

between 67% and 68%, which is only slightly less than the 73% amino acid identity between zebrafish plexinA3 and mouse and human plexinA3, indicating that plexinA3 and plexinA1 are closely related and degenerate primers were not sufficient to distinguish between the two plexins.

To confirm that the newly cloned plexin sequence represents zebrafish plexinA3, the entire ORF of the molecule was amplified from zebrafish brain cDNA by PCR. To avoid unspecific binding of primers in conserved regions and thus, amplification of other plexin homologs, the primers used for this PCR were located in 5' and 3' untranslated regions of the hypothetical plexinA3 gene, which are known to be less conserved than the coding sequences of members of the same gene family. All amplified PCR products were sequenced twice or more. Thus the obtained sequence was verified several times.

Due to genome duplication events that involved large chromosome sections in ray-finned fish, the zebrafish genome often contains two copies of mammalian orthologs (Postlethwait et al., 1999). For example, mammalian sema3A, neuropilin-1 and L1 all have two homologs in zebrafish (Tongiorgi et al., 1995; Roos et al., 1999; Halloran et al., 2000; Yu et al., 2004; Bovenkamp et al., 2004; Martyn and Schulte-Merker, 2004). A second paralog of plexinA3 in zebrafish may exist but a search of the zebrafish genome (Ensembl) did not identify any additional gene. Searching the database for plexins resulted in a large number of plexin-related sequences, none of which was likely to be paralog of plexinA3. To date, only two other members of the plexin family have been characterized, plexinA4 and plexinD1 in zebrafish and neither for plexinA4 nor for plexinD1, paralogs have been described (Yeo et al., 2004; Torres-Vazquez et al., 2004).

4.2 PlexinA3 is expressed in the zebrafish embryonic nervous system

PlexinA3 mRNA was detected in distinct regions of the central nervous system at 24 hpf, including the telencephalon, epiphysis, tegmentum, trigeminal sensory ganglion neurons, hindbrain and spinal cord. At 16 hpf, plexinA3 mRNA is also detectable in the nervous system, but the expression pattern is more diffuse than in 24 hpf embryos. In mammals, plexinA3 is the most ubiquitously expressed plexin family member within regions of the developing nervous system that are known to contain semaphorin-responsive neurons (Cheng

et al., 2001). This finding is in agreement with the broad expression patterns of zebrafish plexinA3 observed in this study.

4.3 PlexinA3 and NRP1a are expressed by primary motor neurons during motor axon growth

The expression patterns of NRP1a and plexinA3 mRNAs during early trunk development were analyzed using in situ hybridization. The distribution of NRP1a mRNA has been previously described (Lee et al., 2002; Bovenkamp et al., 2004; Martyn and Schulte-Merker, 2004; Yu et al., 2004). In these studies, expression of NRP1a mRNA in motor neurons has been identified judged by position. Applying the same probe that was used by Michael Klagsbrun and colleagues (Lee et al., 2002) confirmed the expression of NRP1a in cell clusters at the ventral edge of the spinal cord. Double-labeling of these NRP1a expressing cells with an antibody to acetylated tubulin, which is specific for neurons showed that tubulin-positive ventral axons exited from NRP1a-positive somata. Double-labeling experiments with probes for islet-1 and islet-2, which are common markers for primary motor neurons (Inoue et al., 1994; Appel et al., 1995; Tokumoto et al., 1995), revealed, that the cells in the ventral spinal cord expressing NRP1a are also islet-positive, indicating that these cells are motor neurons.

The two islet mRNAs detect different subtypes of primary motor neurons. Islet-1 specifically labels MiP and RoP while islet-2 is only found in CaP and VaP. Double labeling with the NRP1a probe revealed that NRP1a expression is not detectable in the most rostral motor neuron indicating that NRP1a is only expressed by MiP, CaP and VaP, but not in RoP. Thus, axon guidance of the lateral motor nerve is probably not mediated by NRP1a.

PlexinA3 mRNA in the trunk has been located in cell clusters at the ventral edge of the spinal cord at 24 hpf, and their number and distribution strongly suggests that these cells are motor neurons. NRP1a, L1.1 and L1.2, which are potential co-receptors for plexinA3 are expressed in the same subset of cells (Tongiorgi et al., 1995; Lee et al., 2002; Bovenkamp et al., 2004; Martyn and Schulte-Merker, 2004; Yu et al., 2004) opening the possibility of local interactions between those molecules.

Both, NRP1a and plexinA3 appear to be expressed in primary motor neurons in 16 hpf and 24 hpf embryos before and during motor axon growth in the trunk, which occurs between 18 and 33 hpf. This is in agreement with a functional role in motor axon guidance. At 24 hpf NRP1a expression is only detectable in the most caudal regions of the trunk whereas plexinA3 is also present in putative motor neurons of more rostral segments. This observation could be an indication for distinct roles of the two molecules where, at later time points, plexinA3 is still required, but not NRP1a.

4.4 Morpholino injections probably directly affect motor neurons

Several observations suggest that the effects observed after injection of morpholinos were directly due to reduced NRP1a or plexinA3 expression in the motor neurons, rather than being secondary to alterations of the trunk or spinal cord environment. Two morpholinos of non-overlapping sequence show very similar effects. However, both plexinA3 morpholinos induce the same phenotypes at similar rates, whereas the second NRP1a morpholino was only sufficient to reproduce the branching and multiple exits effects observed after injection of similar concentrations of NRP1a morpholino1, but not displaced cells. This was probably due to a lower efficiency of NRP1a morpholino2, which was also demonstrated by the overall lower frequencies of aberrations. Differences in efficiency of distinct morpholinos to the same mRNA are common and have been observed for other molecules, e.g. tenascin-R (Becker et al., 2003).

Vertical and horizontal myosepta formed and differentiated correctly in NRP1a and plexinA3 morpholino injected embryos as indicated by tenascin-C labeling of vertical myosepta and labeling of muscle pioneer cells at the horizontal myoseptum, a critical choice point for growing motor axons, with an antibody to engrailed (Melancon et al., 1997). This suggests that the somitic pathway of motor axons was not grossly changed in morpholino injected embryos.

Even though NRP1a and plexinA3 mRNAs are expressed in the dorsal spinal cord in uninjected embryos at 16 hpf, the organization of the spinal cord appeared unaltered in morpholino injected embryos at 24 hpf. Labeling with the 3A10 antibody indicated correct positioning of commissural primary ascending motor neurons and their axons in the dorsal

spinal cord. Mauthner axons in the ventral spinal cord were also unaffected by morpholino injections. Immunolabeling with an antibody to islet-1/-2 proteins indicated normal densities and positioning of Rohon-Beard cells and motor neurons, with the notable exception of those putative motor neurons that had migrated out of the spinal cord in NRP1a morpholino treated embryos. Thus, motor axon aberrations were probably not secondary to effects on the spinal cord organization. Several other axon trajectories, such as the dorso-ventral diencephalic tract, the posterior commissure in the head, or peripheral axons of Rohon-Beard neurons all appeared normal, indicating that there was no generalized alteration of axon growth in morpholino injected embryos. However, defects of MiP and RoP axons cannot be excluded, because these could not be selectively labeled.

All three effects of NRP1a morpholino knock down could also be partially rescued by overexpression of NRP1a mRNA. This argues that the effect of the morpholino is due to reduced NRP1a mRNA levels. The fact that the rescue was not complete may best be explained by the mosaic expression of NRP1a protein after mRNA injection. Moreover, the fact that during late phases of axon growth (24 hpf), protein expression from the exogenous mRNA could hardly be detected by immunohistochemistry for the myc epitope indicates diminished abundance of the exogenous protein as embryos develop. A similar incomplete rescue of motor axon phenotypes by mRNA overexpression has also been observed by others (McWhorter et al., 2003). Overexpression of the complete open reading frame of plexinA3 (5679 bp) was not possible since several attempts failed to clone the large full-length gene into the overexpression vector. Similar problems occurred for the overexpression of tenascin-C, which has an open reading frame of 5133 bp (Schweitzer et al., 2005).

4.5 Motor axons and trunk vessels develop independently

In addition to affecting motor axon growth, morpholinos to NRP1a inhibit blood vessel formation (Lee et al., 2002), which was confirmed in this study. However, the motor axon phenotypes observed after NRP1a morpholino injection are probably independent of altered blood vessel formation. This is suggested by the observation that treatment with a morpholino to VEGF inhibits the formation of the vasculature in the trunk, but does not detectably influence the outgrowth of the ventral motor nerve. Sema3A1 morpholinos also affect blood

vessel formation in the trunk (Shoji et al., 2003), but the morpholino used here had no detectable effect on motor axons when injected alone. Thus, early motor axon development is probably independent of blood vessel formation.

4.6 NRP1a and plexinA3 in primary motor neurons may be receptors for repellent signals in the somite environment

Three different phenotypes were observed after application of NRP1a morpholino and two of these were also induced by plexinA3 morpholino: Knockdown of both genes induced branching of ventral motor nerves and additional nerves exiting the spinal cord, whereas the ventral migration of putative motor neurons out of the spinal cord was only observed after injection of NRP1a morpholinos. Branching of the ventral motor nerve was either due to one of the three primary motor axons taking an aberrant path, or due to axonal branching of a primary motor axon. This cannot be differentiated in anti-tubulin labeled preparations. However, this result clearly shows axon growth into territories normally not invaded. This is also true for multiple exit phenotypes and is in agreement with the notion that NRP1a and plexinA3 are receptors for axon-repellent signals (Cheng et al., 2001; Bagri and Tessier-Lavigne, 2002). Reducing NRP1a or plexinA3 expression may release axons from these repulsive signals.

Interestingly, the majority of nerve branches were directed into the posterior part of the somite after injection of NRP1a and plexinA3 morpholinos (NRP1a: 69.6%, plexinA3: 81.9%). Additional exit points from the spinal cord were also most frequently observed in the posterior part of the somite (NRP1a: 74.7%, plexinA3: 72.8%). Transcripts for the potential NRP1a and plexinA3 ligand sema3A2 are concentrated in the posterior part of the somite (Roos et al., 1999) provoking the speculation that sema3A2 acts as a repulsive guidance cue through NRP1a and plexinA3. However, other potential ligands of NRP1a show a different distribution. Sema3A1 is expressed in the dorsal and ventral somite, leaving a corridor at the horizontal myoseptum that is free of sema3A1 transcript.

Overexpression of the putative NRP1a ligands sema3A1 and sema3A2 in transgenic animals or by mRNA injections both induced truncations of ventral motor nerves (Roos et al., 1999; Halloran et al., 2000). This can be considered a complementary phenotype to the abnormal

axon branching and multiple exits observed in NRP1a and plexinA3 morpholino treated animals. Similar complementary phenotypes are also observed when the function of axon-repellent chondroitin sulfates is analyzed in the pathway of the ventral motor nerve. Enzymatic removal of these glycostructures induces abnormal branching of ventral motor nerves, whereas injecting a chondroitin sulfate mixture leads to nerve truncations (Bernhardt and Schachner, 2000). Therefore, the excessive growth of primary motor axons observed in this study, further supports the hypothesis that NRP1a and plexinA3 are receptors for repellent semaphorin ligands in the somite environment.

Overexpression of NRP1a mRNA alone did not induce aberrations in ventral motor nerves while in transgenic mice, overexpression of NRP1 induces abnormal sprouting and defasciculation of nerves (Kitsukawa et al., 1995). It is possible that the dose of NRP1a protein that was reached in our experiments was too low to induce such effects, or that these would occur only later, when secondary motor axons join the nerves.

After injection of NRP1a morpholino, dorso-ventrally elongated cells are found along the ventral motor nerve pathway. The fact that these ectopic cells were labeled by antibodies to the neuronal marker tubulin and to islet-1, a marker of motor neurons in zebrafish (Tokumoto et al., 1995), suggests that ectopic cells were motor neurons. Their shape and position is suggestive of a scenario in which these cells migrated out of the spinal cord along the motor axon pathway. One possible explanation for this phenotype is that normally, repulsive signals from the somite restrict motor neuron somata to the spinal cord and that this repulsion is released under conditions of reduced NRP1a expression. Interestingly, this phenotype is reminiscent of motor neurons exiting the ventral spinal cord after the ablation of so-called boundary cap cells at the motor axon exit point in chicks. The molecular signals from boundary cap cells are unknown (Vermeren et al., 2003). Injection of plexinA3 morpholino did not lead to abnormal positioning of neurons in the somite, suggesting that the restriction of neurons to the spinal cord is not dependent on plexinA3 signaling.

4.7 Multiple guidance cues are present in the trunk environment

Synergistic effects of morpholinos to sema3A1, sema3A2 and VEGF in combination with sub-threshold concentrations of NRP1a or plexinA3 morpholino suggest that these molecules

are interdependent in vivo. The fact that morpholino knock down of individual ligands was ineffective suggests that some of these potential ligands for NRP1a or plexinA3 act redundantly and may substitute for each other in experiments in which morpholinos to only a single ligand were injected. It is speculated, that similar redundant effects are the reason for the more severe abnormalities in peripheral projections of sensory neurons found in neuropilin-1 knockout mice compared to the same, but less severe, phenotypes in sema3A knockout mice where other neuropilin-1 ligands might compensate for the loss of sema3A (Kitsukawa et al., 1997).

The observation that, when injected alone, VEGF morpholino had a severe effect on blood vessel formation but no detectable effect on motor axons indicates that the VEGF signal is indispensable for angiogenesis, but not for axon growth. Nevertheless, VEGF appears to contribute to the guidance of motor axons as revealed in co-injection experiments with NRP1a morpholino. The same is true for sema3A1 and sema3A2. However, not all combinations of morpholinos tested elicit all of the phenotypes observed when NRP1a expression alone is knocked down at above threshold concentrations (Table 5) and the multiple exit phenotype is not elicited by any of the combinations, suggesting some non-overlapping functions of additional ligands. For example, sema3D has been shown to signal through NRP1a in the developing zebrafish CNS (Wolman et al., 2004) and the class 3 semaphorin sema3G (Halloran et al., 1998; Stevens and Halloran, 2005), which may act through NRP1a, is expressed in adaxial cells of the somite during motor axon development.

Interestingly, co-injections of VEGF morpholinos with NRP1a morpholinos induced phenotypes similar to those of co-injecting semaphorin morpholinos with NRP1a morpholinos (branching and ventrally migrating cells), even though mRNAs for VEGF and individual sema3A homologs are all differentially expressed in the somite environment (Fig. 11). Moreover, VEGF and semaphorins have been described as functional competitors in the vascular system (Miao et al., 1999) and VEGF has been reported to promote neurite outgrowth in vitro (Sondell et al., 2000; Bocker-Meffert et al., 2002; Rosenstein et al., 2003), whereas sema3A mostly repels axons (Bagri and Tessier-Lavigne, 2002; He et al., 2002). Disturbing the interactions of different ligands with NRP1a on motor axons in vivo may destabilize a complex axon guidance system. This destabilization may then result in comparable phenotypes. Similarly, overexpression and morpholino knock down of sema3A1

both inhibit the formation of blood vessels in the trunk of embryonic zebrafish (Shoji et al., 2003).

Although NRP1a or plexinA3 morpholinos cause aberrant motor axon growth, there is still a large population of unaffected axons. Only 35.1% or 28.9% of all segments analyzed are affected after injection of NRP1a or plexinA3 morpholinos, respectively. Truncations were rarely found and although ventral motor nerves had abnormal branches, the remaining part of the nerve still grew in its correct position after knockdown of NRP1a or plexinA3. There are multiple guidance cues present in the somite, which may act independently but result in similar responses for motor nerves growing out of the spinal cord. Some of these (sema3A1, sema3A2 and VEGF) may act through NRP1a as shown in this study, whereas others, such as chondroitin sulfates or tenascin-C (Bernhardt and Schachner, 2000; Schweitzer et al., 2005) may act on the axons in a different way. The presence and parallel action of multiple guidance cues in motor axon outgrowth is not unique to zebrafish, but has also been recognized in other vertebrates (Tannahill et al., 2000; Schneider and Granato, 2003).

4.8 Sema3A signals through plexinA3

Contradictory findings have been described in the literature arguing whether sema3A can bind to plexinA3 or not. In vitro studies in transfected COS cells showed, that plexinA1 or plexinA2, but not plexinA3 mediate a contraction response (considered to be the equivalent of growth cone collapse in neuronal cells) to sema3A or sema3F when co-expressed with neuropilin-1 (Takahashi and Strittmatter, 2001) suggesting that plexinA3 does not interact with sema3A. However, the significance of these studies for normal physiological responses of neurons to sema3A and sema3F in vivo was not known but has been investigated by analysis of the plexinA3 knockout mouse, which revealed, that responses of sympathetic ganglion neurons to sema3A are at least partially impaired in these mice (Cheng et al., 2001). The same neurons completely lose their repulsive responses to sema3F, suggesting stronger repulsive effects for sema3F and plexinA3 signaling than for sema3A and plexinA3 signaling. The results obtained from the present study indicating that plexinA3 sema3A morpholinos act synergistically to induce aberrations of motor axon outgrowth, are in agreement with the in

vivo results from Cheng et al., 2001 and further demonstrate that plexinA3 is a functional receptor for sema3A in vivo.

Responses to sema3F are completely and responses to sema3A are partially dependent on plexinA3 (Cheng et al., 2001). The strong effects observed after knockdown of plexinA3 may thus be a result of disrupting the signal from more than on ligand acting through plexinA3, for instance sema3F. Two sema3F homologs have been cloned in zebrafish, but so far, their expression and function has only been characterized in cranial neural crest migration (Yu and Moens, 2005). Whether sema3F is expressed in the zebrafish trunk is currently unknown.

4.9 PlexinA3 and NRP1a may not be co-receptors but function in parallel pathways

Primary motor neurons express NRP1a and plexinA3, knockdown experiments with NRP1a and plexinA3 morpholinos result in partially overlapping phenotypes, and both molecules seem to be receptors for the same ligands as indicated by the sub-threshold experiments with sema3A1, sema3A2 and VEGF. These findings could either be explained by a direct interaction of NRP1a and plexinA3 or by parallel signaling of the two receptors through different co-receptors resulting in similar phenotypes.

Co-injection experiments of NRP1a and plexinA3 morpholinos, both at concentrations that did not induce aberrant growth of motor nerves when injected alone, did not show any synergistic effects of the two morpholinos. Thus, it seems that the two molecules act in different pathways where a slight reduction of NRP1a in one receptor complex and plexinA3 in another does not lead to synergistic effects of single morpholino injections. Instead, both receptor complexes are compromised slightly, but they are still functional. This interpretation is in agreement with the results form other studies showing that sema3A binds preferentially to neuropilin-1 and sema3F has a higher affinity for neuropilin-2 (Chen et al., 1997; Giger et al., 1998; Takahashi et al., 1998). Furthermore, a more recent study demonstrated that neuropilin-1 associates preferentially but not exclusively with plexinA4 and neuropilin-2 with plexinA3 (Yaron et al., 2005) supporting a model where a receptor complex composed of neuropilin-2 and plexinA3 mediates axon repulsion by sema3A whereas sema3F signals preferentially through a receptor complex composed of neuropilin-1 and plexinA4.

Thus, it is likely that NRP1a and plexinA3 function in parallel pathways and their signaling and binding partners are other plexins and neuropilins, respectively. Other A-type plexins have been demonstrated to be potential binding partners for neuropilin-1 in mammals (Takahashi and Strittmatter, 2001; Suto et al., 2003) and their, yet unidentified, zebrafish homologs may be functional co-receptors for NRP1a in motor axon guidance.

Since neuropilin-2 forms a receptor complex with plexinA3 in mice (Yaron et al., 2005) it might also be a component of the plexinA3 receptor in motor axon outgrowth in zebrafish. Zebrafish homologs of neuropilin-2, designated NRP2a and NRP2b, as well as a second homolog of neuropilin-1, NRP1b, have been cloned and their expression patterns have been described (Lee et al., 2002; Yu et al., 2004; Bovenkamp et al., 2004; Martyn and Schulte-Merker, 2004). Strong expression in motor neurons, similarly to NRP1a expression, has not been demonstrated, but it is possible that weaker expression levels might have been overlooked. Alternatively, plexinA3 might bind sema3A independently of neuropilins. For instance, a class 3 semaphorin, sema3E has recently been shown to bind directly to plexinD1 and neuropilins are not required to mediate the effects of sema3E in patterning the vasculature (Gu et al., 2005).

4.10 PlexinA3 might function outside the nervous system

Co-injection of plexinA3 and VEGF morpholinos resulted in a significant increase in the frequency of multiple exits suggesting that VEGF signaling requires plexinA3. Similarly, the sub-threshold experiments with NRP1a and VEGF showed that VEGF acts through NRP1a and plays a role in restricting neurons and axons to the spinal cord. VEGF has been previously described to promote neurite outgrowth in vitro (Sondell et al., 2000; Rosenstein et al., 2003), but in these studies VEGF-R2 (Flk-1) was identified as a receptor component to mediate intracellular signaling. It is possible that VEGF acts through plexinA3 in motor axon outgrowth in zebrafish, but since statistical tests produced only low significance (Fishers Exact test: $P = 0.026$, compared to co-injection of plexinA3 5mm morpholino and sema3A1 morpholino), more specific control experiments, such as co-injection of sub-threshold concentrations of VEGF and plexinA3 5mm morpholinos. In addition, in vitro binding studies, would be required to confirm interactions between VEGF and plexinA3.

Interestingly, there was also expression of plexinA3 mRNA outside the nervous system in the heart and in non-neuronal regions of the tail. These novel findings support the hypothesis that plexinA3 might participate in heart and blood vessel development, similar to zebrafish plexinD1, which mediates sema3A dependent intersegmental vessel patterning (Torres-Vazquez et al., 2004). In the mouse, plexinD1 can enhance sema3A and sema3C binding to neuropilin-1 (Torres-Vazquez et al., 2004). To date, no evidence has been found, that plexins form receptors for VEGF that function in axon guidance. However, VEGF and sema6D have been reported to signal through complexes containing plexinA1 and VEGF-receptor2 in cardiac morphogenesis (Toyofuku et al., 2004). Another member of the plexinA subfamily, plexinA2, plays a role in cardiac neural crest development, probably by mediating sema3C signals (Brown et al., 2001).

4.11 L1.1 may not play a role in primary motor axon guidance

Several findings suggest that L1.1 does not play a crucial role during primary motor axon outgrowth, even though the protein is expressed on growing motor axons. Injection of L1.1 morpholinos does not induce aberrant growth of motor nerves, even at high concentrations of up to 2 mM. This concentration of the morpholino almost completely abolishes detectability of L1.1 protein for up to three days post fertilization as shown by Western blot analysis in 3-day old zebrafish demonstrating that the morpholino is functional. Additionally, co-injection of L1.1 morpholino with the sub-threshold concentration of NRP1a morpholino did not affect motor axon outgrowth. It is possible that L1.2, which is the second zebrafish homolog of L1 and, like L1.1, is expressed in motor neurons (Tongiorgi et al., 1995), could compensate for the loss of L1.1. A potential role of L1.2 in motor axon guidance has not been investigated in this study.

4.12 NRP1a and plexinA3 receptors integrate multiple signals

In combination experiments with plexinA3 and sema3A1 morpholinos, the frequency of aberrantly branched ventral motor nerves (60.2%) was higher than the frequency of multiple exits of motor nerves (37.8%) whereas combination of plexinA3 with sema3A2 morpholinos

induced the multiple exit phenotype (52.3%) rather than the branching phenotype (33.9%) (Table 8). Since comparable numbers of embryos were tested, differences in the frequency of different phenotypes are reflected in the degree of significance that is much stronger for frequencies above 50% ($P < 0.001$), whereas frequencies below 40% showed a low degree of significance ($P < 0.05$). Thus, it seems that knockdown of plexinA3 combined with sema3A1 knockdown induces primarily abnormal branching, whereas the combination with sema3A2 causes preferentially multiple exits of motor nerves (Table 9). Combined injections of plexinA3 and VEGF morpholinos also show only a low degree of significance ($P = 0.026$) suggesting that VEGF may contribute to prevent multiple exits of nerves but does not seem to play a major role (Table 9).

Table 9 Overview of phenotypes induced by single or combined morpholino injections.

receptor	**ligand**	**branching**	**multiple exits**	**displaced neurons**
NRP1a	/	+++	+++	+++
NRP1a +	sema3A1	–	–	+++
NRP1a +	sema3A2	+++	–	+++
NRP1a +	VEGF	++	–	+++
plexinA3	/	+++	+++	–
plexinA3 +	sema3A1	+++	+	–
plexinA3 +	sema3A2	+	+++	–
plexinA3 +	VEGF	–	+	–

Shown are statistical significances obtained from Fisher's Exact tests against appropriate controls. + = $P < 0.05$, ++ = $P < 0.01$, +++ = $P < 0.001$.

Injection of NRP1a morpholinos results in three phenotypes that are only partially reproduced in sub-threshold experiments with potential ligands. The combination of NRP1a morpholino with sema3A1 morpholino does not induce branching or multiple exits, but displaced neurons and the combination of NRP1a morpholino and sema3A2 morpholino leads to branching and displaced neurons (Table 9). Knockdown of VEGF in combination with NRP1a induces branching and displaced neurons (Table 9). These results are summarized in Fig. 29.

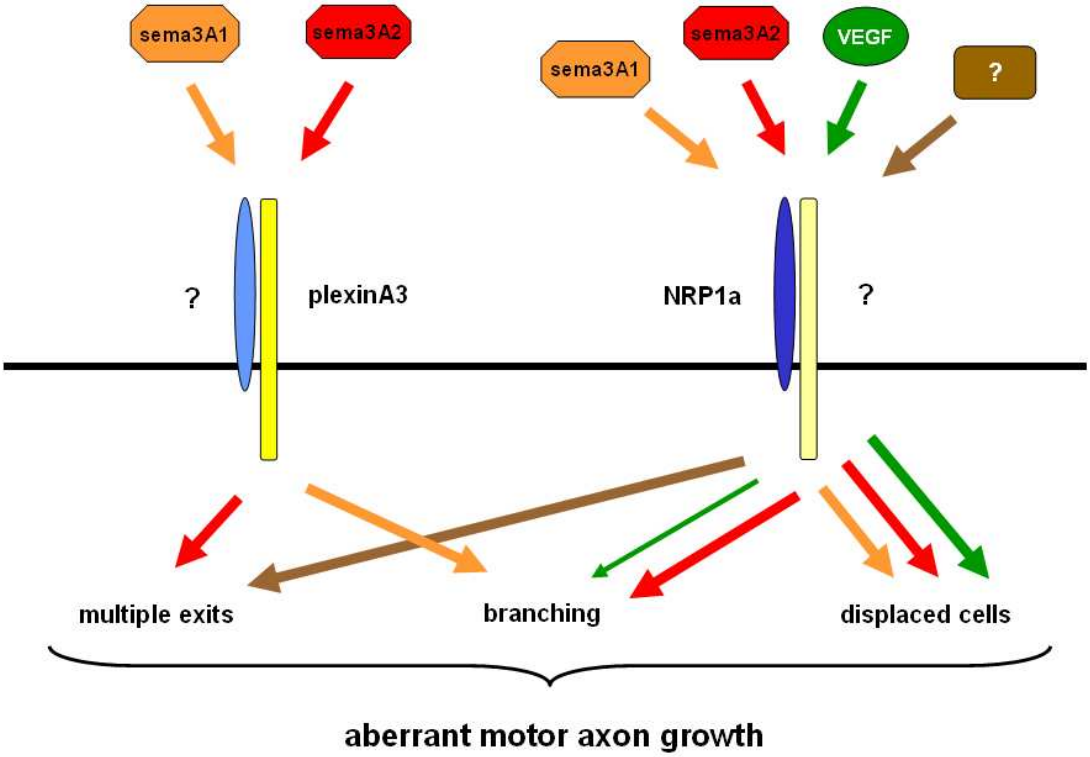

Fig. 29 A model for primary signaling pathway and aberrations induced by the loss of different components in the outgrowth of trunk motor axons. Semaphorins and VEGF signal through NRP1a (blue) and plexinA3 (yellow) receptors. Morpholinos against various ligands (sema3A1: orange, seama3A2: red, VEGF: green, unknown ligand: brown) expressed in the somite environment result in different types of motor axon aberrations. Colors of arrows indicate the identity of the ligand they originate from. Thickness of arrows represents the degree of significance, observed for the corresponding effect of the morpholino injection. Injections that resulted in low levels of significance ($P < 0.05$) have been omitted for clarity.

5 SUMMARY

Neuropilin is the ligand-binding component of a receptor complex for axon-repellent semaphorins, whereas plexin is the signal-transducing component. Neuropilin-1, a receptor for class 3 semaphorins and vascular endothelial growth factor (VEGF), functions both in angiogenesis and axon growth. In zebrafish, neuropilin-1a and a novel zebrafish plexin, homologous to mammalian plexinA3, are strongly expressed in primary motor neurons in the trunk during motor axon development. Reducing the expression of neuropilin-1a or plexinA3 using anti-sense morpholino oligonucleotides induced aberrant branching of ventral motor nerves and additional exit points of motor nerves from the spinal cord. A third phenotype, ventral migration of neurons out of the spinal cord along the motor axon pathway was only found after knockdown of neuropilin-1a. Morpholinos to neuropilin-1a or plexinA3 induced aberrations of motor axons in a dose-dependent manner. Trunk structures and other axons in the spinal cord and head appeared unaffected by the morpholino treatment. The phenotypes induced by the neuropilin-1a morpholino could be partially rescued by co-injecting neuropilin-1a mRNA. In addition, neuropilin-1a morpholino treatment disturbed normal formation of blood vessels in the trunk of 24 hours post-fertilization (hpf) embryos, as shown by microangiography. Morpholinos to VEGF also disturbed formation of blood vessels, but did not affect motor axons, indicating that correct formation of blood vessels is not needed for the growth of primary motor axons. Morpholinos to the semaphorin3A homologs semaphorin3A1 and semaphorin3A2 also had no effect on motor axon growth. However, combined injections of neuropilin-1a morpholino, at a concentration that did not elicit axonal aberrations when injected alone, with VEGF, semaphorin 3A1 or semaphorin 3A2 morpholinos synergistically increased the proportion of embryos showing aberrant motor axon growth. Similarly, injection of sub-threshold concentrations of plexinA3 morpholino in combination with semaphorin3A1, semaphorin3A2 or VEGF morpholinos, reproduces phenotypes observed after injection of plexinA3 morpholino alone. Thus, neuropilin-1a and plexinA3 may integrate signals from several ligands in primary motor neurons and are needed for proper segmental growth of primary motor nerves in zebrafish. These findings suggest that interactions of multiple ligands with neuropilin-1a and plexinA3 play a role in the patterning of peripheral nerves in zebrafish.

6 LITERATURE

Altschul,S.F., Gish,W., Miller,W., Myers,E.W., and Lipman,D.J. (1990). Basic local alignment search tool. J Mol Biol *215*, 403-10.

Appel,B., Korzh,V., Glasgow,E., Thor,S., Edlund,T., Dawid,I.B., and Eisen,J.S. (1995). Motoneuron fate specification revealed by patterned LIM homeobox gene expression in embryonic zebrafish. Development *121*, 4117-25.

Bagnard,D., Lohrum,M., Uziel,D., Püschel,A.W., and Bolz,J. (1998). Semaphorins act as attractive and repulsive guidance signals during the development of cortical projections. Development *125*, 5043-53.

Bagri,A. and Tessier-Lavigne,M. (2002). Neuropilins as Semaphorin receptors: in vivo functions in neuronal cell migration and axon guidance. Adv Exp Med Biol *515*, 13-31.

Bartsch,U. (1996). The extracellular matrix molecule tenascin-C: Expression in vivo and functional characterization in vitro. Prog Neurobiol *49*, 145-161.

Bateman,A., Birney,E., Durbin,R., Eddy,S.R., Howe,K.L., and Sonnhammer,E.L. (2000). The Pfam protein families database. Nucleic Acids Res *28*, 263-6.

Bates,D., Taylor,G.I., Minichiello,J., Farlie,P., Cichowitz,A., Watson,N., Klagsbrun,M., Mamluk,R., and Newgreen,D.F. (2003). Neurovascular congruence results from a shared patterning mechanism that utilizes Semaphorin3A and Neuropilin-1. Dev Biol *255*, 77-98.

Beattie,C.E. (2000). Control of motor axon guidance in the zebrafish embryo. Brain Res Bull *53*, 489-500.

Becker,C.G., Lieberoth,B.C., Morellini,F., Feldner,J., Becker,T., and Schachner,M. (2004). L1.1 is involved in spinal cord regeneration in adult zebrafish. J. Neurosci *24*, 7837-7842.

Becker,C.G., Schweitzer,J., Feldner,J., Becker,T., and Schachner,M. (2003). Tenascin-R as a repellent guidance molecule for developing optic axons in zebrafish. J Neurosci *23*, 6232-6237.

Becker,T., Becker,C.G., Schachner,M., and Bernhardt,R.R. (2001). Antibody to the HNK-1 glycoepitope affects fasciculation and axonal pathfinding in the developing posterior lateral line nerve of embryonic zebrafish. Mech. Dev. *109*, 37-49.

Becker,T., Ostendorff,H.P., Bossenz,M., Schlüter,A., Becker,C.G., Peirano,R.I., and Bach,I. (2002). Multiple functions of LIM domain-binding CLIM/NLI/Ldb cofactors during zebrafish development. Mech Dev *117*, 73-83.

Bernhardt,R.R., Chitnis,A.B., Lindamer,L., and Kuwada,J.Y. (1990). Identification of spinal neurons in the embryonic and larval zebrafish. J. Comp. Neurol. *302*, 603-616.

Bernhardt,R.R., Goerlinger,S., Roos,M., and Schachner,M. (1998). Anterior-posterior subdivision of the somite in embryonic zebrafish: Implications for motor axon guidance. Dev Dyn *213*, 334-47.

Bernhardt,R.R. and Schachner,M. (2000). Chondroitin sulfates affect the formation of the segmental motor nerves in zebrafish embryos. Dev Biol *221*, 206-219.

Bocker-Meffert,S., Rosenstiel,P., Rohl,C., Warneke,N., Held-Feindt,J., Sievers,J., and Lucius,R. (2002). Erythropoietin and VEGF promote neural outgrowth from retinal explants in postnatal rats. Invest Ophthalmol Vis Sci *43*, 2021-6.

Bovenkamp,D.E., Goishi,K., Bahary,N., Davidson,A.J., Zhou,Y., Becker,T., Becker,C.G., Zon,L.I., and Klagsbrun,M. (2004). Expression and mapping of duplicate neuropilin-1 and neuropilin-2 genes in developing zebrafish. Gene Expr Patterns *4*, 361-70.

Brown,C.B., Feiner,L., Lu,M.M., Li,J., Ma,X., Webber,A.L., Jia,L., Raper,J.A., and Epstein,J.A. (2001). PlexinA2 and semaphorin signaling during cardiac neural crest development. Development *128*, 3071-80.

Brümmendorf,T., Kenwrick,S., and Rathjen,F.G. (1998). Neural cell recognition molecule L1: from cell biology to human hereditary brain malformations. Curr Opin Neurobiol *8*, 87-97.

Cai,H. and Reed,R.R. (1999). Cloning and characterization of neuropilin-1-interacting protein: a PSD-95/Dlg/ZO-1 domain-containing protein that interacts with the cytoplasmic domain of neuropilin-1. J. Neurosci. *19*, 6519-6527.

Castellani,V., Chedotal,A., Schachner,M., Faivre-Sarrailh,C., and Rougon,G. (2000). Analysis of the L1-deficient mouse phenotype reveals cross-talk between Sema3A and L1 signaling pathways in axonal guidance. Neuron *27*, 237-49.

Chen,H., Chedotal,A., He,Z., Goodman,C.S., and Tessier-Lavigne,M. (1997). Neuropilin-2, a novel member of the neuropilin family, is a high affinity receptor for the semaphorins Sema E and Sema IV but not Sema III. Neuron *19*, 547-559.

Chen,H., He,Z., Bagri,A., and Tessier-Lavigne,M. (1998). Semaphorin-neuropilin interactions underlying sympathetic axon responses to class III semaphorins. Neuron *21*, 1283-1290.

Cheng,H.J., Bagri,A., Yaron,A., Stein,E., Pleasure,S.J., and Tessier-Lavigne,M. (2001). Plexin-a3 mediates semaphorin signaling and regulates the development of hippocampal axonal projections. Neuron *32*, 249-63.

Chenna,R., Sugawara,H., Koike,T., Lopez,R., Gibson,T.J., Higgins,D.G., and Thompson,J.D. (2003). Multiple sequence alignment with the Clustal series of programs. Nucleic Acids Res *31*, 3497-500.

Cohen,N.R., Taylor,J.S.H., Scott,L.B., Guillery,R.W., Soriano,P., and Furley,A.J.W. (1998). Errors in corticospinal axon guidance in mice lacking the neural cell adhesion molecule L1. Curr Biol *8*, 26-33.

Dahme,M., Bartsch,U., Martini,R., Anliker,B., Schachner,M., and Mantei,N. (1997). Disruption of the mouse L1 gene leads to malformations of the nervous system. Nat Genet *17*, 346-9.

Dickson,B.J. (2002). Molecular mechanisms of axon guidance. Science *298*, 1959-64.

Eisen,J.S. (1994). Development of motoneuronal phenotype. Annu Rev Neurosci *17*, 1-30.

Eisen,J.S., Myers,P.Z., and Westerfield,M. (1986). Pathway selection by growth cones of identified motoneurones in live zebra fish embryos. Nature *320*, 269-71.

Eisen,J.S., Pike,S.H., and Romancier,B. (1990). An identified motoneuron with variable fates in embryonic zebrafish. J. Neurosci. *10*, 34-43.

Ekker,S.C. and Larson,J.D. (2001). Morphant technology in model developmental systems. Genesis. *30*, 89-93.

Giger,R.J., Urquhart,E.R., Gillespie,S.K., Levengood,D.V., Ginty,D.D., and Kolodkin,A.L. (1998). Neuropilin-2 is a receptor for semaphorin IV: insight into the structural basis of receptor function and specificity. Neuron *21*, 1079-1092.

Gluzman-Poltorak,Z., Cohen,T., Shibuya,M., and Neufeld,G. (2001). Vascular endothelial growth factor receptor-1 and neuropilin-2 form complexes. J. Biol. Chem. *276*, 18688-18694.

Goishi,K., Lee,P., Davidson,A.J., Nishi,E., Zon,L.I., and Klagsbrun,M. (2003). Inhibition of zebrafish epidermal growth factor receptor activity results in cardiovascular defects. Mech Dev *120*, 811-22.

Gu,C., Rodriguez,E.R., Reimert,D.V., Shu,T., Fritzsch,B., Richards,L.J., Kolodkin,A.L., and Ginty,D.D. (2003). Neuropilin-1 conveys semaphorin and VEGF signaling during neural and cardiovascular development. Dev Cell *5*, 45-57.

Gu,C., Yoshida,Y., Livet,J., Reimert,D.V., Mann,F., Merte,J., Henderson,C.E., Jessell,T.M., Kolodkin,A.L., and Ginty,D.D. (2005). Semaphorin 3E and plexin-D1 control vascular pattern independently of neuropilins. Science *307*, 265-268.

Halloran,M.C., Sato-Maeda,M., Warren,J.T., Su,F., Lele,Z., Krone,P.H., Kuwada,J.Y., and Shoji,W. (2000). Laser-induced gene expression in specific cells of transgenic zebrafish. Development *127*, 1953-60.

Halloran,M.C., Severance,S.M., Yee,C.S., Gemza,D.L., and Kuwada,J.Y. (1998). Molecular cloning and expression of two novel zebrafish semaphorins. Mech Dev *76*, 165-8.

Haspel,J. and Grumet,M. (2003). The L1CAM extracellular region: a multi-domain protein with modular and cooperative binding modes. Front Biosci. *8*, 1210-25.

He,Z., Wang,K.C., Koprivica,V., Ming,G., and Song,H.J. (2002). Knowing how to navigate: mechanisms of semaphorin signaling in the nervous system. Sci STKE *2002*, RE1.

He,Z.G. and Tessier-Lavigne,M. (1997). Neuropilin is a receptor for the axonal chemorepellent Semaphorin III. Cell *90*, 739-751.

Inoue,A., Takahashi,M., Hatta,K., Hotta,Y., and Okamoto,H. (1994). Developmental regulation of islet-1 mRNA expression during neuronal differentiation in embryonic zebrafish. Develop Dynam *199*, 1-11.

Jowett,T. (2001). Two colour in situ hybridization - sequential alkaline phosphatase staining with chromogenic substrates of zebrafish embryos. In In situ Hybridization - a practical approach, D.G.Wilkinson, ed. (New York: Oxford University Press), pp. 107-127.

Kameyama,T., Murakami,Y., Suto,F., Kawakami,A., Takagi,S., Hirata,T., and Fujisawa,H. (1996). Identification of plexin family molecules in mice. Biochem. Biophys. Res. Commun. *226*, 396-402.

Kawasaki,T., Kitsukawa,T., Bekku,Y., Matsuda,Y., Sanbo,M., Yagi,T., and Fujisawa,H. (1999). A requirement for neuropilin-1 in embryonic vessel formation. Development *126*, 4895-4902.

Kimmel,C.B., Ballard,W.W., Kimmel,S.R., Ullmann,B., and Schilling,T.F. (1995). Stages of embryonic development of the zebrafish. Dev. Dyn. *203*, 253-310.

Kitsukawa,T., Shimizu,M., Sanbo,M., Hirata,T., Taniguchi,M., Bekku,Y., Yagi,T., and Fujisawa,H. (1997). Neuropilin-semaphorin III/D-mediated chemorepulsive signals play a crucial role in peripheral nerve projection in mice. Neuron *19*, 995-1005.

Kitsukawa,T., Shimono,A., Kawakami,A., Kondoh,H., and Fujisawa,H. (1995). Overexpression of a membrane protein, neuropilin, in chimeric mice causes anomalies in the cardiovascular system, nervous system and limbs. Development *121*, 4309-18.

Klagsbrun,M., Takashima,S., and Mamluk,R. (2002). The role of neuropilin in vascular and tumor biology. Adv Exp Med Biol *515*, 33-48.

Kolodkin,A.L., Levengood,D.V., Rowe,E.G., Tai,Y.T., Giger,R.J., and Ginty,D.D. (1997). Neuropilin is a semaphorin III receptor. Cell *90*, 753-762.

Kolodkin,A.L., Matthes,D.J., and Goodman,C.S. (1993). The semaphorin genes encode a family of transmembrane and secreted growth cone guidance molecules. Cell *75*, 1389-1399.

Lee,P., Goishi,K., Davidson,A.J., Mannix,R., Zon,L., and Klagsbrun,M. (2002). Neuropilin-1 is required for vascular development and is a mediator of VEGF-dependent angiogenesis in zebrafish. Proc Natl Acad Sci U S A *99*, 10470-5.

Liang,D., Xu,X., Chin,A.J., Balasubramaniyan,N.V., Teo,M.A., Lam,T.J., Weinberg,E.S., and Ge,R. (1998). Cloning and characterization of vascular endothelial growth factor (VEGF) from zebrafish, Danio rerio. Biochim Biophys Acta *1397*, 14-20.

Maestrini,E., Tamagnone,L., Longati,P., Cremona,O., Gulisano,M., Bione,S., Tamanini,F., Neel,B.G., Toniolo,D., and Comoglio,P.M. (1996). A family of transmembrane proteins with homology to the MET-hepatocyte growth factor receptor. Proc. Natl. Acad. Sci. U. S. A *93*, 674-678.

Mark,M.D., Lohrum,M., and Püschel,A.W. (1997). Patterning neuronal connections by chemorepulsion: the semaphorins. Cell Tissue Res *290*, 299-306.

Martyn,U. and Schulte-Merker,S. (2004). Zebrafish neuropilins are differentially expressed and interact with vascular endothelial growth factor during embryonic vascular development. Dev Dyn *231*, 33-42.

McWhorter,M.L., Monani,U.R., Burghes,A.H., and Beattie,C.E. (2003). Knockdown of the survival motor neuron (Smn) protein in zebrafish causes defects in motor axon outgrowth and pathfinding. J Cell Biol *162*, 919-31.

Melancon,E., Liu,D.W., Westerfield,M., and Eisen,J.S. (1997). Pathfinding by identified zebrafish motoneurons in the absence of muscle pioneers. J Neurosci *17*, 7796-804.

Miao,H.Q., Soker,S., Feiner,L., Alonso,J.L., Raper,J.A., and Klagsbrun,M. (1999). Neuropilin-1 mediates collapsin-1/semaphorin III inhibition of endothelial cell motility: functional competition of collapsin-1 and vascular endothelial growth factor-165. J Cell Biol *146*, 233-42.

Murakami,Y., Suto,F., Shimizu,M., Shinoda,T., Kameyama,T., and Fujisawa,H. (2001). Differential expression of plexin-A subfamily members in the mouse nervous system. Dev. Dyn. *220*, 246-258.

Myers,P.Z., Eisen,J.S., and Westerfield,M. (1986). Development and axonal outgrowth of identified motoneurons in the zebrafish. J Neurosci *6*, 2278-89.

Nakamura,F., Kalb,R.G., and Strittmatter,S.M. (2000). Molecular basis of semaphorin-mediated axon guidance. J. Neurobiol. *44*, 219-229.

Nakamura,F., Tanaka,M., Takahashi,T., Kalb,R.G., and Strittmatter,S.M. (1998). Neuropilin-1 extracellular domains mediate semaphorin D/III-induced growth cone collapse. Neuron *21*, 1093-1100.

Nasevicius,A., Larson,J., and Ekker,S.C. (2000). Distinct requirements for zebrafish angiogenesis revealed by a VEGF-A morphant. Yeast *17*, 294-301.

Neufeld,G., Kessler,O., and Herzog,Y. (2002). The interaction of Neuropilin-1 and Neuropilin-2 with tyrosine-kinase receptors for VEGF. Adv Exp Med Biol *515*, 81-90.

Ohta,K., Mizutani,A., Kawakami,A., Murakami,Y., Kasuya,Y., Takagi,S., Tanaka,H., and Fujisawa,H. (1995). Plexin: a novel neuronal cell surface molecule that mediates cell adhesion via a homophilic binding mechanism in the presence of calcium ions. Neuron *14*, 1189-1199.

Patel,N.H., Martin-Blanco,E., Coleman,K.G., Poole,S.J., Ellis,M.C., Kornberg,T.B., and Goodman,C.S. (1989). Expression of engrailed proteins in arthropods, annelids, and chordates. Cell *58*, 955-68.

Postlethwait,J., Amores,A., Force,A., and Yan,Y.L. (1999). The zebrafish genome. Methods Cell Biol *60*, 149-63.

Raper,J.A. (2000). Semaphorins and their receptors in vertebrates and invertebrates. Curr Opin Neurobiol *10*, 88-94.

Rathjen,F.G. and Schachner,M. (1984). Immunocytological and biochemical characterization of a new neuronal cell surface component (L1 antigen) which is involved in cell adhesion. Embo J. *3*, 1-10.

Rohm,B., Ottemeyer,A., Lohrum,M., and Puschel,A.W. (2000). Plexin/neuropilin complexes mediate repulsion by the axonal guidance signal semaphorin 3A. Mech Dev *93*, 95-104.

Roos,M., Schachner,M., and Bernhardt,R.R. (1999). Zebrafish semaphorin Z1b inhibits growing motor axons in vivo. Mech. Dev. *87*, 103-117.

Rose,T.M., Schultz,E.R., Henikoff,J.G., Pietrokovski,S., McCallum,C.M., and Henikoff,S. (1998). Consensus-degenerate hybrid oligonucleotide primers for amplification of distantly related sequences. Nucleic Acids Res *26*, 1628-35.

Rosenstein,J.M., Mani,N., Khaibullina,A., and Krum,J.M. (2003). Neurotrophic effects of vascular endothelial growth factor on organotypic cortical explants and primary cortical neurons. J Neurosci *23*, 11036-44.

Rupp,R.A., Snider,L., and Weintraub,H. (1994). Xenopus embryos regulate the nuclear localization of XMyoD. Genes Dev. *8*, 1311-1323.

Sambrook,J., Fritsch,E.F., and Maniatis,T. (1989). Molecular cloning. New York Cold Spring Harbour Laboratory Press.

Schneider,V.A. and Granato,M. (2003). Motor axon migration: a long way to go. Dev Biol *263*, 1-11.

Schweitzer,J., Becker,T., Lefebvre,J., Granato,M., Schachner,M., and Becker,C.G. (2005). Tenascin-C is involved in motor axon outgrowth in the trunk of developing zebrafish. Dev Dyn *in press*.

Shoji,W., Isogai,S., Sato-Maeda,M., Obinata,M., and Kuwada,J.Y. (2003). Semaphorin3a1 regulates angioblast migration and vascular development in zebrafish embryos. Development *130*, 3227-36.

Shoji,W., Yee,C.S., and Kuwada,J.Y. (1998). Zebrafish semaphorin Z1a collapses specific growth cones and alters their pathway in vivo. Development *125*, 1275-83.

Soker,S., Takashima,S., Miao,H.Q., Neufeld,G., and Klagsbrun,M. (1998). Neuropilin-1 is expressed by endothelial and tumor cells as an isoform-specific receptor for vascular endothelial growth factor. Cell *92*, 735-745.

Sondell,M., Sundler,F., and Kanje,M. (2000). Vascular endothelial growth factor is a neurotrophic factor which stimulates axonal outgrowth through the flk-1 receptor. Eur J Neurosci *12*, 4243-54.

Sonnhammer,E.L., Eddy,S.R., Birney,E., Bateman,A., and Durbin,R. (1998). Pfam: multiple sequence alignments and HMM-profiles of protein domains. Nucleic Acids Res *26*, 320-2.

Stevens,C.B. and Halloran,M.C. (2005). Developmental expression of sema3G, a novel zebrafish semaphorin. Gene Expr. Patterns. *5*, 647-653.

Summerton,J. (1999). Morpholino antisense oligomers: the case for an RNase H-independent structural type. Biochim. Biophys. Acta *1489*, 141-158.

Summerton,J., Stein,D., Huang,S.B., Matthews,P., Weller,D., and Partridge,M. (1997). Morpholino and phosphorothioate antisense oligomers compared in cell-free and in-cell systems. Antisense Nucleic Acid Drug Dev. *7*, 63-70.

Suto,F., Murakami,Y., Nakamura,F., Goshima,Y., and Fujisawa,H. (2003). Identification and characterization of a novel mouse plexin, plexin-A4. Mech. Dev. *120*, 385-396.

Takagi,S., Hirata,T., Agata,K., Mochii,M., Eguchi,G., and Fujisawa,H. (1991). The A5 antigen, a candidate for the neuronal recognition molecule, has homologies to complement components and coagulation factors. Neuron *7*, 295-307.

Takahashi,T., Fournier,A., Nakamura,F., Wang,L.H., Murakami,Y., Kalb,R.G., Fujisawa,H., and Strittmatter,S.M. (1999). Plexin-neuropilin-1 complexes form functional semaphorin-3A receptors. Cell *99*, 59-69.

Takahashi,T., Nakamura,F., Jin,Z., Kalb,R.G., and Strittmatter,S.M. (1998). Semaphorins A and E act as antagonists of neuropilin-1 and agonists of neuropilin-2 receptors. Nat. Neurosci. *1*, 487-493.

Takahashi,T. and Strittmatter,S.M. (2001). Plexina1 autoinhibition by the plexin sema domain. Neuron *29*, 429-439.

Tamagnone,L., Artigiani,S., Chen,H., He,Z., Ming,G.I., Song,H., Chedotal,A., Winberg,M.L., Goodman,C.S., Poo,M., Tessier-Lavigne,M., and Comoglio,P.M. (1999). Plexins are a large family of receptors for transmembrane, secreted, and GPI-anchored semaphorins in vertebrates. Cell *99*, 71-80.

Taniguchi,M., Yuasa,S., Fujisawa,H., Naruse,I., Saga,S., Mishina,M., and Yagi,T. (1997). Disruption of semaphorin III/D gene causes severe abnormality in peripheral nerve projection. Neuron *19*, 519-30.

Tannahill,D., Britto,J.M., Vermeren,M.M., Ohta,K., Cook,G.M., and Keynes,R.J. (2000). Orienting axon growth: spinal nerve segmentation and surround-repulsion. Int J Dev Biol *44*, 119-27.

Taylor,J.S., Van de Peer,Y., and Meyer,A. (2001). Revisiting recent challenges to the ancient fish-specific genome duplication hypothesis. Curr Biol *11*, R1005-R1008.

Tessier-Lavigne,M. and Goodman,C.S. (1996). The molecular biology of axon guidance. Science *274*, 1123-1133.

Tokumoto,M., Gong,Z., Tsubokawa,T., Hew,C.L., Uyemura,K., Hotta,Y., and Okamoto,H. (1995). Molecular heterogeneity among primary motoneurons and within myotomes revealed by the differential mRNA expression of novel islet-1 homologs in embryonic zebrafish. Dev Biol *171*, 578-89.

Tongiorgi,E., Bernhardt,R.R., and Schachner,M. (1995). Zebrafish neurons express two L1-related molecules during early axonogenesis. J. Neurosci. Res. *42*, 547-561.

Torres-Vazquez,J., Gitler,A.D., Fraser,S.D., Berk,J.D., Van,N.P., Fishman,M.C., Childs,S., Epstein,J.A., and Weinstein,B.M. (2004). Semaphorin-plexin signaling guides patterning of the developing vasculature. Dev. Cell *7*, 117-123.

Toyofuku,T., Zhang,H., Kumanogoh,A., Takegahara,N., Suto,F., Kamei,J., Aoki,K., Yabuki,M., Hori,M., Fujisawa,H., and Kikutani,H. (2004). Dual roles of Sema6D in cardiac morphogenesis through region-specific association of its receptor, Plexin-A1, with off-track and vascular endothelial growth factor receptor type 2. Genes Dev. *18*, 435-447.

Van de Peer,Y., Taylor,J.S., Joseph,J., and Meyer,A. (2002). Wanda: a database of duplicated fish genes. Nucleic Acids Res. *30*, 109-112.

Vermeren,M., Maro,G.S., Bron,R., McGonnell,I.M., Charnay,P., Topilko,P., and Cohen,J. (2003). Integrity of developing spinal motor columns is regulated by neural crest derivatives at motor exit points. Neuron *37*, 403-15.

Walsh,F.S. and Doherty,P. (1997). Neural cell adhesion molecules of the immunoglobulin superfamily: Role in axon growth and guidance. Annu Rev Cell Dev Biol *13*, 425-456.

Westerfield,M., McMurray,J.V., and Eisen,J.S. (1986). Identified motoneurons and their innervation of axial muscles in the zebrafish. J Neurosci *6*, 2267-77.

Winberg,M.L., Noordermeer,J.N., Tamagnone,L., Comoglio,P.M., Spriggs,M.K., Tessier-Lavigne,M., and Goodman,C.S. (1998). Plexin A is a neuronal semaphorin receptor that controls axon guidance. Cell *95*, 903-16.

Wolman,M.A., Liu,Y., Tawarayama,H., Shoji,W., and Halloran,M.C. (2004). Repulsion and attraction of axons by semaphorin3D are mediated by different neuropilins in vivo. J. Neurosci. *24*, 8428-8435.

Yaron,A., Huang,P.H., Cheng,H.J., and Tessier-Lavigne,M. (2005). Differential requirement for Plexin-A3 and -A4 in mediating responses of sensory and sympathetic neurons to distinct class 3 Semaphorins. Neuron *45*, 513-523.

Yee,C.S., Chandrasekhar,A., Halloran,M.C., Shoji,W., Warren,J.T., and Kuwada,J.Y. (1999). Molecular cloning, expression, and activity of zebrafish semaphorin Z1a. Brain Res Bull *48*, 581-93.

Yeo,S.Y., Miyashita,T., Fricke,C., Little,M.H., Yamada,T., Kuwada,J.Y., Huh,T.L., Chien,C.B., and Okamoto,H. (2004). Involvement of Islet-2 in the Slit signaling for axonal branching and defasciculation of the sensory neurons in embryonic zebrafish. Mech Dev *121*, 315-24.

Yu,H.H., Houart,C., and Moens,C.B. (2004). Cloning and embryonic expression of zebrafish neuropilin genes. Gene Expr Patterns *4*, 371-8.

Yu,H.H. and Moens,C.B. (2005). Semaphorin signaling guides cranial neural crest cell migration in zebrafish. Dev. Biol. *280*, 373-385.

Yu,T.W. and Bargmann,C.I. (2001). Dynamic regulation of axon guidance. Nat. Neurosci. *4 Suppl*, 1169-1176.

7 APPENDIX

7.1 Abbreviations

∅	“without”, diameter
µ	micro (10^{-6})
× g	g-force
°C	grad celsius
aa	amino acid
A	adenine
Amp	ampicillin
ATP	adenosine triphosphate
bp	base pairs
BSA	bovine serum albumine
C	Cytosine
cDNA	complementary deoxyribonucleic acid
CTP	cytosine triphosphate
Da	dalton
dATP	2’-desoxyadenosinetriphosphate
dCTP	2’-desoxycytidinetriphosphate
DEPC	diethylpyrocarbonate
dGTP	2’-desoxyguanosinetriphosphate
DMSO	dimethylsulfoxide
DNA	deoxyribonucleic acid
DNase	desoxyribonuclease
dNTP	2’-desoxyribonucleotide-5’-triphosphate
dpf	days post fertilization
DTT	dithiothreitol
E. coli	escherichia coli
Fig.	Figure
EDTA	ethylendiamintetraacetic acid
g	gramm

G	guanosine
h	human, hour
HEPES	2-(4-(2-Hydroxyethyl)-piperzino)-ethansulfonic acid
hpf	hours post fertilization
IPTG	isopropyl-β-D-thiogalactoside
Kan	kanamycin
kb	kilo base pairs
l	litre
LB	Luria Bertani
m	milli (10^{-3})
min	minute
MO	morpholino
MOPS	(4-(N-morpholino)-propan)-sulfonic acid
mRNA	messenger ribonucleic acid
n	nano (10^{-9}), number of animals
Nt	nucleotide(e)
OD	optic density
ORF	open reading frame
p	pico (10^{-12})
PAGE	polyacrylamide gel electrophoresis
PBS	phosphat-buffered saline
PCR	polymerase chain reaction
rpm	rounds per minute
psi	pounds per square inch
RNA	ribonucleic acid
RNase	ribonuclease
RT	room temperature
s	second
SDS	sodium dodecyl sulfate
T	thymine
T_A	annealing temperature
TABS	(N-tris(Hydroxymethyl)methyl-3-aminopropane-sufonic acid
TE	tris-EDTA

TEMED	N,N,N',N'-tetraethylenamine
Tet	tetracycline
T_m	melting temperature
TM	transmembrane segment
Tris	tris(-hydroxymethyl)-aminomethane
U	unit (emzymatic)
V	volt
v/v	volume per volume
Vol.	volume
w/v	weight per volume
ZMNH	Zentrum für Molekulare Neurobiologie Hamburg

7.2 Morpholino sequences

L1.1 MO1	5'-ATGAAAACAGCCCCGACTCCAGACA-3'
NRP1a MO1	5'-GAATCCTGGAGTTCGGAGTGCGGAA-3'
NRP1a 4mm MO1	5'-GATTCCAGGAGTTCGGACTGCCGAA-3'
NRP1a MO2	5'-GATCAACACTAATCCACAATGCATC-3'
PlexinA3 MO1	5'-ATACCAGCAGCCACAAGGACCTCAT-3'
PlexinA3 5mm MO1	5'-ATACCACCACCCAGAACGACCTGAT-3'
PlexinA3 MO2	5'-AGCTCTTCCCTCAAGCGTATTCCAG-3'
Sema3A1 MO	5'-AAAAATCCCAACAAGGTAATCCATG-3'
Sema3A2 MO	5'-GTACAATCCACCACAAGTAGTCCAT-3'
VEGF MO	5'-GTATCAAATAAACAACCAAGTTCAT-3'
VEGF 4 mm MO	5'-GTAACAATTAAACAACCATGTTGAT-3'

7.3 Primer sequences

Codehop plexin primer

plexinU2-5’	5’-CCCGATACTCCCTGTCCGA(AG)GA(AGCT)AA(AG)(CT) -3’
plexinY1-3’	5’-GCAGAGGCAGGCAGTTGG(AT)(CT)TTCCA(AGCT)G(CT)(AG)T-3’

Nested PCR primer

RoRi dT_{17}	5’-ATCGATGGTCGACGCATGCGGATCCAAAG CTTGAATTCGAGCTC$(T)_{17}$-3’
Ro	5’-ATCGATGGTCGACGCATGCGGATCC-3’
Ri	5’-GGATCCAAAGCTTGAATTCGAGCTC-3’
plexinN1a-5’	5’-CAGACCAGCGGGAAGGAG-3’
plexinN2a-5’	5’-GCACTCTGCAGAAGTTTGTGG-3’

pCS2+MT primer

NRP1ClaI low	5’-CGATCGATGCGCTTCCGAGTACGAGTTCTGT-3’
NRP1ClaI up	5’-CGATCGATATGCATTGTGGATTAGTGTTGATCCT-3’
Plexin/Cla-3’	5’-GCATCGATCCAGCAGCAATTTGTTGAC-3’
Plexin/Bam-5’2	5’-GTGGATCCACCACTGAGACAGCAAAAG-3’
Sema3Aa/Bam-5’	5’-CTGGATCCAGCACCATGGATTACCTTG-3’
Sema3Aa/Cla-NEW-3’	5’-CCATCGATCGCGTTTGGAAGGTGTGGC-3’
Sema3Ab/Bam-5’	5’-CTGGATCCATGGACTACTTGTGGTGGATTG-3’
Sema3Ab/Cla-3’	5’-GCATCGATCTCGTCGAGAAGGTGAAGAA-3’

Plexin full-length primer

Plexin5496Chr8-5'5	5'-TGCGATAAGGACAGAGAGGCTCTTC-3'
Plexin5496Chr8-3'	5'-TCCCAGAAAGATGGATATTTCCTTCCATG-3'

Plexin sequencing primer

PlexinChr8-seq5'1	5'-TTCTCACCAGACCGG-3'
PlexinChr8-seq5'2	5'-TCTACGGGTTCTCCAG-3'
PlexinChr8-seq5'3	5'-TCTCTGCCGTGGTTG-3'
PlexinChr8-seq5'4	5'-TACACAGCTGAGTGTG-3'
PlexinChr8-seq5'5	5'-TCACATTGCGAGCCC-3'
PlexinChr8-seq5'6	5'-TCAGAGCCAAATATGGAG-3'
PlexinChr8-seq5'7	5'-CTCTCACGTTGCCTG-3'
PlexinChr8-seq5'8	5'-AACAGCTGCTAGCCG-3'
PlexinChr8-seq5'9	5'-ACTGACCAGAATCATCC-3'
PlexinChr8-seq5'10	5'-ACAAGAGGCAGATCAC-3'
PlexinChr8-seq5'11	5'-TGGAGTTCGCTGTAAC-3'
PlexinChr8-seq5'12	5'-CATGGCAACGAGTTCAA-3'
PlexinChr8-seq3'1	5'-AACCGCAGGAACTGG-3'
PlexinChr8-seq3'5	5'-TGTGGCGATATTTACACC-3'
PlexinChr8-seq3'7	5'-ACTCGACTGAAGCTCG-3'
PlexinChr8-seq3'8	5'-AATCATCACTCGCTGTTC-3'

7.4 Full length coding sequence of plexinA3

ATGAGGTCCTTGTGGCTGCTGGTATTTTCCTTCTCTGTTTTGACTGGGACCAACATGGCATT
TCCAATGATTCTGTCGGAGCGCCCTGAAGTCACCGGGAGCTTCAAGGTTAAAGACACGAGTC
TCACTCACCTCACAGTGCACCGCAAAACTGGTGAGGTGTTCGTGGGTGCTATAAACCGAGTC
TACAAGCTTTCTGCCAATCTCACCGAAACGCGTTCTCACCAGACCGGTCCCGTGGAAGACAA
CGCCAAGTGCTATCCACCCCCCAGTGTACGAGCTTGCACGCAGAAACTGGAGTCTACAGACA
ACGTCAACAAATTGCTGCTGGTTGATTATGCGGGCAACCGTCTGGCGGCCTGTGGAAGCATC
TGGCAGGGCGTGTGCCAGTTCCTGCGGTTGGAAGATCTGTTCAAGCTTGGTGAACCACATCA
CCGTAAAGAGCACTACCTCTCGGGAGCCAAAGAGTCTGATGGGATGGCTGGAGTCGTGGTGG
GTGATGATGACGGAGACTTGAAGAAGAAAAAGAAAGGTGGCAGTCGACTCTTCATTGGTGCT
GCAATCGATGGCAAATCAGAGTATTTTCCAACCCTCTCTAGCCGTAAACTGGTGGCGGATGA
GGAAAGTGTTAACATGTTCAGTTTGGTCTACCAAGATGAGTTTGTGTCTTCTCAAATCAAGA
TACCTTCAGACACCCTCTCTCAGTATCCCGCATTTGATATCTACTACGTCTACGGGTTCTCC
AGCCGGACTTACATCTATTTCCTCACTTTGCAACTGGATACTCAGCTCACTCAGGTGGATGT
GACGGGGGAGAAGTTCTTCACCTCAAAAATAGTCCGCATGTGCTCCAATGACACTGAGTTTT
ACTCCTACGTAGAGTTCCCGCTTGGGTGCACCAAGGATGGCGTGGAATACAGACTTGTTCAA
GCTGCCTACAAGCATCGTCCTGGAAAGATTCTGGCACAGGCTTTGGGCCTGTCTGAGGATGA
GGATGTCCTGTTCGTGATCTTCTCCCAGGGTCAGAAGAACAGGGCTAACCCACCGAGAGAAA
CAGTGCTGTGCCTCTTCACACTGCACCAGATTAACCTGGCCATGCGAGAGAGGATCAAGTCA
TGCTACCGCGGAGAGGGAAAGCTGTCTCTGCCGTGGTTGCTCAACAAGGAGCTGCCTTGCAT
TAATACGCCCAAGCAGATTGGTGATGATTTCTGCGGCCTGGTCTTGAATCAGCCCCTTGGGG
GATTGATGGTGATCGAGGGCATTCCTCTGTTTGACGACCGCACTGACGGCATGGCATCAGTG
GCTGCATACACATACGGAGACCATTCGGTGGTGTTTGTGGGCACTCGCAGCGGCCACCTCAA
GAAGATTCGAGTGAATGGTGTTCCTCCGCCGTCAGAAAACGCTTTGCTGTACGAGACCGTGA
CCGTTGTGGAGGGAAGCCCCATCCTGAGGGACATGGTGTTCAGTCCAGACTATCAGTACATC
TATCTGCTGAGCGACAAACAGGTGAGTCGTCTGCCGGTGGAGAGCTGTTCTCAGTACAGCAG
CTGTAAGACGTGTCTGGGCTCTGGAGATCCTCACTGCGGCTGGTGTGTCCTGCATAACAAGT
GCTCCAGAAAGGAGGCCTGTGAGAAGTGGGCCGAGCCGCTTCACTTCAGTACAGAGCTGAAG
CAGTGTGTGGACATTACCGTCACTCCGGATAACATGTCTGTGACCTCCGTGTCTACACAGCT
GAGTGTGAAGGTGGCGAACGTCCCGAACCTCTCTGCGGGGGTGACGTGTGTGTTTGAGGAGC
TCACCGAGAGTCCAGGAGAAGTGCTGGCTGAAGGACAAATCCTCTGCATGTCCCCTTCCCTT
CGGGACGTCCCGTCTGTCACTCAGGGATATGGCGATAAACGGGTCGTGAAGCTTTCTCTGAA
GTCCAAAGAGACGGGGCTCAAATTCATCACCACCGACTTCGTCTTCTACAACTGCAGCGTTC
TGCAATCGTGTTCATCGTGTGTTAGCAGTTCTTTCCCTTGCAACTGGTGTAAATATCGCCAC
ATCTGCACTAATAATGTAGCCGAGTGCTCTTTCCAGGAAGGTCGGGTGAGCAGTGCAGAGGG
CTGCCCACAGATTTTGCCCAGCAGTGACATCCTGGTACCGGCGGGGATCGTTCGGCCAATCA
CATTGCGAGCCCGAAACTTGCCCCAGCCTCAGTCTGGACAGAAGAACTATGAGTGCGTCTTT
AACATCCAGGGAAAAGTGCAGCGTATTCCTGCGGTCCGCTTCAACAGTTCCTGCATCCAGTG
TCAGAACACCTCGTACTGGTATGAAGGGAACGAGATGGGGGATCTGCCTGTGGATTTCTCCA
TCGTGTGGGACGGTGACTTTCCCATCGACAAACCCTCATCCATGAGAGCTCTCCTGTATAAG
TGTGAGGCTCAGAGGGACAGCTGTGGACTATGTCTGAAGGCTGACAGCACATTTGAGTGTGG
CTGGTGTTTGGCCGATAAGAAGTGTCTCCTAAAGCAACACTGTCCATCAGCCGAACACAACT
GGATGCATCAGGGACGACGCAACATTCGCTGCAGCCATCCGCGCATTACCAAGATTCGTCCT
CTGACGGGCCCGAAAGAAGGAGGCACACGCGTCACCATTGAAGGGGAGAATCTGGGGCTGCA
GGTTCGAGAAATCACTCACGTGCGTGTGGCTGGAGTTCGCTGTAACCCTGCTGCAGCTGAAT
ACATCAGCGCTGAGAGGATTGTGTGTGATATGGAGGAGTCCCTGATGTCCAGTCCTCCCGGA
GGTCCGGTGGAGCTGTGTATCGGAGACTGCAGCGCTGAGTACAGGACTCAATCCACACAGAC
TTACTCCTTTGTGATGCCGAGCTTCAGTCGAGTGCGCCCTGAGAAAGGCCCGGTGTCCGGCG
GGACGAGGCTGACCATCTCAGGCCGACATCTGGACGCCGGCAGCGCTGTGACCGTGTTTTTG

GCCCAGGAGGAGTGTCTGTTCGTCAGGAGGACGGTGCGTGAGATTGTGTGTGTGACGCCTCC
ATCAGCTTCAGGATCTGGACCTTCATCTGTGAAGCTGTTTATTGATAAAGCAGAGATCACCA
GCGACACCCGCTACATCTACACTGAAGACCCAAATATCTCCACCATCGAGCCCAACTGGAGC
ATCATCAACGGCAGCACAAGCCTCACGGTCACAGGAACCAACCTGCTCACCATTCAGGAGCC
CAAAGTCAGAGCCAAATATGGAGGAGTGGAGACCACAAACATCTGTAGTCTGGTCAATGACT
CTGTGATGACGTGCTTGGCTCCGGGCATCATCTACACTAAACGTGAGGCTCCAGAAAGCGGC
GTTCACCCGGACGAGTTCGGCTTCATCCTGGATCACGTCTCTGCCCTCCTCATCCTCAACGG
GACTCCGTTCACTTACTATCCCAACCCGACCTTTGAACCTCTTGGGAATGCCGGGATTCTGG
AGGTCAAACCAGGATCACCCATCATCCTGAAGGGCAAGAACCTGATTCCTCCTGCGCCTGGG
AACATCCGTCTGAATTACAGCGTGACGATCGGAGAAACGCCCTGCCTGCTAACAGTCTCTGA
ATCTCAGCTGCTCTGCGATTCGCCAGATCTGACCGGAGAACAGCGAGTGATGATTCTTGTCG
GCGGTCTGGAATATTCCCCCGGAATGCTTCACATTTATTCGGACAGCACTCTCACGTTGCCT
GCCATCATCGGGATCGGAGCAGGTGGAGGAGTCCTCCTCATCGCCATCATCGCTGTGCTCAT
CGCTTACAAGCGCAAGACGCGGGACGCCGACCGCACACTCAAACGCCTGCAGCTGCAGATGG
ACAACCTGGAGTCCCGGGTTGCGCTGGAGTGCAAGGAAGCATTCGCTGAGCTGCAGACAGAC
ATCCAAGAGCTGACGAATGACATGGACGGTGTGAAAATCCCTTTCCTGGAGTATCGTACCTA
CACCATGAGAGTGATGTTCCCTGGCATCGAGGAGCACCCGGTTCTGAAGGAGCTGGACTCTC
CAGCTAATGTGGAGAAGGCCCTGCGCTTGTTCAGTCAGCTGCTGCACAACAAGATGTTCCTG
CTGACCTTCATCCACACGCTGGAGGCGCAAAGGTCCTTCTCCATGCGGGATCGTGGCAATGT
GGCCTCCCTCCTCATGGCGGCACTGCAGGGACGGATGGAGTACGCCACTGTGGTTCTCAAAC
AGCTGCTAGCCGACCTGATCGAGAAGAACTTGGAGAACCGAAACCACCCTAAACTACTGCTT
AGACGAACTGAATCTGTGGCAGAGAAGATGCTCACCAACTGGTTCACGTTCCTTCTGCACCG
CTTCCTCAAGGAGTGTGCGGGCGAGCCTCTGTTTATGCTGTACTGTGCTATAAAACAGCAGA
TGGAGAAAGGCCCCATAGACGCCATCACAGGAGAGGCCAGATACTCCCTGAGCGAAGACAAG
CTCATCCGACAGCAAATCGACTACAAGCAGCTGACGCTGATGTGTATTCCTCCTGAAGGAGA
AGCCGGGACAGAAATCCCTGTTAAGGTGCTAAACTGTGACACGATCACTCAGGTGAAGGACA
AGCTGTTGGACGCTGTTTATAAAGGCATCCCGTACTCGCAGAGACCACAGGCGGACGACATG
GACCTGGAATGGCGGCAGGGTCGACTGACCAGAATCATCCTCCAAGATGAAGACGTCACCAC
AAAGATCGAGAGCGACTGGAAGAGACTGAACACACTGGCACATTACCAGGTGACAGATGGGT
CTTTGGTGGCTTTGGTTCAGAAGCAAGTATCCGCTTACAACATCGCCAACTCTTTCACGTTC
ACTCGCTCTCTCAGTCGATACGAGAGCCTCTTGAGGACGTCCAGTAGTCCAGACAGCCTGCG
CTCCAGGGCTCCCATGATCACTCCTGACCAGGAAACGGGTACCAAACTCTGGCACCTGGTGA
AGAACCATGAGCATGCAGACCAGCGGGAAGGAGACCGCGGCAGCAAGATGGTGTCTGAGATT
TACCTCACACGCTTACTAGCTACCAAGGGCACTCTGCAGAAGTTTGTGGACGATCTGTTTGA
GACGGTCTTCAGTACAGCTCACCGCGGCAGCGCTCTCCCGCTGGCCATCAAATACATGTTTG
ATTTCCTGGATGAACAGGCGGACAAGAGGCAGATCACCGACCCAGACGTACGGCACACCTGG
AAGAGCAACTGCCTTCCTCTGCGGTTTTGGGTCAACGTGATCAAAAACCCTCAGTTTGTGTT
TGACATCCACAAGAACAGTATTACAGATGCCTGTCTGTCGGTGGTGGCTCAGACATTTATGG
ACTCCTGCTCCACGTCTGAGCATCGTCTGGGAAAAGACTCTCCGTCAAACAAACTGCTCTAC
GCTAAAGACATCCCCAACTACAAGAGCTGGGTGGAGAGATATTACCGTGACATCAGCAAGAT
GCCAAGTATCAGTGATCAGGATATGGATGCCTATCTGGTCGAGCAGTCTCGTCTCCATGGCA
ACGAGTTCAACACACTGAGCGCGCTCAGTGAACTGTATTTCTACATCAACAAGTACAAAGAA
GAGATTTTGACAGCGCTGGACAGAGACGGTTACTGTCGCAAACACAAGCTACGACACAAACT
GGAACAAGCCATTAACCTGATGTCTGGCAGCAGCTGA

Publications and poster presentations

Publications

Becker CG, Schweitzer J, Feldner J, Becker T, Schachner M. Tenascin-R as a repellent guidance molecule for developing optic axons in zebrafish. J Neurosci. 2003 Jul 16; 23(15): 6232-7.

Becker CG, Schweitzer J, Feldner J, Schachner M, Becker T. Tenascin-R as a repellent guidance molecule for newly growing and regenerating optic axons in adult zebrafish. Mol Cell Neurosci. 2004 Jul; 26(3): 376-89.

Becker CG, Lieberoth BC, Morellini F, Feldner J, Becker T, Schachner M. L1.1 is involved in spinal cord regeneration in adult zebrafish. J Neurosci. 2004 Sep 8; 24(36): 7837-42.

Feldner J, Becker T, Goishi K, Schweitzer J, Lee P, Schachner M, Klagsbrun M, Becker CG. Neuropilin-1a is involved in trunk motor axon outgrowth in embryonic zebrafish. Dev Dyn. (in press)

Feldner J, Becker CG, Schachner M, Becker T. Outgrowth of ventral motor axons in embryonic zebrafish requires PlexinA3. (in preparation)

Poster presentations

Feldner, J, Becker, T, Goishi, K, Schweitzer, J, Lee, P, Klagsbrun, M, Schachner, M, Becker, CG. Guidance of motor axons in the trunk of embryonic zebrafish. 15th International Society of Developmental Biologists Congress, 3 - 7 September 2005, Sydney, Australia

Danksagung

Hiermit möchte ich mich bei Frau Prof. Schachner bedanken, für die Überlassung dieses interessanten Themas und die Möglichkeit meine Doktorarbeit in ihrem Institut durchführen zu können, sowie für Ihre stetige Unterstützung.

Herrn Prof. Renwrantz am Zoologischen Institut der Universität Hamburg danke ich für die Übernahme der Begutachtung meiner Dissertation.

Mein besonderer Dank gilt PD Dr. Catherina Becker und Dr. Thomas Becker für die freundschaftliche Zusammenarbeit, ihre Hilfsbereitschaft in allen Lebenslagen und nicht zuletzt für die hervorragende Betreuung meiner Arbeit.

Den (ehemaligen) Mitgliedern der Zebrafisch Gruppe, Anselm Ebert, Bettina Lieberoth, Michell Reimer, Linda Schuldt, Jörn Schweitzer, Annika Slavetic, Inga Sörensen und Britta van Veen danke ich für die freundschaftliche Zusammenarbeit und die Unterstützung im Laboralltag.

Ganz besonders möchte ich mich beim „festen Kern“ der Zebrafischgruppe, Dr. Jörn Schweitzer bedanken, der durch seine stetige Hilfsbereitschaft bei Problemen jeder Art und konstruktiven Ideen diese Arbeit entscheidend mitgeprägt hat.

Außerdem möchte ich mich bei allen Kollegen des Instituts für ihre Hilfsbereitschaft und die freundschaftliche Atmosphäre bedanken, besonders Vasudha für unsere gemeinsamen Mittagspausen und Barbara für die Einführung ins „Hörbuch hören beim Mikroskopieren“, sowie für ihre Freundschaft.

Meinen Eltern, meinem Bruder Stefan und meinen Großeltern danke ich für ihre Geduld und Unterstützung.